Coordination Chemistry Reviews 254 (2010) 1977–2006

Contents lists available at ScienceDirect

Coordination Chemistry Reviews

journal homepage: www.elsevier.com/locate/ccr

Review

Thallium(I) supramolecular compounds: Structural and properties consideration

Kamran Akhbari, Ali Morsali*

Department of Chemistry, Faculty of Sciences, Tarbiat Modares University, P.O. Box 14155-4838, Tehran, Islamic Republic of Iran

Contents

Abbreviations: Cp^{x}, $Cp^{*} = C_5(CH_3)_5$; Cp, C_5H_5; dpa^{-}, diphenylacetate; 2Cl-PhCO, 2-chlorophenyl(oximino)acetonitrile; 3-np, 3-nitrophenoxide; Ph_2pz, 3,5-diphenylpyrazolate; MePhpz, 3-methyl-5-phenylpyrazolate; H_2tdp, 4,4′-thiodiphenol; acac, acetylacetonate; 2-(3(5)-pzH)py, 2-[3(5)-pyrazolyl]pyridine; HAB, 4-aminobenzoic acid; $1,3,5\text{-}H_3btc$, 1,3,5-benzenetricarboxylic acid; 2-np, 2-nitrophenoxide; OAr^{F}, OC_6F_5; OAr′, $3,5\text{-}OC_6H_3(CF_3)_2$; $HAnthAnthO^{-}$, (anthranoyl)anthranilate; DBM^{-}, 1,3-diphenylpropane-1,3-dionate; $PhTt^{t\text{-}Bu}$, phenyltris((t-butylthio)methyl)borate; Tbz, hydrotris(mercaptobenzothiazolyl) borate; Tp^{4py-}, hydrotris[3-(4-pyridyl)pyrazol-1-yl]borate; py-3,5-dc, pyridine-3,5-dicarboxylate; BPC, biphenyl-2-carboxylate; ADC^{2-}, acetylenedicarboxylate; oxa^{2-}, oxalate; H_2SB, 4-[(4-hydroxyphenyl)sulfonyl]-1-benzenol; 2,4-dnp, 2,4-dinitrophenoxide; $pydcH_2$, pyridine-2,6-dicarboxylic acid; $1,2,3\text{-}H_3btc$, 1,2,3-benzenetricarboxylic acid; $1,2,4,5\text{-}H_4btc$, 1,2,4,5-benzenetetracarboxylic acid; 4-np, 4-nitrophenoxide; DMeOPrPE, 1,2-(bis(dimethoxypropyl)phosphino)ethane; 4Br-PhCO, 4-bromophenyl(oximino)acetonitrile; HBTCO, 2-heteroarylcyanoximes; $MeB(3,5\text{-}Me_2pz)_3$, tris(3,5-dimethylpyrazol-1-yl)methylborato; Cym, cymantrenyl; L^{1}, bis[3-(2-pyridyl)pyrazol-1-yl]phosphinate; DNB^{-}, 3,5-dinitrobenzoate; HL^{2}, 4-hydroxybenzylidene-4-aminobenzoic acid; 2,5-DMe-DCNQI, 2,5-dimethyl-N,N′-dicyanoquinone-diimine; CSB^{2-}, 4-[(4-carboxyphenyl)sulfonyl]-1-benzenecarboxylate; $RN\text{–}B^{Ph}\text{–}NR$, N,N′-dithalliobis(alkylamido)phenylboranes; L^{3}, bis[3-(2-pyridyl)-pyrazolyl]dihydroborate; $TPPB^{-}$, tris[3-(2-pyridyl)-pyrazol-l-yl]borate; PFSCp, (pentafluoro-λ^{6}-sulfanyl)cyclopentadiene; D,L-penD,L, -penicillamine; L^{4}, bis[3-(2-pyrazinyl)-pyrazol-1-yl]dihydroborate; Bm^{Me}, bis(2-mercapto-1-methylimidazolyl)borate; Tp, hydrotris(pyrazolyl)borate; Ar^{Mes2}, $C_6H_3\text{-}2,6\text{-}(C_6H_2\text{-}2,4,6\text{-}Me_3)_2$; HBQA, bis(8-quinolinyl)amine; HCPMEF, 9-(1-cyclopentadienyl-1-methylethyl)fluorenyl; DMP, $OC_6H_3(CH_3)_2\text{-}2,6$; pz, pyrazolyl; $P_3C_2Bu^{t}_2$, 3,5-di-tert-butyl-1,2,4-triphospholyl; Pc, phthalocyanine; D-penD, -penicillamine; Hdcp, 2,4-dichlorophenol; HB^{-}, 4-hydroxybenzoate; $Tp^{Ph,4CN}$, hydrotris(4-cyano-3-phenyl)pyrazolylborate; $C_5H_3Ph_2$, 1,4-diphenylcyclopentadiene; L^{5}, commo-3,3′-Ga(3,1,2-$GaC_2B_9H_{11}^{-}$; L^{6}, commo-3,3′-Al(3,1,2-$AlC_2B_9H_{11})_2^{-}$; DACH, 1,2-diaminocyclohexane; dmg-H, dimethylglyoximate dianion; mnt, maleonitriledithiolate; pda, 1,2-propyldiamine; acacH, acetylacetone; bipy, 4,4′-bipyridine; L^{7}, hydrotris(imidazolyl)borate; L^{8}, dihydrobis(1,2,4-triazolyl)borate; HL^{9}, dimethyl-N-trichloracetylamidophosphate; L^{10}, 1-methylcytosine; HL^{11}, phenylmethanethiol; HL^{12}, malonohydroxamic acid; L^{13}, (N,N-diethyl-N′-benzoylselenoureato); HL^{14}, Lasalocid acid; *m*-Nbs^{-}, *m*-nitrobenzenesulfonate; $Ohyo^{2-}$, oxalohydroxamate; (H)phthalate, hydrogenphthalate; pyn-2-ol, pyrimidin-2-olate-N1,N3; eda, ethylenediaminium; dme, 1,2-dimethoxyethane; $S\text{-}t\text{-}C_4H_9$, tert.-butanethiolate; QtmCp, 1-(8-Quinolyl)-2,3,4,5-tetramethylcyclopentadiene; BX_4^{-}, tetrakis(imidazolyl)borate; BY_4^{-}, tetrakis-(4-methylimidazolyl)borate.

* Corresponding author. Tel.: +98 2166906597; fax: +98 88009730.
E-mail address: morsali_a@modares.ac.ir (A. Morsali).

0010-8545/$ – see front matter
doi:10.1016/j.ccr.2010.03.006

ARTICLE INFO

Article history:
Received 20 January 2010
Accepted 13 March 2010
Available online 23 March 2010

Keywords:
Supramolecular
Coordination polymers
Thallium(I)
Polyhapto
Thallophilic
Agostic
Secondary interactions

ABSTRACT

During the last two decades, supramolecular compounds and especially coordination polymers have received great attention and the number of their synthesized compounds is still growing, which is mainly due to their potential application in various fields such as microelectronics, nonlinear optics, ion exchange, catalysis, gas storage, separation and luminescence. Formation of polymers with main group metal ions such as thallium(I) is disproportionately sparse when compared with those of other metals. Because of the interest structures, properties and applications of thallium polymers, it is necessary to understand thallium's ability to bind donors and form supramolecular compounds. This review tries to give an overview of all supramolecular compounds which were reported from thallium(I) after 1990 and to investigate their properties and applications. Thallium(I) usually forms neutral species and exhibits greater tendency to forming one-dimensional supramolecular compounds. Thallium(I) also favors secondary interactions on its coordination sphere (especially with unsaturated carbon atoms forms organometallic polymers) with stereochemically active lone pair and hemidirected coordination sphere around it.

1. Introduction

Thallium, when compared with the remainder of the group 13 elements, shows a preference for the oxidation state +1. This has been attributed to the effect of the inert pair of electrons which is generally used in introductory textbooks to explain the tendency of the heavier main group elements to adopt oxidation numbers that are two less than the respective group number. This phenomenon which could also be observed in Pb^{2+} and Bi^{3+} [1–6], originates from a combination of shell structure effects and relativity. Owing to the relativistic downshift in energy of the 6s orbital, Tl does indeed favor the oxidation state +1 over +3. Moreover [7], Tl might be regarded as a relativistic alkali metal because Tl chemistry parallels that of the alkali metals in many ways [8] and the well-known toxicity of thallium compounds may also be associated with the high affinity for sulfur functions and the non-reversibility of the complexation reactions as compared to the action of alkali cations [9]. Specially thallium(I) compounds are similar in structure and chemical properties to potassium and silver salts [10]. In modern coordination chemistry the role of most metals as clustering centers for ligands appears to be predictable and the coordination number and coordination geometry can be extrapolated for most of the common metal/ligand combinations with quite high certainty. Although this is generally true, the situation is surprisingly difficult for main group metals in their low oxidation states in which they are assigned lone pairs of electrons [11]. Although such a pair of s electrons beyond a completed shell is always stereoactive with an obvious gap in Tl^{I} coordination sphere in the thallium(I) complexes with lower coordination number (three to five), this activity cannot be predicted in complexes with higher coordination number (six to twelve) [12]. Thallium(I) has atomic, ionic, covalent and van der waals radii of $1.70 < r(Tl) < 1.90$, 1.47, 1.55 and 1.96 Å, respectively [13,14]. Owing to the relativistically contracted valence shell and the low electrical charge, the Tl^{+} cation is intermediate between standard hard and soft character and has affinity for both hard and soft donor atoms, like oxygen and sulfur, or chloride and iodide, and so forth [11].

The design and construction of supramolecular arrays utilizing non-covalent bonding of tectons would be called supramolecular synthesis. Thus, the supramolecular synthesis successfully exploits hydrogen bonding and other types of non-covalent interactions, in building supramolecular systems such as intermolecular coordination bonds, which leads to formation of coordination polymers, polyhapto, metallophilic or agostic interactions which are introduced below.

In contrast to transition-metal arene complexes, arene π-complexes of monovalent p-block metals are rather scarce [15]. Tl^{I} also forms π-complexes with aromatic hydrocarbons [16] as first demonstrated for the anionic cyclopentadienyl ligands in 1957, and in 1985 for neutral arenes [11], but structural reports on thallium(I) arene complexes have only appeared in the literature in the last 20 years. It was not until 1985 that Schmidbaur isolated the first structurally characterized Tl(I) arene complex, with $Tl\cdots\pi_{(centroid)}$ distances between 2.94 and 3.03 Å [17]. The reported Tl···C separations range is 3.20–4.00 Å in recent reported species [11,18] and the sum of the van der Walls radii of carbon and Tl atoms is 3.66 Å [14]. The M–M bonded clusters, in which the metal ion has a +1 oxidation state and weakly interacting ns^2 lone pairs, are of particular interest due to the nature of the bonding and the unusual optical properties that can be produced by M–M interactions, in particular those in thallium(I) centers [19]. The strength of this interaction is generally considered to be of a magnitude similar to that of a typical hydrogen bond [20]. Recent ab initio calculations on thallocene dimers suggest energy minima with Tl···Tl distances slightly under 4 Å and interaction strengths of the order 10 kJ/mol [21]. Though positioning in a structural analysis of a H so close to the heavy Tl atom may not be given too much credibility, however M···H interactions have recently reported [20,22–24]. This interaction is observed when the H atoms situated above the proposed site on the lone pair of Tl are oriented such that they might be thought to be forming a Tl–Lp···H–C– (Lp = lone pair) as a weak hydrogen bond [22] or Tl···H–C– as agostic interactions with distances smaller than 3.30 Å [25].

In this review we summarize three types of thallium(I) supramolecular compounds: thallium(I) coordination polymers, thallium(I) compounds aggregate from secondary interactions and finally thallium(I) polymeric compounds obtained from Tl–M (M = Pt, Au or Ni) bonds. Also we take distances that fall within the sum of the covalent or ionic radii, as primary bond and distances falling within the sum of the van der waals radii or near it, as secondary interactions, in addition we consider much attention in Tl···C, Tl···Tl and Tl···H secondary interactions due to role of these interactions in aggregate Tl^{I} supramolecular compounds. Scheme 1 shows the figures of some complex ligands which are used to fabricate thallium(I) supramolecular compounds.

2. Thallium(I) coordination polymers

Coordination polymers are a very important topic of modern solid-state chemistry. Especially porous compounds like MOF-5 [26], MIL-53 [27] or HKUST-1 [28] have attracted a lot of attention due to their potential as heterogeneous catalysts or adsorbates for gases like hydrogen. Besides porosity there are also attractive aspects of non-porous coordination polymers, e.g. magnetic, lumi-

nescent, vaporochromism or conducting properties to name a few [29–31]. Coordination polymers offer significant advantages over conventional molecular compounds due to very low solubility in conventional organic solvents and water, and much higher thermal stability. They have also several applications in sensors, organic light emitting diodes (OLED) and full-colored LCD displays [32]. In this section we classified coordination polymers on the basis of their dimensions and secondary interactions in the Tl^{I} coordination sphere. Tl(I)–ligand bonding is generally divided into two types, primary and secondary. Primary bonding is said to exist if the Tl–X (X = hetero atom) bond distance falls within the sum of the covalent or ionic radii. Secondary bonding occurs if the Tl–X (X = hetero atom) bond distance falls within the sum of the van der Waals radii [33].

2.1. One-dimensional coordination polymers with secondary interactions in Tl^{I} coordination sphere

$[Tl(\mu_4\text{-AB})]_n$ (**1**) [34], $Tl[C_8H_8NO_2]$ (**2**) [11], $[HAnthAnthOTl(H_2O)_{0.5}]$ (**3**) [9], *catena*-[bis(μ_3-salicylato)dithallium(I)] (**4**) [35], *catena*-[bis(μ_3-4-aminosalicylato)dithallium(I)] (**5**) [35], *catena*-[μ_3-(3,5-dimethoxybenzoato)thallium(I)] (**6**) [35], $[Tl(\mu_4\text{-dpa})]_n$ (**7**) [36] and $[Tl_2(\mu\text{-}1,3,5\text{-}H_3btc)(H_2O)]_n$ (**8**) [37] form 1D coordination polymers with the carboxylate group of the related

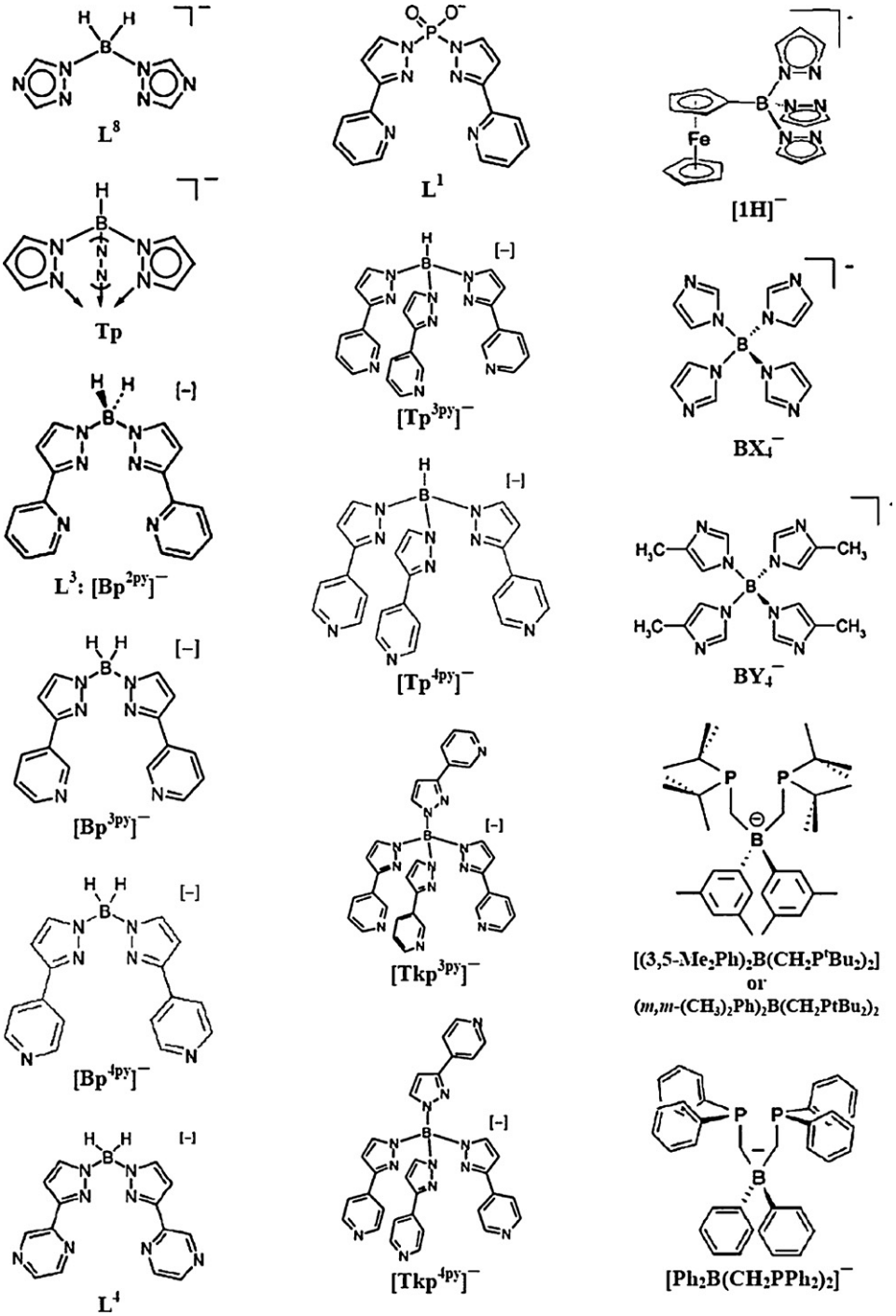

Scheme 1. Shows the figures of some complex ligands which used in fabricate thallium(I) supramolecular compounds. In L^5 and L^6 hydrogen atoms omitted for clarity.

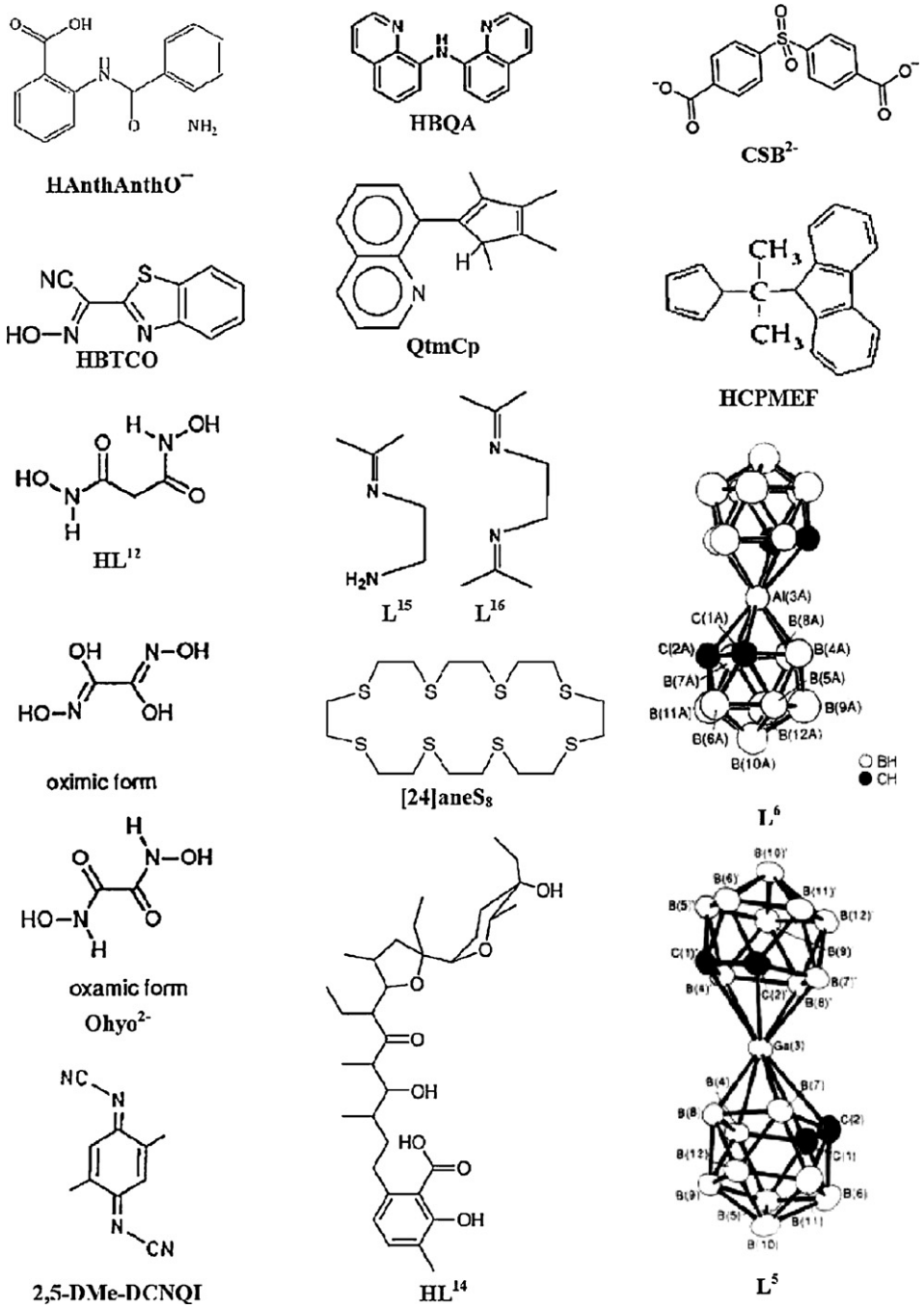

Scheme 1. (*Continued*).

ligand. In **1** (Fig. 1a) the thallium atoms have an irregular coordination sphere containing stereochemically active lone pair and bi-hapto (η^2) interactions. Thus the Tl(I) atoms are linked to two carbon atoms of phenyl groups with distances Tl···C of 3.362(2) and 3.617(5)Å, attaining a total hapticity of seven with O_5**Tl**···C_2 coordination environment. The oxygen atom of the carboxylate groups and hydrogen atom of $-NH_2$ groups of AB^- anions in compound **1** are involved in a hydrogen bonding network (Fig. 1b). Compound **1** does not melt and sublimation of this compound occurs between 222 and 239 °C. The ligand HAB and compound **1** are luminescent in the solution state, with emission maxima at 395 nm.

In thallium(I) 2-amino-3-methyl-benzoate (**2**) the anion is chelating the metal atom to form a wedge-like four-membered ring. These fundamental units aggregate to give dimers, the geometry also suggests intramolecular hydrogen bonding. Complexation of the metal atom through four oxygen atoms in a small quadrant of the coordination sphere is supplemented by a weak polyhapto contact with Tl···$\pi_{(centroid)}$ distance of 3.230(11) Å. In the dinuclear units of **3**, the thallium ions accommodate one nitrogen and four oxygen atoms of the anions in their coordination sphere and in addition entertain weak Tl-arene contacts forming 3D supramolecular networks. Relatively short contacts of three carbon atoms with Tl^I ion have 3.47, 3.59 and 3.47 Å distances. The water molecules are not involved in metal complexation, but contribute to a network of hydrogen bonding. In compounds **4** and **5**, adjacent units are held together by secondary Tl–O3 interactions, resulting in stair-like, infinite one-dimensional polymers. The Tl^+ ion is in a distorted square pyramidal geometry, with the four oxygen atoms in the

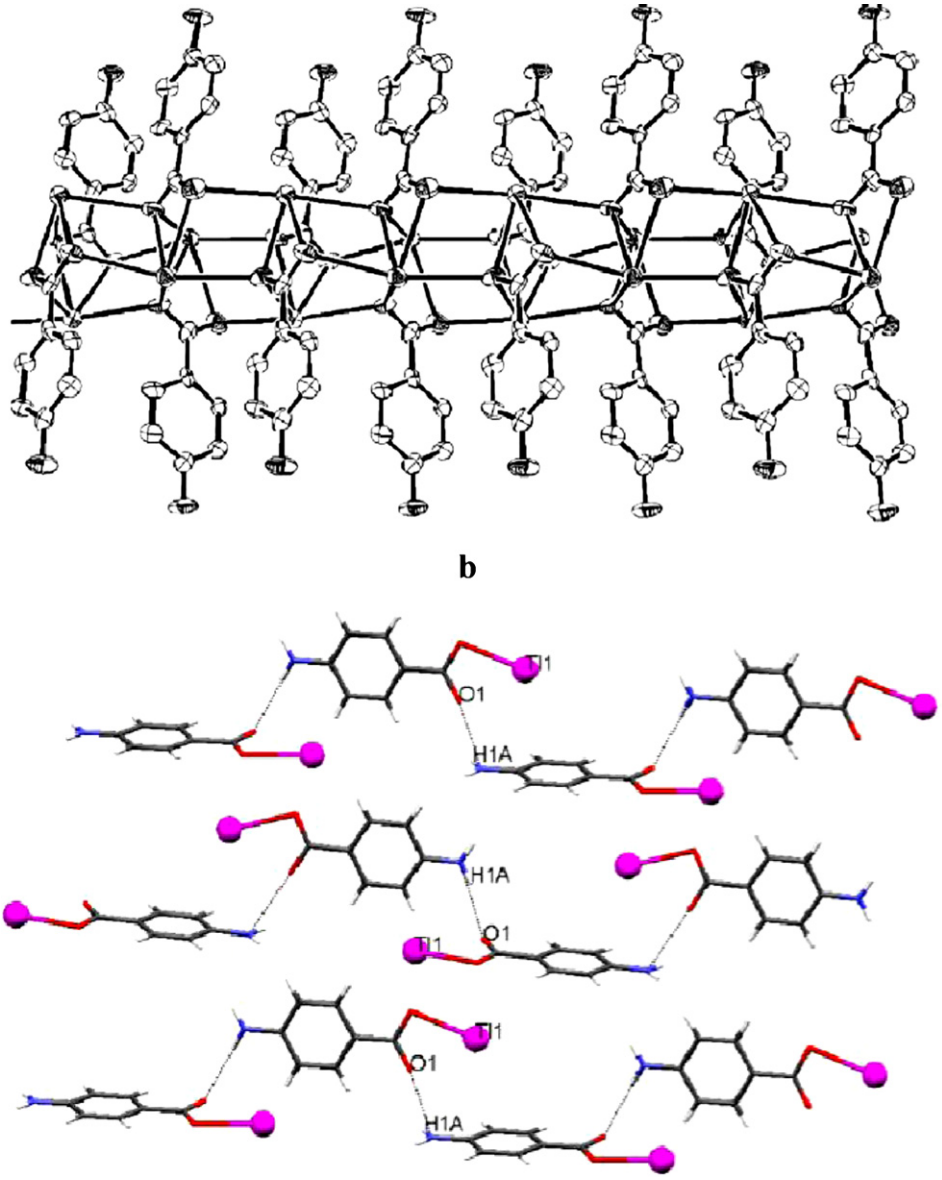

Fig. 1. (a) A fragment of the one-dimensional coordination polymer in $[Tl(\mu_4\text{-AB})]_n$ (**1**). H atoms are omitted for clarity. (b) Hydrogen bonding in the compound **1** [34]. Reproduced with permission of Elsevier.

basal plane and the stereoactive lone pair occupying the apex position of the pyramid, in a hydrophobic environment provided by two neighboring phenyl groups with O_4**Tl**$\cdots 2\eta^6$-C_6 coordination environment. In **4** the distance between the planes of the phenyl rings and the Tl^+ cation is 3.29 Å and in **5** the distance between the planes of the phenyl rings and the Tl^+ cation are 3.31 and 3.68 Å. In addition to the strong intramolecular hydrogen bond, weak hydrogen bonds are also formed between the amino protons and O2 atoms of adjacent units, resulting in a 3D supramolecular compound. Compound **4** was obtained from H_2O with empirical formula of $(C_7H_5O_3Tl)_2$ crystallizing in the monoclinic system with $P2_1/n$ space group. In similar work in our laboratory a polymorth of **4**, with empirical formula of $C_7H_5O_3Tl$, thallium(I) salicylate **47** [8] was obtained from a mixture of H_2O and CH_3OH. It crystallizes in the orthorhombic system with Pbca space group. Compound **47** illustrates completely different structural packing compared with **4** which will be discussed in section 2.3. In **6** each Tl^+ ion is coordinated on one side to four oxygen atoms of three carboxylate groups. The Tl^+ cation is therefore in a distorted square pyramidal geometry as in compound **4** and an η^6–C_6 polyhapto interaction could be also seen between Tl^+ ion and the phenyl ring. The distance between the planes of the phenyl rings and the Tl^+ cation are 3.42 Å. In **7** the five-coordinate Tl centers involving Tl$\cdots$C interactions with distances between 3.379(5) and 3.995(2) Å, resulting in a total hapticity of eleven with an O_5**Tl**$\cdots C_6$ coordination environment (Fig. 2).

Compound **8** which is stable up to 350 °C after removal of coordinated water molecule, has two types of Tl^+-ions with the coordination sphere of O_4**Tl1**$\cdots Tl_2$ and O_6**Tl2**$\cdots Tl_2$. In **8**, there is one coordinated water molecule and this 1D polymeric compound is further interconnected by an extensive network of hydrogen bonds between the 1,3,5-$Hbtc^{2-}$ anions and the oxygen atoms of coordinated water molecules. Compound **8** also shows a broad intraligand fluorescence emission band with the maximum intensity at 400 nm upon excitation at 350 nm.

Structural determination of $[Tl(2\text{-np})]_n$ (**9**) [38], $[Tl(3\text{-np})]_n$ (**10**) [39] and $TlOAr^F$ (**11**) [40] show the complexes to be one-dimensional classical 'stair-polymer' array by phenoxide oxygen atoms and with some thallophilic interactions in **9** and **10**. In **9** thallium atoms are linked by five phenoxide oxygen atoms. The Tl atoms have an unsymmetrical three-coordinate, **Tl**O_3 geometry in

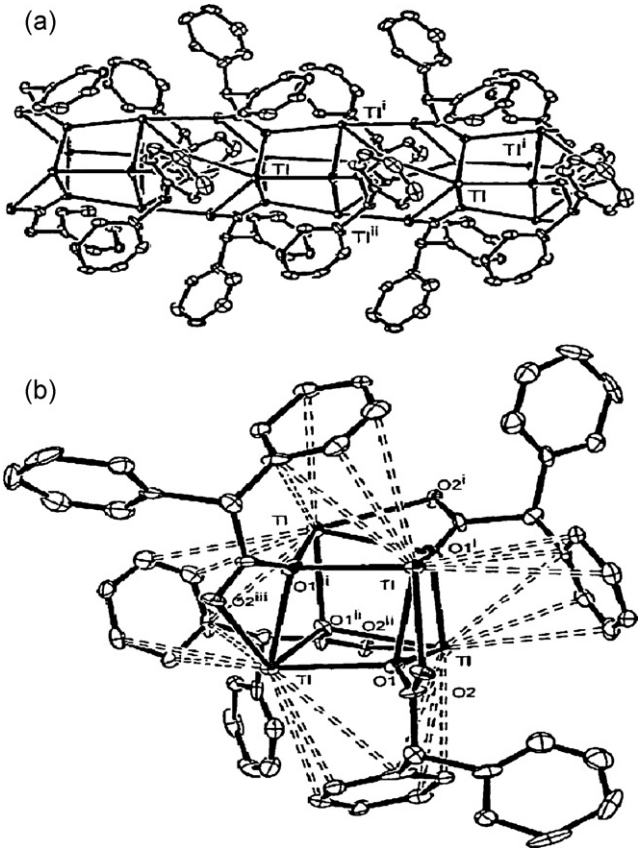

Fig. 2. (a) Fragment of 1D coordination polymer in $[Tl(\mu_4\text{-dpa})]_n$ (**7**); (b) bonding and polyhapto interactions within a fragment of **7** after extending the bonding limit [36].
Reproduced with permission of Wiley-VCH Verlag GmbH & Co. KGaA.

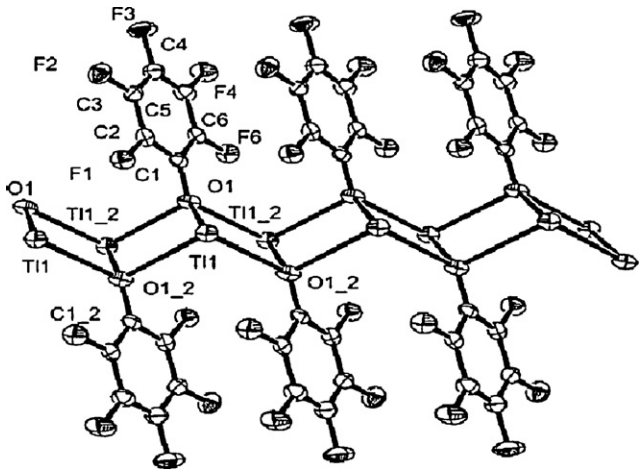

Fig. 3. ORTEP of $TlOAr^F$ (**11**) [40] with ellipsoids at the 50% level.
Reproduced with permission of American Chemical Society.

10 and **11**. Weak interaction of thallium(I) with oxygen atoms of an adjacent molecule and π–π-stacking interaction between the parallel aromatic rings could be observed in the solid state of **10**. When **11** is recrystallized from CH_2Cl_2, no solvent is incorporated and an infinite ladder chain is observed (Fig. 3), close contacts are that of Tl(1) to F(1), F(2), and F(4). If $TlOAr^F$ is recrystallized from THF, a monomeric $[Tl_2(\mu_2\text{-}OAr^F)_4]$ unit with pseudo-octahedron structure is formed and if TlOAr′ is recrystallized from THF, a disordered cubic unit, $\{TlOAr'\}_4$.THF is formed [40].

Compound [Tl(2Cl-PhCO)] (**12**) [41,42], has an exactly similar structure as observed in **11**, but compounds $[Tl(OC_6H_3(Me)_2\text{-}2,6)]_n$ (**13**) [43] and $[Tl(OC_6H_3(CHMe_2)_2\text{-}2,6]_n$ (**14**) [43], are one-dimensional polymers that possess a $[Tl–O–]_\infty$ backbone with two-coordinate Tl^I centers (Fig. 4). With a low coordination number and a stereoactive lone pair, both compounds form Tl–π interactions with the aromatic phenyl ring with distances of 3.16 and 3.08 Å for **13** and **14**, respectively.

When recrystallized from C_6D_6/d_8-THF, compound $Tl_2Cu(OAr^F)_4$ (**15**) [40], reveals a unique helical chain. The $\{Tl_2(\mu_2\text{-}OAr)_4\}$ pseudo-octahedron unit bridges the Cu(1) and Cu(2) centers. Tl(1), Tl(6), Tl(8), and Tl(10) are coordinated in an η^6-fashion to benzene molecules with average Tl···C distances of 3.42(5), 3.53(6), 3.42(6), and 3.42(6) Å, respectively. Four other thallium atoms are coordinated, in addition to the bridging aryloxide groups, intramolecularly to fluorine atoms at distances less than 3.5 Å. There are also intermolecular Tl–F contacts less than 3.5 Å in **15**. $Tl_2Cu(OAr')_4$ and $Tl_2Cu(OAr')_4{\cdot}2THF$ form dimeric and monomeric structures, respectively [40].

In $[Tl(acac)]_n$ (**16**) [44], $[Tl_2(DBM)_2]_n$ (**17**) [45] and $[Tl\{(O{=}CPhOMe)_2CH\}]$ (**18**) [46], $acac^-$ or similar ligands were used as the bridging ligand. The structure of **16** consists of mononuclear Tl(acac) units in which the chelating acetylacetonate ligands bind the thallium atom through both oxygen atoms and can be also described as an infinite two-dimensional supramolecular compound, formed via Tl···Tl interactions and oxygen bridges with $O_3\mathbf{Tl}\cdots Tl_2$ coordination environment. **16** is luminescent and shows an emission at 418 nm (exc at 351 nm), which is shifted to 410 nm (exc at 344 nm) when the measurement is carried out at 77 K. TD-DFT calculations show that $Tl_2(acac)_2$ units would be responsible for the luminescent behavior of **16** in acetonitrile solution. In **17** there are two types of Tl^+-ions, Tl1 and Tl2, with the coordination number four. The Tl1 and Tl2 atoms interact with two neighboring thallium atoms with thallophilic interactions

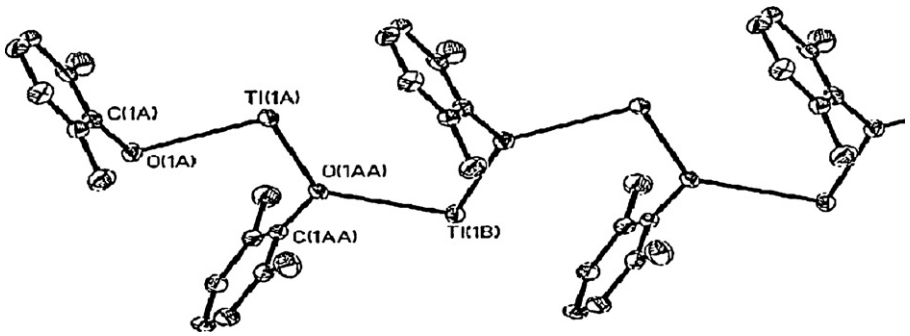

Fig. 4. Thermal ellipsoid plot of $[Tl(OC_6H_3(Me)_2\text{-}2,6)]_n$ (**13**) [43]. Ellipsoids are drawn at 30% level.
Reproduced with permission of American Chemical Society.

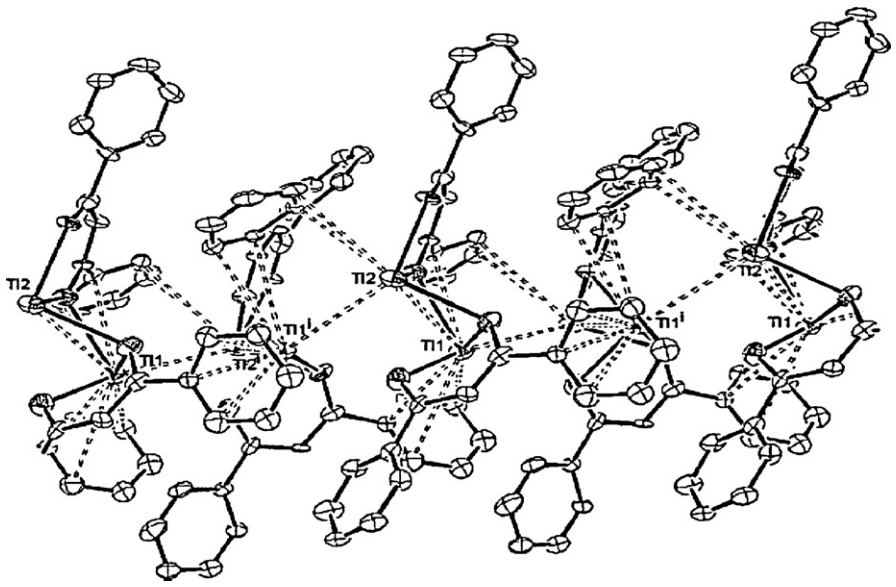

Fig. 5. A fragment of the 1D coordination polymer in $[Tl_2(DBM)_2]_n$ (**17**) [45], showing polyhapto interactions after extending the bonding limit. *i*: *x*, −*y*, *z* + 1/2. Reproduced with permission of Elsevier.

of 3.974(2) and 3.897(3) Å. Tl1 and Tl2 atoms in this compound may also be involved in a η^6 and η^2 interactions with the phenyl groups, respectively. Hence, the Tl^I ions attain O_4**Tl1**$\cdots C_6Tl_2$ and O_4**Tl2**$\cdots C_2Tl_2$ coordination sphere (Fig. 5). In **18**, the organic ligand coordinates to the metal center through both ketonic oxygen atoms in a slightly asymmetrical chelate fashion. Each monomeric unit is linked to an identical, symmetry-related group through an intermetallic bridged bonding interaction to form a disk-like dimer. The Tl–Tl separation observed is 3.747(1) Å. The whole dimeric moiety (44 atoms) is roughly planar. The dimeric units form a polymeric columnar arrangement and the thallium coordination environment could be described as a highly distorted octahedron with a vacant position occupied by the stereochemically active lone pair of the Tl(I) atom.

$[Tl(Ph_2pz)]$ crystallizes in two forms. In the first form, benzene has trinuclear molecules $[Tl_3(Ph_2pz)_3]$ (**19**) [47], linked by intermolecular Tl3–π–η^6–Ph contacts, forming a one-dimensional polymeric chain. In addition to these contacts, there are four other intermolecular Tl$\cdots$C distances of a similar magnitude but, unlike the Tl3$\cdots\eta^6$–Ph interactions, these other contacts do not appear to have a significant influence on the overall arrangement of $(\mathbf{19})_n$. Within **19** the three thallium atoms are different, having coordination numbers of two (**Tl3**N_2) with the Tl$\cdots\eta^6$–Ph contact, three (**Tl2**N_3) with Tl$\cdots\eta^2$–Ph contact and four (**Tl1**N_4). Crystallization of $[Tl(Ph_2pz)]$ from dme gives tetranuclear molecules $[Tl_4(Ph_2pz)_4]$ (**20**) [47] solvated by dme. Three or four-coordinate Tl atoms are observed with pyrazolate coordination. In addition there is an intermolecular Tl–π–η^3–Ph interaction linking the tetranuclear molecules into a polymer and secondary intramolecular Tl$\cdots$C contacts (Tl1, Tl2, Tl3 and Tl4 with eight, six, six and one aromatic C atoms, respectively), the most important of which is an unsymmetrical Tl–π–η^5–Ph_2pz interaction. Crystallization of $[Tl(Ph_2pz)]$ or [Tl(MePhpz)] from dichloromethane afforded the partially hydrolysed tetranuclear cages $[Tl_4(Ph_2pz)_3(OH)]$ (**21**) [47] or $[Tl_4(MePhpz)_3(OH)]$ (**22**) [47], which associate to give a dimer and a polymer respectively owing to Tl$\cdots$Tl interactions, supported for the dimer by an intercage distant Tl–π–η^5–Ph_2pz contact. Complex **21** features three (Tl3) and four (Tl1, Tl2 and Tl4) coordinate Tl atoms, Tl1 also form secondary interactions with two aromatic C atoms of the ligand. In **21**, the dichloromethane of solvation is well behaved in refinement with the chloride atoms contacting phenyl hydrogen atoms, one of the hydrogen atoms contacting a distant thallium, whilst **22** has three (Tl4), four (Tl3) and five (Tl1 and Tl2) coordinate thallium atoms, which formed a tetranuclear cage which is linked to adjacent cages by metal$\cdots$metal interactions between Tl(1) and Tl(2′) (3.685(2) Å) giving an overall polymeric structure. Secondary Tl$\cdots$C interactions are observed in Tl1 and Tl4 with six carbon atoms. $[Tl(2\text{-}(3(5)\text{-}pz)py)]_n$ (**23**) [48] (Fig. 6) demonstrates one-dimensional chain structures with a zigzag arrangement of pyrazolato-bridged thallium atoms, featuring a distorted trigonal pyramidal coordination geometry. Orientation of the aromatic rings in **23** toward the Tl^I ion, make us to have a search in CIF of this compound. We found that Tl^I ion has a short contact with the pyrazolyl ring ($Tl\cdots\pi_{(centroid)}$ = 3.35 Å) and the two carbon atom of pyridine ring of (2-(3(5)-pzH)py ligand, thus the thallium(I) ion attained the total N_3**Tl**$\cdots N_2C_5$ coordination sphere.

One-dimensional polymeric chains in $[Tl(Tbz)]_\infty$ (**24**) [49], comprise a zigzag array of Tl and S atoms (Fig. 7a). The full coordination sphere of the Tl ion is shown in Fig. 7b. The vacant coordination sites on Tl interact (albeit weakly) with the π-systems of benzothiazole units in neighboring ligands with S_4**Tl**$\cdots 2\eta^6$–C_6 coordination sphere. In one case the interaction is approximately symmetrical, whereas in the other the metal is placed significantly 'off-center' with respect to the ring. In the solid-state $Tl[PhTt^{t\text{-}Bu}]$ (**25**) [50] forms a one-dimensional coordination polymer. Each thallium ion is coordinated to three sulfur donors and a phenyl ring in an η^6-mode that may be described roughly as a three-legged piano stool coordination environment. The Tl$\cdots$C distances range is from 3.272(8) to 3.446(8) Å.

In $[Tl\{Cp^*Fe(\mu,\eta^5{:}\eta^5{:}\eta^1\text{-}P_5)\}_3]_n[Al\{OC(CF_3)_3\}_4]_n$ **(26)** [51] the Tl^+ ion is surrounded by three π-coordinating units of $[Cp^xFe(\eta^5\text{–}P_5)]$. The geometry around each Tl^+ ion is trigonal pyramidal, owing to an additional σ bond of one of the phosphorus atoms of each P_5 rings to the neighboring Tl^+ ion and a 1D coordination polymer is formed which contains the cyclo-P_5 moieties of $[Cp^xFe(\eta^5\text{–}P_5)]$ in a hitherto unknown bridging $\eta^5{:}\eta^1$-coordination mode (Fig. 8). Thus, the geometry around the thallium ions may be considered as a distorted octahedron.

Structural determination of $\{[Ph_2B(CH_2PPh_2)_2][Tl]\}_n$ (**27**) [52], revealed the formation of 1D coordination polymer. The thallium atom is best described by two Tl–P bonds and two η^6–aryl interactions. The Tl–C_{aryl} average distance is 3.31 Å (Fig. 9).

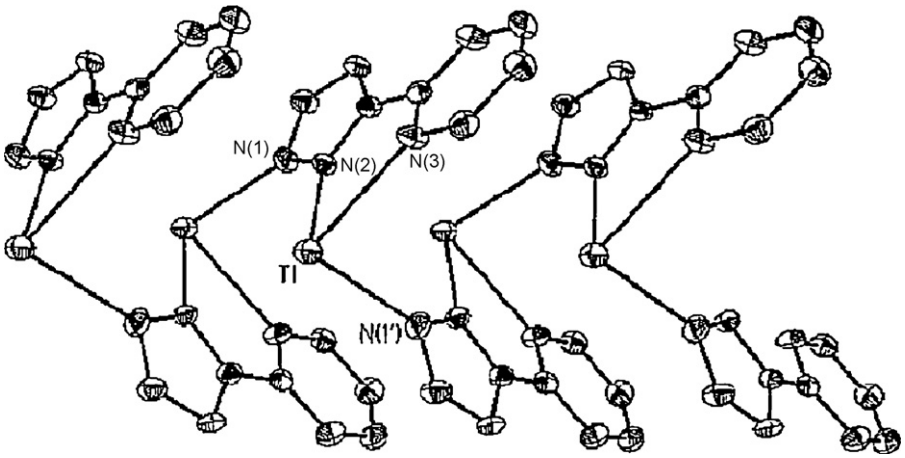

Fig. 6. Structure of the $[Tl(2\text{-}(3(5)\text{-}pz)py)]_n$ (**23**) [48], extended chain showing 30% probability ellipsoids and the atom-labeling scheme. Reproduced with permission of American Chemical Society.

Compound TlL^9 (**28**) [53], forms a polymeric ladder structure from centrosymmetric dimers that are formed by the bridging function of the phosphoryl oxygen atom with a central planar four-membered Tl_2O_2 ring. One nitrogen atom and methoxy group oxygen atoms of the neighboring dimer moieties are also involved in coordination to each thallium atom with the O_4N**Tl**···Cl coordination environment. In TlL^7 (**29**) [54,55], each of three imidazolyl rings coordinate to a different metal atom. A one-dimensional ladder-like strand is formed from this. The packing of adjacent strands in **29** is most likely dictated by electrostatic interactions between the thallium ion and imidazolyl π manifolds. These non-bonded Tl···C and Tl···N distances are in the range of 3.69–4.00 Å.

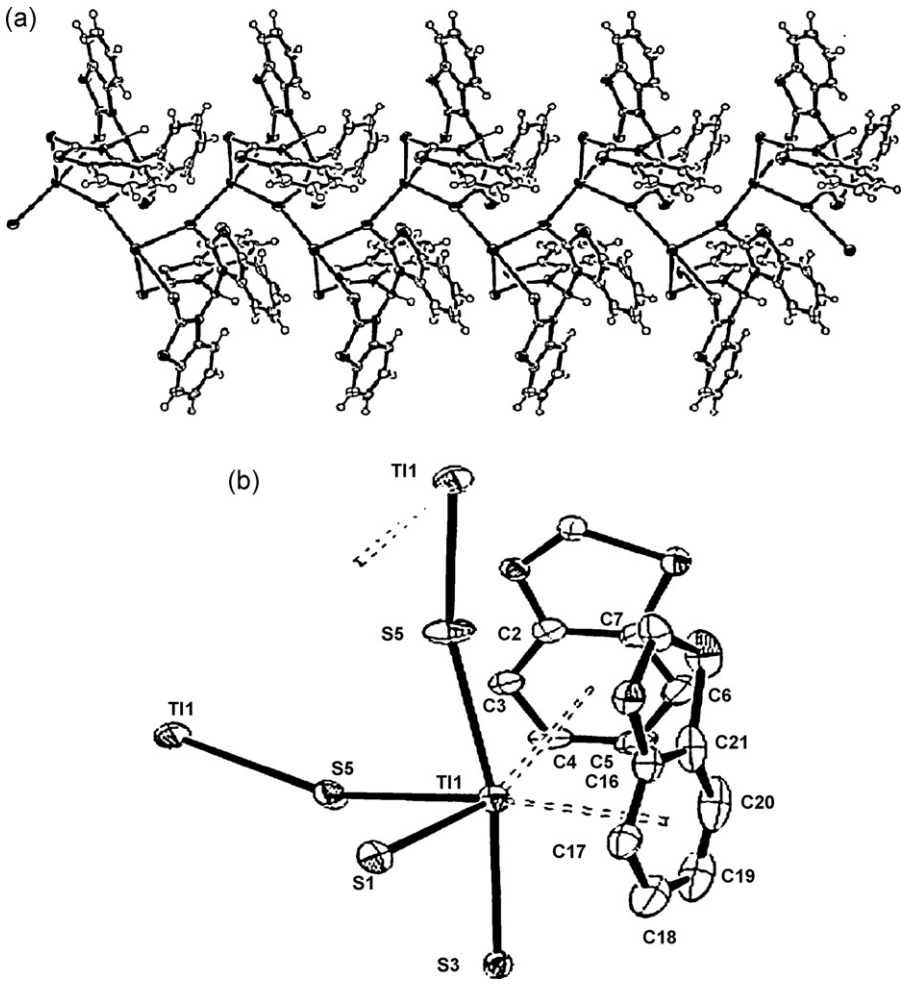

Fig. 7. (a) A view of a section of the infinite polymeric chain in $[Tl(Tbz)]_\infty$ (**24**) [49], emphasising the zigzag –Tl–S–Tl– arrangement. (b) The thallium coordination sphere in TlTbz.
Reproduced with permission of Elsevier.

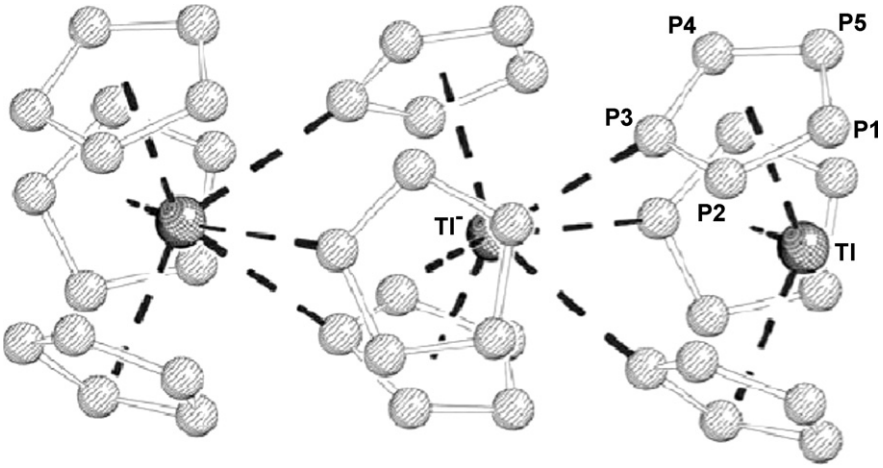

Fig. 8. Portion of the polycationic chain in $[Tl\{Cp^*Fe(\mu,\eta^5{:}\eta^5{:}\eta^1\text{-}P_5)\}_3]_n[Al\{OC(CF_3)_3\}_4]_n$ (**26**) [51], ({Cp*Fe} fragments are omitted for clarity).
Reproduced with permission of Wiley-VCH Verlag GmbH & Co. KGaA.

The basic structural feature of $Tl(L^{10})NO_3$ (**30**) [56], is the formation of infinite stacks of pairs of cytosine rings with the metal ions linking the nucleobases forming 1D coordination polymer. Tl^+ forms eight bonds to two N(3), three O(2) as well as three nitrate oxygen atoms. Thallophilic interaction with distance of 3.79 Å could be observed in **30**. A search was made for Tl···C interactions revealing that the Tl^I ion has a short contact with three of the aromatic carbon atoms, thus attaining the coordination sphere of O_6N_2**Tl**···C_3Tl.

2.2. One-dimensional coordination polymers without secondary interactions in Tl^I coordination sphere

The crystal structure of Tl(4Br-PhCO) (**31**) [42] and Tl(BTCO) (**32**) [32] is similar to that of **12** with no thallophilic interactions. The separation between two phenyl rings in **12** is 0.22 Å lower than the same separation for **31**. This difference is very close to the van der Waals radii difference between Cl and Br atoms: 0.15 Å. The anion is non-planar and adopts a *trans-anti*-configuration in **32**. The solid-state UV–vis absorption spectrum of **32** possesses an intense broad band of $n \rightarrow \pi^*$ transition. Compound **32** also exhibits strong room temperature blue emission in the solid state. The crystal structure of TlL^{11} (**33**) [57] is similar to **11** but with four-membered Tl_2S_2 rings and **Tl**S_3 coordination sphere. Our search also indicates the existence of a Tl···H interaction (3.126 Å) which leads to formation of 2D supramolecular network in **33**. Compound $[Tl_2(\mu\text{-Htdp})_2(\mu\text{-}H_2O)]_n$ (**34**) [58], which is stable up to 216 °C, forms a large tetranuclear $(\mu\text{-Htdp})_2(Tl(\mu\text{-}H_2O)Tl)_2$ metallacycle (Fig. 10). This polymer consists of horseshoe-shaped $(\mu\text{-Htdp})Tl(\mu\text{-}H_2O)Tl(\mu\text{-Htdp})$ subunits with **Tl**O_3 coordination sphere. The individual strands of one-dimensional polymer are further interconnected by an extensive network of hydrogen bonds, extending the $[Tl_2(\mu\text{-Htdp})_2(\mu\text{-}H_2O)]_n$ chains to infinite two-dimensional supramolecular sheets. In the solid state both ligand H_2tdp and **32** have fluorescence emission with a band at 475 and 465 nm upon excitation at 300 nm, respectively.

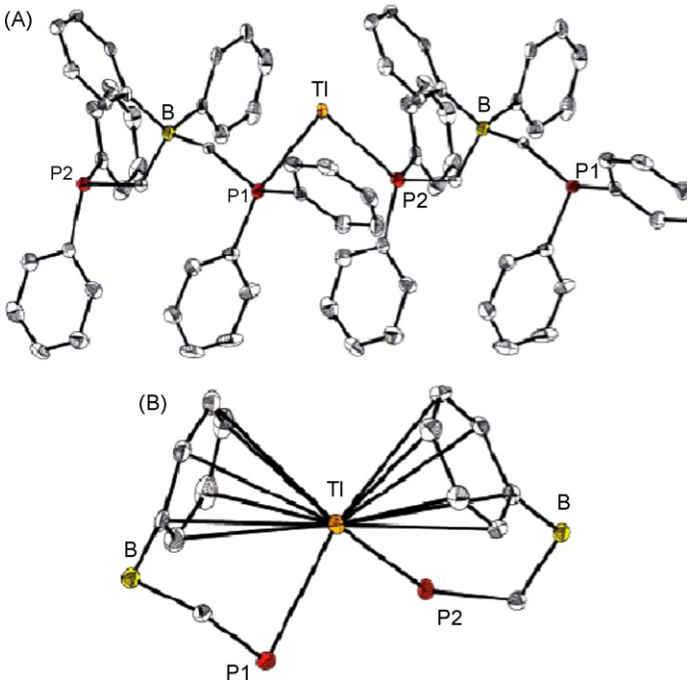

Fig. 9. (a) A 50% displacement ellipsoid representation of $\{[Ph_2B(CH_2PPh_2)_2][Tl]\}_n$ (**27**) [52], hydrogen atoms are omitted for clarity. (b) Expanded view of the thallium coordination sphere.
Reproduced with permission of American Chemical Society.

Tl[trans-Ru(DMeOPrPE)$_2$Cl$_2$]PF_6 (**35**) [33] is a 1D coordination polymer in which the Tl(I) centers have an unusual slightly distorted octahedral **Tl**O_4Cl_2 coordination geometry with a stereochemically active $6s^2$ lone pair (Fig. 11). The formation of product **35** is solvent and temperature dependent.

Complex Tl(18-crown-6)[H{ONC(CN)C(O)C_6H_5}$_2$] (**36**) [59] exists as a hybrid coordination/H-bonded one-dimensional polymer (Fig. 12a) with eight-coordinate thallium. The polymeric chain can be formally described to consist of macrocyclic cations Tl(18-crown-6), oximate anions $(bco)^-$ and oxime molecules H(bco). Complex hydrogen oximate anions $H(bco)_2^-$ that possess a centrosymmetric structure with two (bco) fragments being symmetry equivalents. Compound **36** is illustrated in Fig. 12b.

$TlBp^{3py}$ (**37**) [60] forms a one-dimensional polymeric chain (Fig. 13a) and crystallizes in a centrosymmetric space group, implying that the crystal contains equal numbers of chains of either helicity. Each Tl(I) center in **37** is in a pyramidal three-coordinate environment with **Tl**N_3 coordination sphere, arising from the two chelating pyrazolyl donors from one ligand and a 3-pyridyl donor from an adjacent complex unit. $TlBp^{4py}$ (**38**) [60,61] forms one-dimensional chiral helical chains (Fig. 13b) with similar connectivity to that of **37**. The chiral space group indicates that each crystal only containing helical chains which all have the same chirality. The structure of $TlTp^{4py}$ (**39**) [60,61] reveals a chiral one-dimensional polymeric chain results by virtue of a bridging

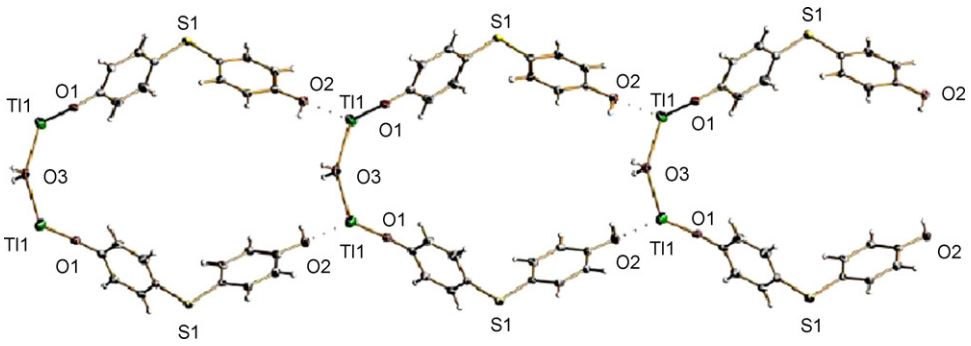

Fig. 10. Schematic representation of the one-dimensional chains in $[Tl_2(\mu\text{-Htdp})_2(\mu\text{-}H_2O)]_n$ (**34**) [58].
Reproduced with permission of Elsevier.

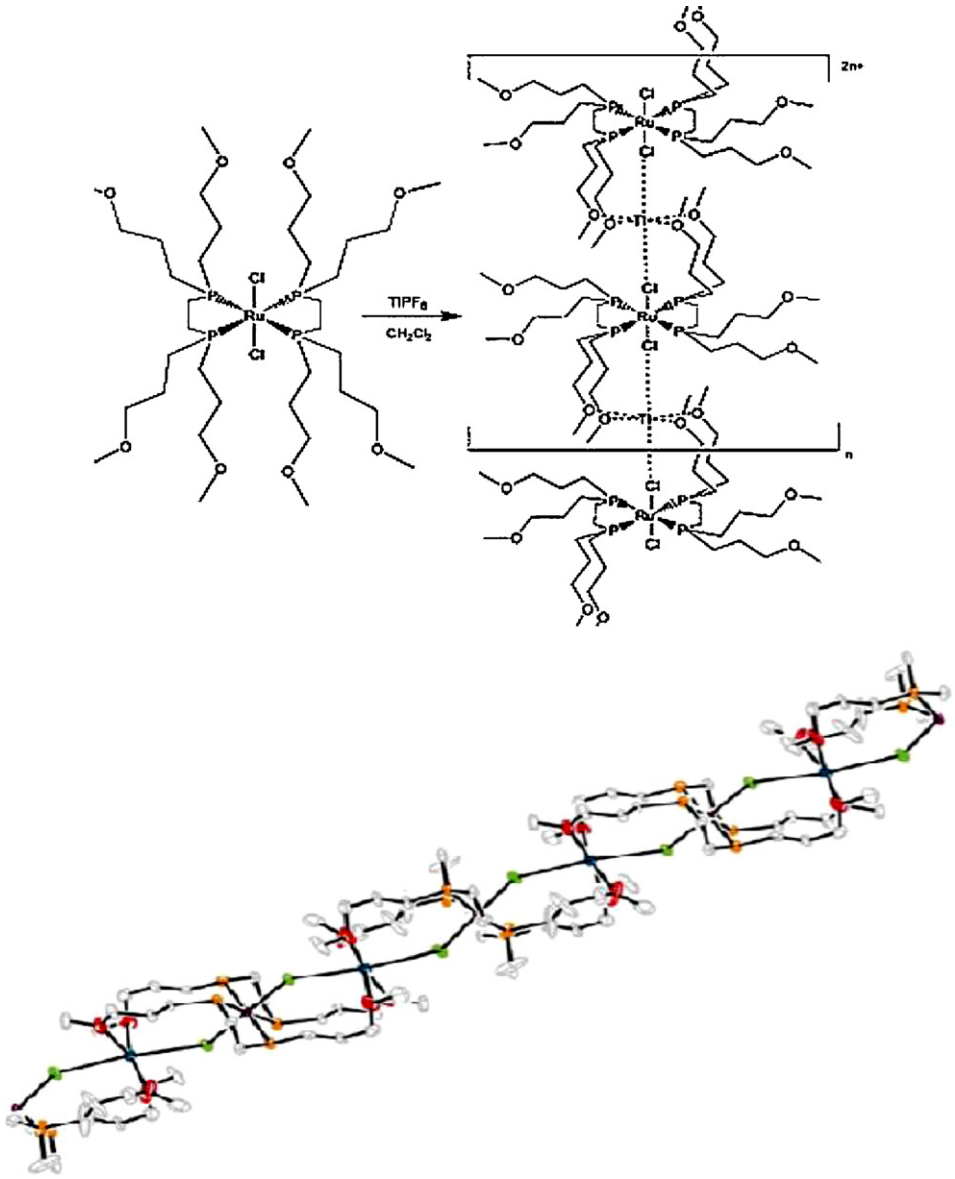

Fig. 11. Schematic representation of $Tl[trans\text{-}Ru(DMeOPrPE)_2Cl_2]PF_6$ (**35**) [33] formation and thermal ellipsoid plot of a fragment of **1** (50% probability level); O (red), Cl (green), C (gray), Ru (maroon), Tl (blue). Hydrogen atoms, PF^{6-} anions and non-coordinated methoxypropyl groups have been removed for clarity. (For interpretation of the references to color in this figure legend, the reader is referred to the web version of the article.)
Reproduced with permission of The Royal Society of Chemistry.

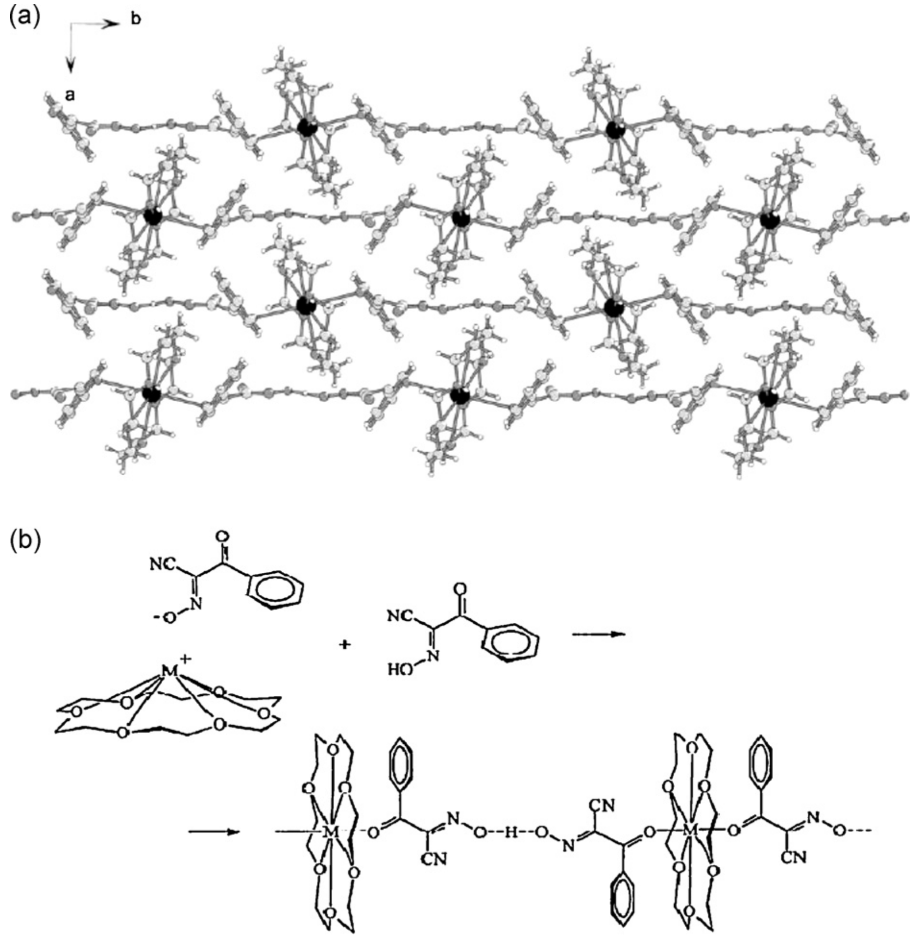

Fig. 12. (a) View of one-dimensional polymeric structure of Tl(18-crown-6)[H{ONC(CN)C(O)C_6H_5}$_2$] (**36**) [59]. (b) Schematic representation of compound **36** formation with M = Tl^+.
Reproduced with permission of Elsevier.

interaction between a pendant 4-pyridyl donor on one complex unit and the Tl(I) center of another. In the structure of Tl[MeB(3,5-$Me_2pz)_3$] (**40**) [62] the bridging action of the ligand between two thallium atoms leads to a 2_1-helicoidal chain and in CymB$(pz)_3$Tl (**41**) [63] each ligand binds to one Tl(I) ion in an η^2 fashion. In **40** and **41** one thallium atom is coordinated by two pyrazolyl rings and the third pyrazolyl ring binds the adjacent symmetry-related thallium center in a monodentate fashion, finally forming a **Tl**N_3 coordination sphere. Bulky substituents attached to the boron center apparently disfavor a η^3 binding mode of the scorpionate ligand, probably due to steric congestion. ^{1}H and ^{13}C NMR signal patterns observed for **41** suggest that oligomeric structures are restricted to the solid state, while monomeric thallium scorpionates are formed when **41** is dissolved in benzene or DMSO. 1H-Tl (**42**) [64] form 1D polymeric rods with **Tl**N_3 coordination sphere. Steric congestion due to a ferrocene substituent at boron facilitates the formation of **42** as a coordination polymer.

The compound [TlL^1]·MeOH (**43**) [65] is a one-dimensional helical polymer of TlL^1 units (Fig. 14), with each ligand bridging two metals and each Tl ion in a '2 + 3' coordination geometry with two short and three longer, weak bonds to ligand. A combination of interstrand aromatic π-stacking interactions, inter- and intrastrand hydrogen bonding interactions involving the lattice MeOH molecule, stabilized the structure of **43** in the crystal packing.

In TlL^{12} (**44**) [12], the coordination environment of Tl^I ion is square pyramidal with the lone pair electrons oriented in the axial direction. In this complex, each malonohydroxamate ligand acts as a bridge between two thallium centers to generate a 1D polymer and these polymers are further interlinked by hydrogen bonds to form a three-dimensional supramolecular compound. [Tl([24]aneS_8)]PF_6 (**45**) [66] adopts a polymeric structure in which each Tl^I bridges two thioether crowns to give an infinite sinusoidal chain. The [S_4 + S_4] coordination sphere at the metal center is satisfied by two half ligands in a sandwich arrangement. Overall [4 + 4] thioether coordination at each metal center results with two Tl–S bond distances, lying within the sum of the formal ionic radii of S and Tl^I suggesting a substantial covalency. The two other Tl–S distances are rather longer. In TlL^{13} (**46**) [67], Tl($C_{12}H_{15}N_2OSe$) units exist in a dimeric form and the two complex molecules are connected by Tl–Se bonds to form a planar four-membered ring with **Tl**OSe_3 coordination sphere. The considerably bent chelate rings are nearly at right angles to the central four-membered rings; finally form a 1D coordination polymer.

2.3. Two-dimensional coordination polymers with secondary interactions in Tl^I coordination sphere

[Tl(salicylate)]$_n$ (**47**) [8], *catena*-[μ_4-(3,4-dimethoxybenzoato) thallium(I)] (**48**) [35], [Tl_3(μ-BPC)$_2$(μ-NO_3)]$_n$ (**49**) [68] and [Tl(L^{14})]$_n$ (**50**) [69,94], all form 2D polymeric compounds with carboxylate donor atoms and Tl···C interactions. The coordination number of the Tl^I ion in compound **47** is four with the coordination environment of **Tl**O_4 (Fig. 15). It appears that the Tl atom in compound **47** may also be involved in an η^6 interaction with

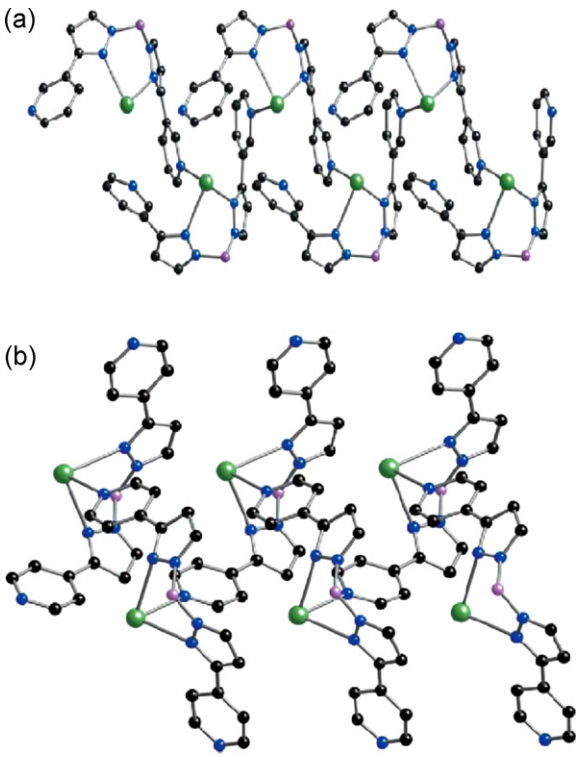

Fig. 13. Views of the one-dimensional chain formed by bridging (a) 3-pyridyl interactions in [Tl(Bp^{3py})] (**37**) [60] and 4-pyridyl interactions in (b) [Tl(Bp^{4py})] (**38**) [60] [Tl, green; B, purple; N, blue; C, black]. (For interpretation of the references to color in this figure legend, the reader is referred to the web version of the article.) Reproduced with permission of The Royal Society of Chemistry.

the Tl···$\pi_{(centroid)}$ distance of 3.541 Å, giving a total hapticity of ten with the coordination environment of O_4**Tl**···C_6. Crystal structure of **48** is based on dimeric $Tl_2(C_7H_6NO_3)_2$ units, each dimeric unit is extensively cross-linked to adjacent units resulting in infinite two-dimensional, puckered sheets. Tl^+ ion is coordinated on one side to five oxygen atoms of four carboxylic groups. In this case the other side is also completely naked due to the stereoactive lone pair and has a short contact with the aromatic phenyl ring (Tl···$\pi_{(centroid)}$ = 3.47 Å). In **49** there are three types of Tl^I ions with coordination numbers of 5 (Tl1 and Tl2), and 4 (Tl3). Two of the thallium atoms, Tl1 and Tl3, contain close Tl···C contacts with a Tl···$\pi_{(centroid)}$ separation of 3.43 (Tl1) and 3.32 Å (Tl3), thus attaining a total hapticity of 11 and 10 with coordination environments of O_5**Tl1**···C_6 and O_4**Tl3**···C_6, respectively. It appears that in **49**, there are thallophilic interactions between Tl1···Tl2 and Tl2···Tl3 too. Compound **50** is based on dimeric, non-centrosymmetric $Tl_2(L^{14})_2$ units without μ_2-bridging carboxylic groups. In bis [Tl(L^{14})] (**50**) with **Tl**O_5 coordination sphere, adjacent units are held together by secondary Tl–(phenyl) π interactions (with Tl···$\pi_{(centroid)}$ distance of 3.22 Å) resulting in a crystal organization which can be described as half sandwich, infinite two-dimensional polymer. The pseudocyclic conformation is stabilized by hydrogen bonds, with most of the polar oxygen atoms directed inward to capture the metal ion and with all nonpolar groups outward, but in [Tl_2(phthalate)]$_n$ (**51**) [70] and [Tl_2(py-3,5-dc)]$_n$ (**52**) [71] only thallophilic interactions observed. There are six (**Tl1**O_6) and five (**Tl2**O_5) coordinate Tl atoms and some "weak" Tl···Tl bonds in the polymeric state of **51** and the exact distances are Tl1–Tl2 ($x-1$, y, z) = 3.8572(8) Å. In **51** also there is a π–π-stacking interaction between the parallel aromatic rings of adjacent chains. Compound **52** which is stable up to 330 °C has six (**Tl**O_5N) coordinate Tl atoms with some "weak" Tl···Tl interactions in the polymeric state and the exact distances are Tl(1)–Tl(1I) = 3.5563(8) Å, Tl(1)–Tl(1I) = 3.6849(8) Å and Tl(1)–Tl(1II) = 3.8188(8) Å. The ligand and compound **52** show fluorescent emission in the solid state. λ_{max} emission bands of the ligand and compound **52** in the solid states are the same and equal to 465 nm upon excitation at 300 nm.

Fig. 15. A view of 2D coordination polymer in [Tl(salicylate)]$_n$ (**47**) [8].

In 2D coordination polymer of Tl(*m*-Nbs) (**53**) [72], both Tl(I) cation and the sulfonate group display high coordinating ability: one thallium(I) cation is surrounded by nine oxygen atoms and one sulfonate anion is coordinated to six different thallium(I) cations. The Tl/O distances are at long end of the range for Tl(I)–O distances, suggesting a predominantly ionic character for metal–ligand bonding in this complex. This might be interpreted as an indication that

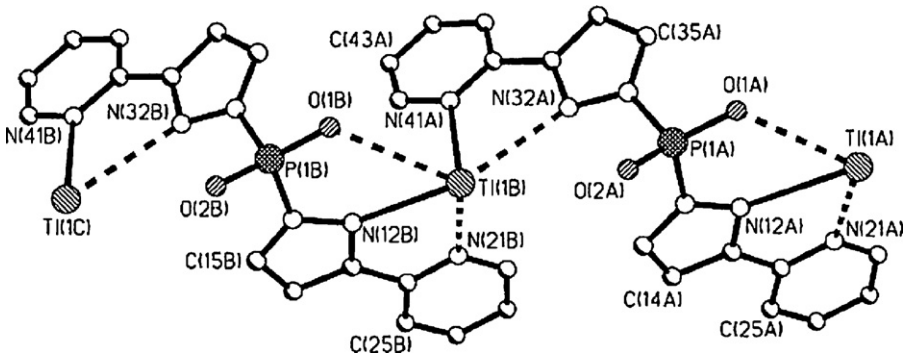

Fig. 14. Crystal structure of the one-dimensional helical chain of [TlL^1]·MeOH (**43**) [65]. Reproduced with permission of The Royal Society of Chemistry.

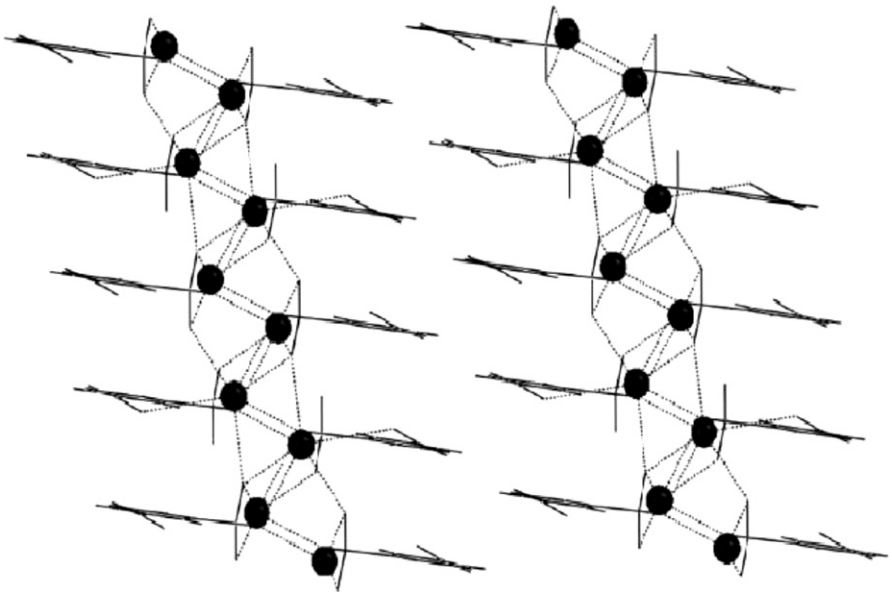

Fig. 16. Packing diagram of Tl(*m*-Nbs) (**53**) [72], as viewed along the *y*-axis, of the stacked *m*-nitrobenzenesulfonate anions arranged in columns along the *z*-axis. The thallium cations reside in between pairs of columns that have their sulfonate groups directed inwards.
Reproduced with permission of Elsevier.

the $6s^2$ lone pair of thallium ion is not stereochemically active. The crystal structure can be viewed as consisting of inorganic and organic layers (Fig. 16). The organic layers are formed by *m*-Nbs^- anions arranged in columnar stacks along the *z*-axis. The sulfonate groups are situated outside these layers and directed towards the inorganic layers within which they interact with the Tl^+ cations. Besides the ionic and stacking interactions, the packing is stabilized by the C–H/O hydrogen bonds. A relatively short contact between Tl(I) cation and aromatic proton H(2) equal to 3.05 Å and thalophilic interactions at a distance of 3.857(1) Å also deserves attention, resulting in O_9**Tl**···TlH coordination sphere.

In Tl(Ohyo) (**54**) [12], the coordination polyhedron around the Tl^I can be described as a distorted dodecahedron; the eight Tl–O bonds are divided into sets of six short and two long, the latter lying at one side of the Tl^I ion which show the lone pair electrons are stereoactive. The oxalohydroxamate groups comprise a hydrogen-bonded, two-dimensional ligand layer; layers of this type are, in turn, interlinked by the aforementioned strong hydrogen bonds to form a three-dimensional supramolecular network.

The main structural unit of the polynuclear thallium complex with dialkyldithiocarbamates is the centrosymmetric binuclear molecule $Tl_2\{S_2CN(CH_2)_6\}_2]_n$ (**55**) [73] (Tl···Tl 3.6776 Å) involving two bridging ligands. Both thallium atom simultaneously coordinate all four S atoms of two dithio ligands. The geometry of the dimer can be represented by a tetragonal bipyramid with four equatorial S atoms and the thallium atoms as its vertices. The geometry of the seven-membered heterocyclic fragments $–N(CH_2)_6–$ can be approximately represented as a "twist chair". The complexing metal in structure **55** becomes coordinatively saturated via additional coordination of the S atoms of adjacent dimeric molecules. Thus, each binuclear fragment is united with two neighbors through pairs of additional Tl–S bonds and the resulting zigzag polymer chain is aligned with the crystallogaphic *z*-axis. In turn, polymer chains are united into a layer through additional coordination by each Tl atom and an S atom in an adjacent chain. The distance between the closest Tl atoms in adjacent chains is 3.7264 Å. The thallium atom has two agostic interactions with two hydrogen atoms too, thus attaining the total coordination sphere of S_6**Tl**···H_2Tl_2.

In [Tl(Tp^{3py})] (**56**) [60], the monomer units are associated into two-dimensional sheets (Fig. 17a). Pairs of pyrazolyl–pyridine units oriented in opposite directions are associated by π-stacking. Each metal center accordingly has rather irregular coordination geometry with two relatively short Tl–N contacts to two of the pyrazolyl ligands, and four much longer ones, to the third pyrazolyl ring and the three bridging pyridyl ligands lead to N_2**Tl**···N_4 coordination sphere for Tl^I ion. It is noticeable that the six Tl–N bonds do not define anything like an octahedral geometry, but that there is a large gap in the coordination sphere of Tl(I) consistent with the lone pair retaining some stereochemical activity. In [Tl(Tkp^{3py})]·H_2O (**57**) [60] and [Tl(Tkp^{4py})]·2MeOH (**58**) [60] the Tl^I ion is coordinated by two or three of the four pyrazolyl arms with N_3**Tl**···N_4 and N_2**Tl**···N_3 coordination sphere, respectively; bridging interactions of pendant 4-pyridyl groups with adjacent Tl(I) centers result in a two-dimensional sheet forming in each case. In **57** a third pyrazolyl group lies approximately 'face-on' to the Tl atom. The fourth pyrazolyl group of $(Tkp^{3py})^-$ is uncoordinated. Three of the pyridyl groups also interact with adjoining Tl atoms. Thus Tl(I) is nominally seven coordinate, if we count the side-on N–N bond as two donors. The two stronger Tl–N(pyridyl) interactions connect the complexes into a 1D ladder-like motif. The weaker Tl–N(pyridyl) interactions then cross-link the ladders into 2D sheets (Fig. 17b). In **58** the fourth pyrazolyl is uncoordinated. In addition, two of the pyridyl groups coordinate to adjacent Tl(I) atoms. Thus each Tl(I) atom is five coordinate, with distorted square pyramidal geometry; the lone pair on the metal again appears to be stereochemically active. The coordinating pyridyl groups link the complexes into 2D (4,4) sheets, as shown in Fig. 17c. These sheets are chiral, (as indicated by the space group). The uncoordinated pyridyl groups hydrogen bond to methanol molecules are intercalated between the sheets.

2.4. Two-dimensional coordination polymers without secondary interactions in Tl^I coordination sphere

{[Tl(L^2)(HL^2)](H_2O)$_{0.77}$}$_n$ (**59**) [74] which melts at 162 °C, is the first thallium(I) coordination polymer with a Schiff base ligand forming 2D network with the thallium atom weakly coordinated to seven oxygen atoms of the L^- and HL ligands. The Tl^I coordination sphere is holodirected with no observed gap in the coordina-

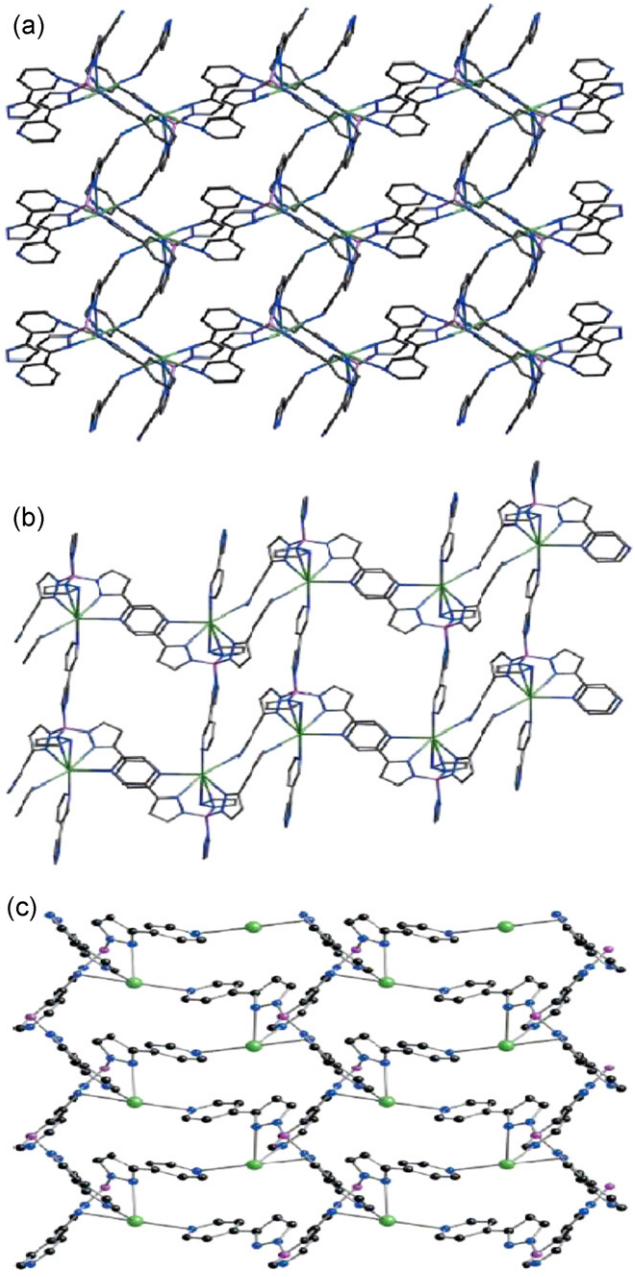

Fig. 17. Views of the two-dimensional sheet formed by bridging (a) 3-pyridyl interactions in [Tl(Tp^{3py})] (**56**) [60], (b) 4-pyridyl interactions in [Tl(Tkp^{3py})]·H_2O (**57**) and (c) 4-pyridyl interactions in [Tl(Tkp^{4py})]·2MeOH (**58**), only the two bridging pyrazolyl-pyridine arms are shown for each ligand; the arms where the 4-pyridyl group is not coordinated are not shown for clarity [Tl, green; B, purple; N, blue; C, black]. (For interpretation of the references to color in this figure legend, the reader is referred to the web version of the article.)
Reproduced with permission of The Royal Society of Chemistry.

tion sphere and inactivity of $6s^2$ lone pair of Tl^I ion is obvious. The individual layers of the two-dimensional polymer are further interconnected by an extensive network of hydrogen bonds extending compound **59** layers to an infinite three-dimensional supramolecular network. [Tl(μ-DNB)]$_n$ (**60**) [75] is a novel two-dimensional polymer with eight-coordinate Tl atoms. Each DNB^- anion is octadentate connecting eight Tl^I ions. The carboxylate group of the DNB^- ligand is both bidentate chelating, and bridging. One of the nitro groups of this ligand has chelating and the other nitro group has only bridging coordination behavior. Structural determination of {Tl[(H)phthalate)]}$_n$ (**61**) [8,76] shows the

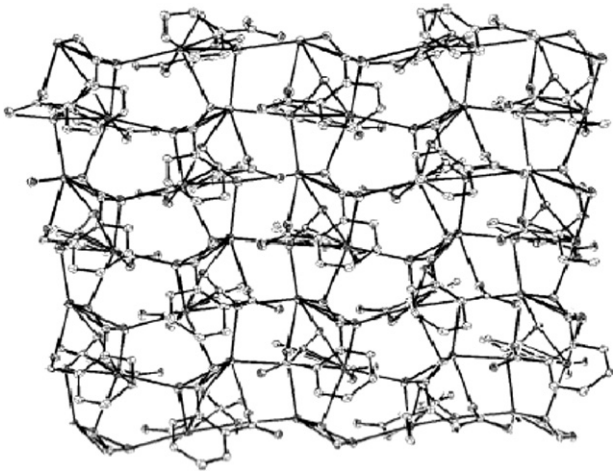

Fig. 18. A view of two-dimensional coordination polymer in {Tl[(H)phthalate)]}$_n$ (**61**) [8].

formation of two-dimensional coordination polymer (Fig. 18). The coordination number of the Tl^I ion is six with the coordination environment of **Tl**O_6. The arrangement of the O atoms suggests a gap in the coordination geometry around the thallium atom in compound **61**, due to a stereochemically 'active' electron lone pair of Tl^I.

In Tl[B(Im)$_4$] (**62**) [77] and Tl[B(4-MeIm)$_4$] (**63**) [77], the thallium borate units form two-dimensional layers, with the metal sites facing the interlayer spacing. In both compounds Tl^I ion has **Tl**N_4 coordination sphere and one of these coordination bonds is longer than 2.7 Å. The arrangement of the N atoms suggests a gap in the coordination geometry around the thallium atom, due to a stereochemically 'active' electron lone pair of Tl^I. [Cu(pyn-2-ol)$_2$]$_n$.[Tl(NO_3)$_m$]$_{n/2}$ (**64**) [78], forms a two-dimensional coordination polymer with four-coordinated Tl^+ ion, being bound to only the four exocyclic oxygen atoms of a metallacalix[4]arene moiety. Due to "stereochemical activity" of Tl^I lone pair, nitrate ions does not increase its coordination number (Fig. 19).

The layer structure of Tl_2[Ag{N(SO_2Me)$_2$}$_3$] (**65**) [79], displays two unprecedented characteristics; one $(MeSO_2)_2N^-$ ion that strongly deviates from the C_2-symmetric standard conformation of this species and approximates to mirror symmetry and a tris(dimesylamido)argentate anion featuring a trigonal planar AgN_3 core. The independent thallium ions are coordinated by the

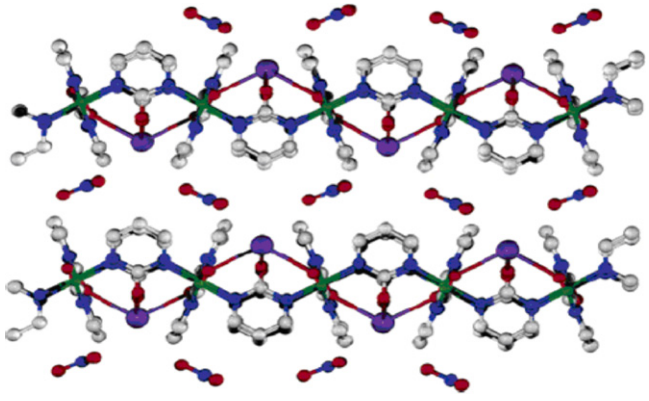

Fig. 19. Representation, down [001], of the crystal packing in [Cu(pyn-2-ol)$_2$]$_n$.[Tl(NO_3)$_m$]$_{n/2}$ (**64**) [78] shows two layers. For the sake of clarity granting ordered nitrate ions, hydrogen atoms and methanol molecules have been omitted (carbon, gray; nitrogen, blue; oxygen, red; copper, green; thallium, violet). (For interpretation of the references to color in this figure legend, the reader is referred to the web version of the article.)
Reproduced with permission of American Chemical Society.

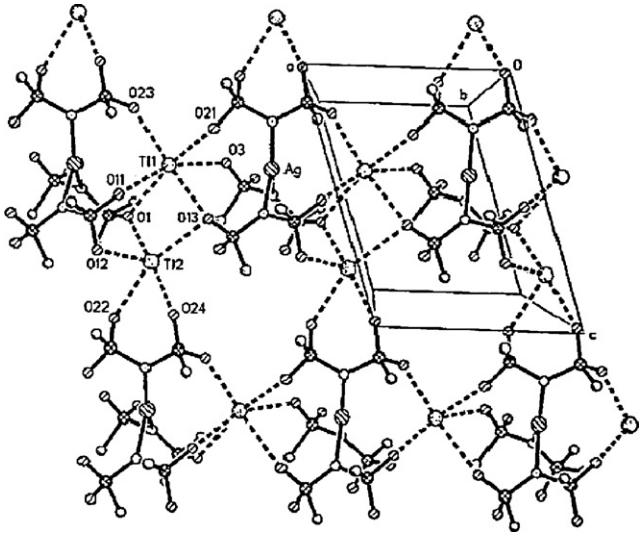

Fig. 20. Portion of 2D polymeric sheets in $Tl_2[Ag\{N(SO_2Me)_2\}_3]$ (**65**) [79].
Reproduced with permission of Wiley-VCH Verlag GmbH & Co. KGaA.

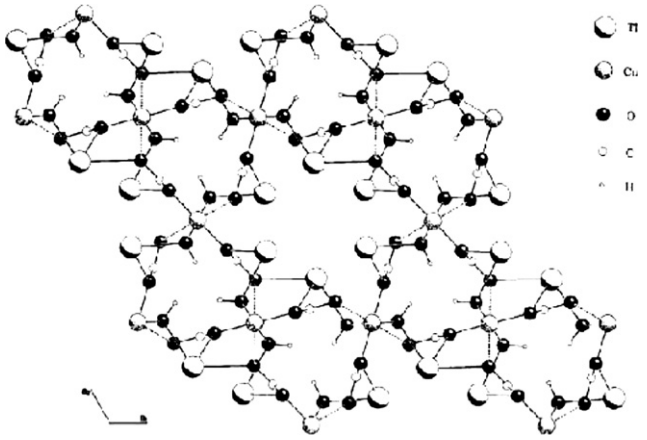

Fig. 21. Representation, down [0 0 1], of the crystal packing in $TlCu(OH)CO_3$ (**74**) [86].
Reproduced with permission of Wiley-VCH Verlag GmbH & Co. KGaA.

complex anions to form monolayer substructures, in which Tl(I) attains an O_6 and Tl(2) an O_5 environment; the monolayers are associated into bilayers via one independent set of Tl(2)–O bonds that concomitantly raise the coordination number for Tl(2) to six (Fig. 20). The two-dimensional Ag–N/Tl–O bonding system is reinforced by a three-dimensional network of weak C–H···O hydrogen bonds.

2.5. Three-dimensional coordination polymers with secondary interactions in Tl^I coordination sphere

$[Tl_2(\mu_9\text{-ADC})]_n$ (**66**) [80,81], is a 3D coordination polymer which is stable up to 430 °C. In **66** there are two types of Tl^+-ions with coordination numbers of six **Tl1**O_6 and five **Tl2**O_5. The Tl1 and Tl2 atoms in **66** interact with one neighboring thallium atom. Tl2 in **66** may also be involved in an η^2 interaction with acetylene of neighboring molecules. Thus, the Tl2 atoms in **66** are linked to two carbon atoms of neighboring acetylene groups, with distances of 3.398(2) and 3.628(5) Å, respectively. Hence, the Tl^I coordination sphere could be considered as Tl···**Tl1**O_6 and C_2Tl···**Tl2**O_5 with the stereochemically 'active' lone pair in the solid state. $Tl_4(ADC)(oxa)$ (**67**) [80] is stable up to 150 °C. In **67**, Tl1 and Tl2 are 5-coordinate. Again a search for Tl···C and Tl···Tl interactions shows that in addition of thallophilic interactions in **67**, Tl1 ion has a short distance (3.628 Å) with one of the ADC^{2-} carbon atoms resulting in 3D coordination polymer with O_5**Tl1**···Tl_2C and O_5**Tl2**···Tl_2 coordination sphere. $Tl_4(ADC)(oxa)$ can be synthesized without adding oxalic acid. Thus H_2ADC has been oxidized under very mild reaction conditions to form oxalic acid. Compounds **66** and **67** crystallize in non-centrosymmetric space groups. This is probably caused by the influence of stereochemically active lone pairs at Tl(I). Thallium(I) ion in $Tl^I_2(oxa)$ (**68**) [82] has an O_7**Tl**···Tl_3 environment with an irregular coordination and a lone pair which clearly squeezes the T–O bonds in the polyhedron. $[K_2Tl(\mu\text{-succinate})(\mu\text{-}NO_3)]_n$ (**69**) [83] with mixes succinate and nitrate ligands, shows two types of K^+-ions with coordination numbers of seven and eight and one Tl^+-ion with a coordination number of five. Two hydrogen atoms of succinate situated 3.26 Å above the proposed site on the lone pair of Tl^I is oriented in such a way that it might be forming a weak Tl–Lp···H–C hydrogen bond or agostic interaction, thus attaining a coordination environment of O_5Tl···H_2. In $[Tl_3(\mu\text{-1,2,3-btc})]_n$ (**70**) [37] it appears that there are three types of Tl^+-ions (Tl1, Tl2 and Tl3), two of them contain the weak Tl···Tl interactions with distances of 3.771 and 3.972 Å. The Tl1 in compound **70** is linked to two carbon atoms of neighboring phenyl group, with distances Tl1···C15^i and Tl1···C6^i (i: $-x$, $y+1/2$, $-z+1/2$) of 3.408(2), and 3.430(2) Å, respectively. Thus the thallium(I) ions in **70** attaining the total coordination sphere of O_5**Tl1**···C_2, O_4**Tl2**···Tl_2 and O_6**Tl3**···Tl_2. In $[Tl_4(\mu\text{-1,2,4,5-btc})]_n$ (**71**) [37], there are two types of Tl^+-ions, Tl1 and Tl2. A search for Tl···H interactions shows that Tl atoms in compound **71** may also be involved in an additional interaction with two H atoms of 1,2,4,5-btc^{4-} anion with distance Tl1···H5^i (i: $-x$, $y+1/2$, $-z+1/2$) = 3.05 Å. Thus the thallium(I) ions in **71** attaining the total coordination sphere of O_5**Tl1**···H_2 and **Tl2**O_6. Compounds **70** and **71** are stable up to 350 and 300 °C, respectively and do not show emission upon excitation at 350 nm in solution state. $\{(eda)[Tl_2(\mu\text{-1,2,4,5-btc})(H_2O)_2)]\}_n$ (**72**) [84] is another coordination polymer of Tl^I ion with 1,2,4,5-btc ligand, the Tl^I atom is seven coordinated by three 1,2,4,5-btc ligands and two water molecules in an irregular geometry due to the stereochemically active lone pair on the Tl center. The water molecule and 1,2,4,5-btc ligand are bonded to the Tl atoms in μ- and μ_6-forms, respectively, leading to a three-dimensional structure. The crystal structure involves O–H···O, N–H···O and C–H···O hydrogen bonds, and also a Tl···π interaction at a Tl-centroid distance of 3.537(1) Å, resulting in O_7**Tl**···C_6 coordination sphere. Compound $[(Tl(pydcH)]_n$ (**73**) [85], has only one type of Tl^+-ion with coordination number seven, but with long Tl–N and Tl–O bond distances indicating that these bonds are not strong chemical bonds. The Tl^I ion has a short distance with aromatic pyridine ring with Tl···$\pi_{(centroid)}$ distance of 3.535 Å. Thus compound **73** could be considered as 3D coordination polymer with NO_6**Tl**···C_5N coordination sphere. $TlCu(OH)CO_3$ (**74**) [86] which is prepared from carbonate solutions, is stable up to 160 °C and decomposition occurs in two steps to the products Tl_2O and CuO. The Structural features are Cu–O chains bridged by carbonate groups and tunnels parallel [0 0 1] (Fig. 21), our studies illustrate that Tl^I ion has O_4**Tl**···O_3H coordination sphere with a short Tl···H distance that could be considered as agostic, finally resulting in a 3D coordination polymer. The magnetic measurements show Curie-paramagnetism with θ_{Curie} = 2.7 K. A ferromagnetic arrangement of the Cu^{2+}-moments was detected below 4.8 K.

Although Tl(4-np) (**75**) [38] and [Tl(2,4-dnp)] (**76**) [39] have approximately similar ligands, they show different structural motifs. The structure of **75** is based on a tetranuclear cubane motif with **Tl**O_3 coordination sphere. Tl···Tl interactions within the cube are 3.858(2) Å and [Tl(*O*-phenoxide)]$_4$ units linked into a three-dimensional network by further Tl···O–nitro interactions from adjacent units. The crystal structure of **76** shows a three-

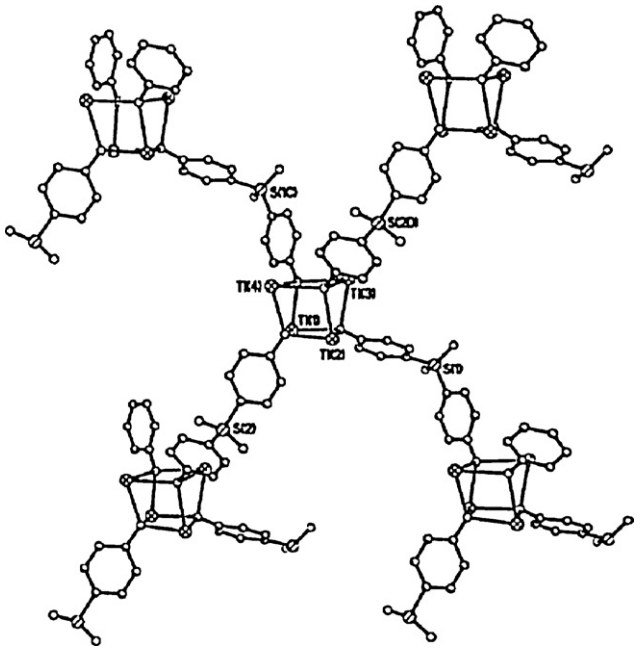

Fig. 22. Fragment of the three-dimensional coordination polymer in $[Tl_4(\mu_8\text{-}SB)_2]_n$ (**77**) [87].
Reproduced with permission of Elsevier.

dimensional polymer as a result of bridging 2,4-dnp ligands. In **76**, the Tl atoms have **Tl**O_2 coordination sphere with weak thallophilic interactions (3.740 Å), π–π-stacking interactions between the parallel aromatic rings also exist. $[Tl_4(\mu_8\text{-}SB)_2]_n$ (**77**) [87], another compound with phenolic group, is a novel three-dimensional coordination polymer involving the tetranuclear cubic cage nodes as a result of bridging "SB_2^{-}" ligands with basic repeating $[Tl_4(\mu_8\text{-}SB)_2]$ units (Fig. 22). There are four thallium atoms with different coordination spheres (**Tl1**O_4, O_4**Tl2**···Tl_2, O_4**Tl3**···Tl and O_3**Tl4**···Tl) in the cubic cage. These thallium atoms contain an irregular coordination sphere with stereochemically active lone pair and thallium–thallium interactions.

2.6. Three-dimensional coordination polymers without secondary interactions in Tl^{I} coordination sphere

CSB^{2-} ligand in compound $[Tl_2(\mu_{10}\text{-}CSB)]_n$ (**78**) [81] is similar to SB^{2-} in **77** but with caboxylate donor groups instead of phenolate group. Compound **78** is a 3D coordination polymer which is stable up to 410 °C. In **78** the thallium atoms have an irregular coordination sphere containing a stereochemically active lone pair with **Tl**O_5 coordination environment. There are two known forms of [Tl(picrate)] (**79**) [88], showing approximately similar coordination environments for the thallium atoms but the 'high temperature', yellow form has a bond to the phenoxide oxygen atom which is 0.2 Å shorter than the equivalent bond in the 'low temperature', red form. The yellow polymorph of **79** has **Tl**O_9 and the red polymorph of **79** has O_{11}**Tl**···C coordination sphere with Tl···C distance of 3.463 Å, finally resulting in a 3D coordination polymer with inactive lone pair in both polymorphs. Transition from the red to the yellow polymorph occurs in the solid state only at 400 K and above, but the yellow polymorph does not transform to red, neither on heating nor on cooling. Addition of a small amount of solvent to the system accelerates the transformations in both directions.

TlL^8 (**80**) [55] form an extended 3D coordination polymer with N_3**Tl**···N_3 coordination sphere around Tl^{I} ion. $[2,5\text{-DMe-DCNQI}]_2Tl$ (**81**) [10], is a 3D coordination polymer with **Tl**N_8 coordination sphere and inactive $6s^2$ lone pair of Tl^{I} ion which shows semiconductor-like behavior. The acceptor molecules form a network linked by thallium ions, therefore, one of the two thallium atoms is to be visualized as being above the plane of the diagram while the other is below the plane. More interestingly, **81** is the first non-copper radical anion salt in which a significant Knight shift of the $^{205}Tl^{+}$ nucleus (referenced to $TlNO_3$) has been observed (4200 ppm at 290 K), shows that the s-orbitals of the thallium ion become polarized onto the DCNQI stacks as a result of the mobility of the electron spin.

In $[Tl\{HO_3P(CH_2)_2PO_3H_2\}]$ (**82**) [89], the thallium atoms are coordinated dodecahedrally to oxygen atoms O(1)–O(6) of both diphosphonates. **Tl**O_8 dodecahedra, share O(1)–O(1) and O(6)–O(6) edges to form "**Tl**$O_{6/}$" chains parallel to the *a*-axis; these chains are linked to one another through the O(4) atoms. The diphosphonate is bonded, in a monodentate fashion, to six thallium atoms. Similarly, the thallium atom is bonded to six phosphonate moieties of different diphosphonates resulting in 3D coordination polymer. A network of hydrogen bonds is also present in **82**. $Tl_2(MoO_3)_3PO_3CH_3$ (**83**) [90] which is stable up to 435 °C, is a new layered phase build up from vertex-sharing MoO_6 and PO_3CH_3 units. Interlayer Tl^{+} cations complete the crystal structure with **Tl1**O_6 and **Tl2**O_{12} coordination sphere. The thallium cations serve to link adjacent anionic sheets by way of Tl–O bonds.

In $Tl\{ONC(CN)_2\}$ (**84**) [91], the thallium(I) center has four shorter bonds than the sum of the ionic radii bonds (three with N and one with O atoms) and three longer electrostatic (ionic) contacts with the anion. The $6s^2$ lone pair is stereoactive, and the coordination polyhedron is best described as a distorted square pyramid. The $ONC(CN)_2^{-}$ anion in this complex is planar and in the nitroso form. Compound **84** at 293 K exhibited structured metal-based red photoluminescence in the range of 690–800 nm that depends on the excitation wavelengths. An assignment of a metal-to-ligand charge transfer (MLCT) state from Tl(I) to π^* of the $ONC(CN)_2^{-}$ anion is very likely since thallium is known to form a stable Tl(III) oxidation state. $[T1(SC_6H_5)]$ (**85**) [57], is built up by the two novel structure units; $[Tl_7(SC_6H_5)_6]^{+}$ and $[Tl_5(SC_6H_5)_6]^{-}$ with six different Tl^{I} ions as Tl1, Tl2, Tl5 with **Tl**S_1 coordination sphere, Tl3 and Tl4 with **Tl**S_3 coordination sphere and finally Tl6 with **Tl**S_4 coordination sphere, resulting in a 3D coordination polymer with stereoactive electron lone pair (Fig. 23).

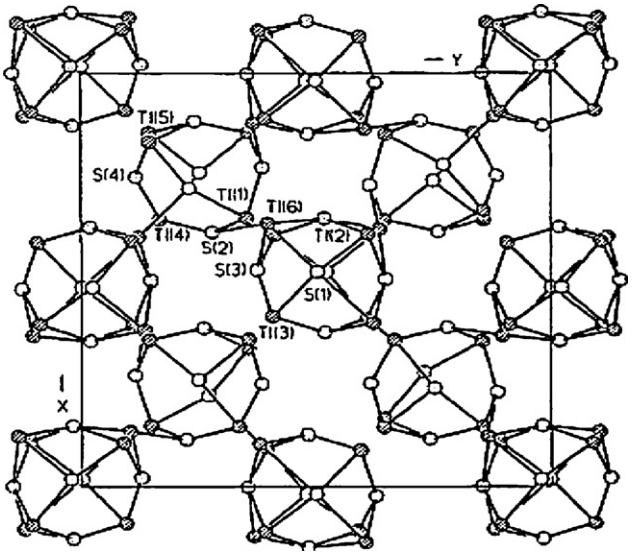

Fig. 23. Representation, down [0 0 1], of the crystal packing in three-dimensional coordination polymer of $[T1(SC_6H_5)]$ (**85**) [57], the phenyl groups have been omitted for clarity.
Reproduced with permission of Wiley-VCH Verlag GmbH & Co. KGaA.

3. Thallium(I) supramolecular compounds aggregate from secondary interactions

The utilization of intermolecular interactions which generate specific supramolecular motifs has greatly enhanced the systematic approach to both the understanding and the design of highly organized molecular arrays in solids. Intermolecular hydrogen bonding has been the most widely employed 'directional forces' in this context. More recently, the attractive interactions between heavy closed shell metal centers (with d^{10} or $d^{10}s^2$ configuration) and the way they affect the intermolecular aggregation in solids have been investigated [92,93]. In addition polyhapto and agostic interactions play important role in formation of Tl^I supramolecular compounds. In Section 2 we considered Tl^I coordination polymers which cover a wide area of supramolecular compounds, in this section we consider Tl^I compounds which aggregate from secondary interactions.

3.1. One-dimensional supramolecular compounds

Thallium(I) 2-amino-benzoate (anthranilate) (**86**) [11], thallium(I) 2-amino-4-methyl-benzoate (**87**) [11], thallium(I) 2-Hydroxy-4-methyl-benzoate (4-methyl-salicylate) (**88**) [11], and thallium(I) 2-hydroxy-3-methyl-benzoate (3-methyl-salicylate) (**89**) [11], all form 1D supramolecular compounds, the first two having Tl···π interactions with the aromatic ring. In **86**, the monomers dimerize to give a four-membered ring. Through stacking of the flat dimers each thallium atom builds contacts with an amino group on one side and an η^6 arene ring on the other with a $Tl\cdots\pi_{(centroid)}$ distance of 3.372(6) Å. The vacancy appears to be finally compensated by inter-string thallophilic contacts, finally lead to $O_3N\mathbf{Tl}\cdots C_6Tl_2$ environment around Tl^I ion. In **87**, both Tl1 and Tl2 are thus tricoordinated by nearest oxygen atoms in steep trigonal pyramids and η^6-capped by one arene group with $Tl\cdots\pi_{(centroid)}$ distance of 3.166(13) and 3.181(15) Å, lead to $O_3\mathbf{Tl}\cdots C_6$ coordination sphere. Pairs of symmetry-related water molecules which are located in the voids between the tetramers in **87**, stabilized the crystalline phase through a set of hydrogen bonds. Compound **88** has tricoordinated Tl^I ion by oxygen atoms and η^6-capped by one arene group with $Tl\cdots\pi_{(centroid)}$ distance of 3.304(8) Å. A longer Tl–O contact also observed, lead to $O_3\mathbf{Tl}\cdots OC_6$ coordination sphere around Tl^I ion. The set of five oxygen atoms covers just about one hemisphere of the thallium environment in **89** and no other contacts are discernible in the other half of the coordination sphere. A hydrogen bond between the hydroxy group and one of the carboxylate oxygen atoms result to 1D supramolecular compound. Another polymorph of compound **50** [94] forms a monomer, $Tl^+(L^{14-})$, where the metal ion is coordinated, on one side, to six oxygen atoms of the anionic ligand. The other side of the metal ion is, however, completely naked. The L^{14} molecule again assumes the pseudocyclic conformation stabilized by three types of hydrogen bonds. The thallium atom in $[Tl(18\text{-crown-6})][H_2N\{B(C_6F_5)_3\}_2]\cdot 2CH_2Cl_2$ (**90**) [95], is bonded to all six crown-ether O atoms and is positioned slightly out of the plane formed by the six oxygen atoms. The coordination sphere is completed by two Tl···F interactions, which lead to 1D supramolecular compound.

Compounds $TlN(Me)Ar^{Mes2}$ (**91**) [96], $HB(pz)_3Tl$ (**92**) [97], [Tl][BQA] (**93**) [98], $CH_2[CH_2N(Tl)SiMe_3]_2$ (**94**) [92], $MeSi[SiMe_2N(T1)Bu^t]_3$ (**95**) [99], $[(C_6H_5)C\{CH_2N(Tl)SiMe_3\}_3]$ (**96**) [100], all form complexes with Tl–N bonds and supramolecular compounds from polyhapto and/or thallophilic interactions. Compound **91** features an apparent Tl-arene interaction with the flanking mesityl substituent [$Tl\cdots\pi_{(centroid)} = 3.026(2)$ Å] in addition to two types of Tl^I ion which are coordinated by one N atom. A longer interaction of 3.569(2) Å to the centroid of an aryl ring of a neighboring molecule and agostic interactions of Tl^I ion with H atom of -CH_3 (Tl1) and arene (Tl2) groups with distances of 3.109 and 3.006 Å respectively, result in a 1D supramolecular compound with $N\mathbf{Tl}\cdots C_{12}H$ coordination sphere. Compound **92** indicates the formation of 1D double strand chain from short contact of Tl^I ion with one of the pyrazolyl ring with $N_3\mathbf{Tl}\cdots C_3N_2$ coordination sphere and $Tl\cdots\pi_{(centroid)}$ distance of 3.512 Å. In **93**, a possible weak π-stacking or Tl–Tl interaction is observable in the zigzag arrangement of extended structure (Fig. 24) with $N_3\mathbf{Tl}\cdots Tl_2$ coordination sphere. Notably, the nearest neighbor Tl cation is located at a distance of 3.5336(5) Å.

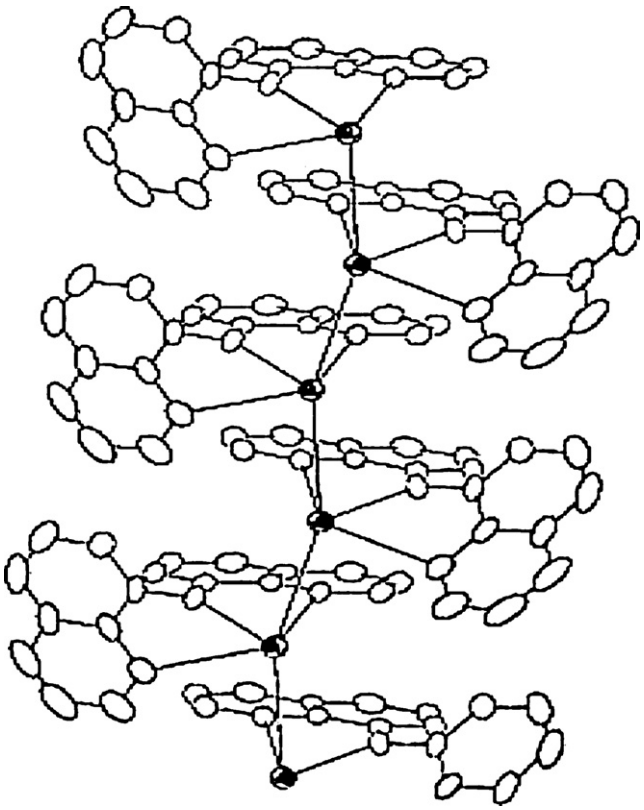

Fig. 24. Displacement ellipsoid (50%) representation of [Tl][BQA] (**93**) [98], extended along the crystallographic *a*-axis.
Reproduced with permission of American Chemical Society.

In the solid the two amido-N atoms and the two Tl^I centers of **94** form a puckered four-membered ring and the molecular units of **94** aggregate via Tl···Tl contacts to form infinite, double-stranded bands. One of the two metal atoms in the monomers not only forms a direct contact to its neighbor within a strand [Tl···Tl 3.775(3) Å] but also across to the opposite strand [Tl···Tl 3.697(3) Å], lead to $N_2\mathbf{Tl1}\cdots Tl_3$ and $N_2\mathbf{Tl2}\cdots Tl_2$ coordination sphere around Tl^I ions. Metal exchange between the lithium amide $MeSi[SiMe_2N\text{-}(Li)Bu^t]_3$ and TlCl (Fig. 25a), yields the corresponding thallium amide **95** which aggregates in the solid through weak attractive Tl···Tl interactions (3.673(2) Å) to form infinite molecular chains (Fig. 25b). Short interamolecular Tl···Tl contacts also exist in **95**, finally result in $N_2\mathbf{Tl}\cdots Tl_2$ environment for three types of Tl^I ions. In **96** there are three types of Tl^I ion with $\mathbf{Tl}N_2$ coordination sphere. Although Tl3 adopts a slightly slipped η^6 coordination of the aryl ring with Tl···C distances lying in the range 3.34–3.74 Å and Tl1 is located close to the ipso and two *ortho* phenyl carbon atoms with Tl···C distances of 2.87, 3.24 and 3.22 Å. In the solid the amidothallium units are dimeric and form infinite chains which are defined by intermolecular Tl···Tl contacts of 3.75 Å. Thus we could consider $N_2\mathbf{Tl}\cdots C_3Tl$ and $N_2\mathbf{Tl}\cdots C_6$ coordination environment for Tl1 and Tl3 respectively.

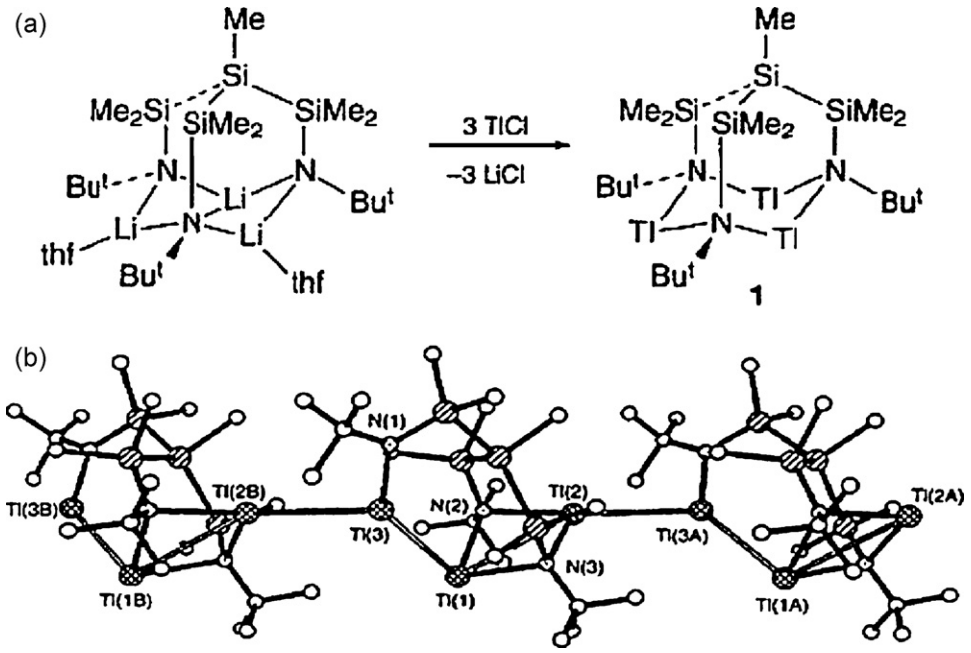

Fig. 25. (a) Schematic representation of $MeSi[SiMe_2N(T1)Bu^t]_3$ (**95**) [99] formation and (b) the polymeric chain viewed onto the *ac* plane. Reproduced with permission of The Royal Society of Chemistry.

[TpTl] (**97**) [55,101], TlL^3 (**98**) [102], TlL^4 (**99**) [103], Tl(TPPB) (**100**) [104], $Tl_2[1,3\text{-}C_6H_4(tBuBpz_2)_2]$ (**101**) [105], $[^tBuN–B^{Ph}–N^tBu]Tl_2$ (**102**) [106], $[^iPrN–B^{Ph}–N^iPr]Tl_2$ (**103**) [106] and $[(m,m\text{-}(CH_3)_2Ph)_2B(CH_2PtBu_2)_2][Tl]$ (**104**) [52], all form 1D supramolecular compounds which we will consider in detail here. Compound **97** forms a double 2_1-helical strand. The molecular structure of **97** shows the usual pyramidal geometry of the thallium atom with two different chain types present in the unit cell and the two crystallographically different Tl centers with $N_3\mathbf{Tl}\cdots C_6N_4$ coordination sphere and $Tl\cdots\pi_{(centroid)}$ distances of 3.555 and 3.748 Å for Tl1 and 3.500 and 3.665 Å for Tl2. Each Tl^I ion in **98** is in a "2 + 2" coordination environment, with two short bonds to the pyrazolyl donors and two longer bonds to the pyridyl donors, therefore each Tl^I ion is in an approximately square pyramidal geometry, with the four nitrogen donor atoms occupying the basal plane and the stereochemically active lone pair occupying the obvious gap in the metal ion coordination sphere at the apex of the pyramid. The molecules lie in a stack along the Tl···Tl axis with secondary $Tl\cdots\pi_{(pyrazolyl)}$ interactions (3.423 and 3.427 Å). In **99** the Tl^I ion is coordinated in the N_4 binding pocket of the ligand and the externally directed N atoms involved only in intermolecular N···H–C hydrogen bonding interactions. Similar to **98**, the two Tl–N bonds to the pyrazolyl N atoms are much shorter than the bonds to the pyrazinyl N atoms. Tl···H–B (3.079 Å) and $Tl\cdots\pi_{pyrazolyl}$ (3.255 Å) interactions in **99** lead to a $N_2\mathbf{Tl}\cdots C_3N_4H$ coordination environment around the Tl^I ion. The Tl^I ion in **100**, is in a '3 + 3' coordination environment, with three short bonds to the pyrazolyl N atoms and three long interactions with the pyridyl N atoms. The relatively open structure of the complex leads to aromatic π-stacking interactions between the pyridyl rings (3.56 Å) of adjacent complex units and three agostic interactions with Tl···H separations of 3.52, 3.35 and 3.36 Å per metal ion (Fig. 26).

Compound **101** is a 1D supramolecular compound with two types of Tl^I ion being coordinated to two pyrazolyl nitrogen atoms of its scorpionate ligand. In **101** each Tl^I ion forms two π-contacts to the two pyrazolyl rings of a neighboring scorpionate ligand with $Tl\cdots\pi_{(centroid)}$ contacts of 3.360 and 3.458 Å for Tl1 and 3.302 and 4.019 Å for Tl2, resulting in $N_2\mathbf{Tl}\cdots C_6N_4$ coordination spheres for Tl^I ions. In compound **102**, the asymmetric unit of the complex possesses a single dithallium unit that has a molecular structure in which two nitrogen and two thallium(I) atoms form a puckered spirocycle. Two types of Tl^I ion in **102** have $N_2\mathbf{Tl1}\cdots Tl_3$ and $N_2\mathbf{Tl2}\cdots Tl_3$ coordination spheres (Fig. 27a). The asymmetric unit in $[^iPrN–B^{Ph}–N\ ^iPr]Tl_2$ (**103**) possesses four dithallium units, all of which possess similar Tl_2N_2 cores and ligand metrics as **102**. Two of these monomeric units aggregate to form an infinite chain of edge sharing triangles with $N_2\mathbf{Tl}\cdots Tl_5$ coordination sphere (Fig. 27b). The other two monomeric units are not involved in aggregation, but instead demonstrate a metal–arene interaction with $N_2\mathbf{Tl}\cdots C_6$ environment. One thallium from each of these units has a contact of 3.496(18) Å from the plane of the phenyl rings of the ligands in the aggregation polymer. The thallium cation in **104** is coordinated by two phosphines and garners additional electron density from the aryl ring of an adjacent arylborate group. In fact there are two Tl^I ions with the same coordination sphere in **104** which is best

Fig. 26. Part of the packing diagram for Tl(TPPB) (**100**) [104] showing two intermolecular interactions: aromatic stacking between pyridyl rings, and Tl···H interactions.
Reproduced with permission of The Royal Society of Chemistry.

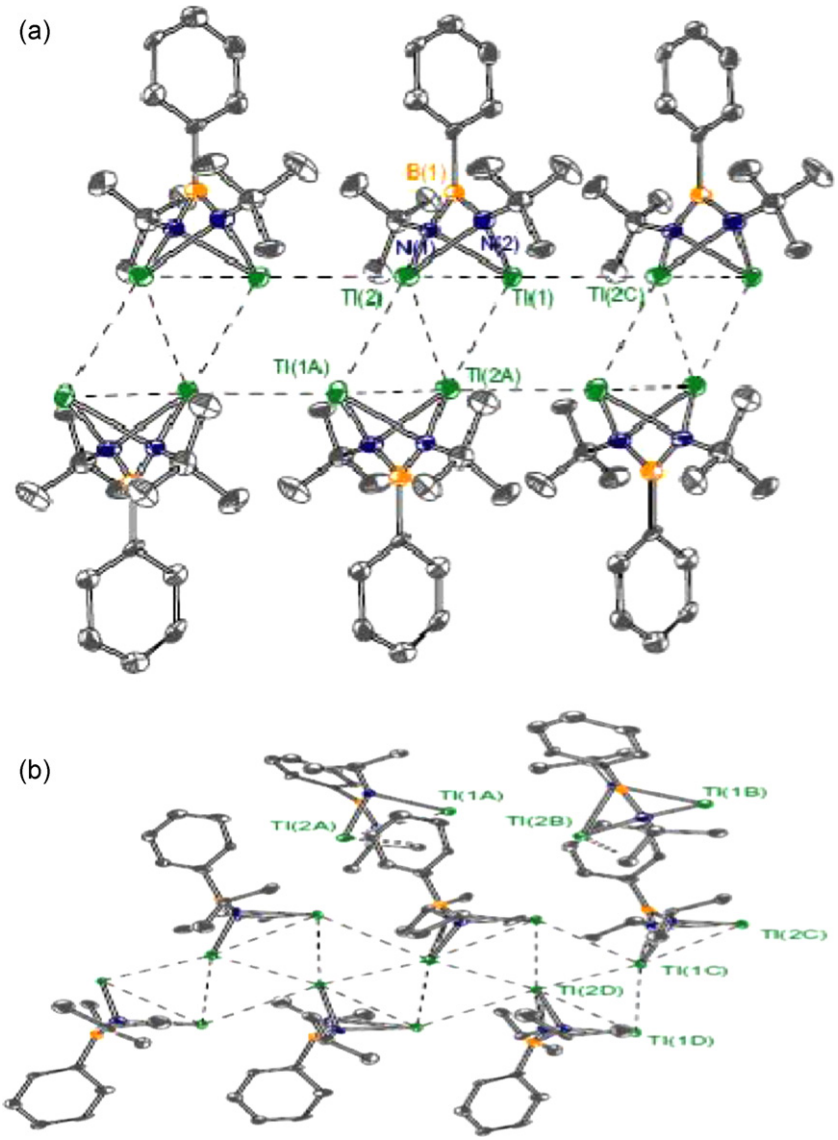

Fig. 27. Solid-state structure of [RN–B^{Ph}–NR]Tl_2 [106] with (a) R = ^{t}Bu (**102**) show casing three dimeric units and weak intermolecular thallium–thallium contacts and (b) R = ^{i}Pr (**103**) demonstrating both thallium–thallium and thallium–arene interactions. Thermal ellipsoids are shown at the 50% probability level.
Reproduced with permission of Elsevier.

described with two phosphine donors and a single η^2–aryl interaction. Tl1···$\pi_{(centroid)}$ and Tl2···$\pi_{(centroid)}$ distances are 3.35 and 3.38 Å, respectively.

In [TlS-t-C_4H_9] (**105**) [57], [NEt_4]$_2$[{Tl(1,2-(μ-S)$_2$$C_6H_4$)}$_2$] (**106**) [107] and Tl_2[Ni(H_2O)$_6$][Ni^{II}(D-pen)(L-pen)]$_2$(Ni^{II}(SCN)$_2$(H_2O)$_4$] (**107**) [108] the donor atom which coordinates to Tl^I ion is sulfur. Compound **105** forms 1D supramolecular network from intermolecular Tl···Tl interactions. In **105** there are four types of Tl^I ions as Tl1, Tl4 with **Tl**S_3 coordination sphere, Tl2 with S_3**Tl**···Tl_2 coordination sphere and Tl3 with S_4**Tl**···Tl coordination spheres. In addition to intermolecular Tl···Tl interactions in **105**, intramolecular thallophilic interactions also observed. Compounds **106** and **107** contain rectangular bipyramidal [TlS_4Tl] cages with the four sulfur atoms defining the equatorial plane and the two thallium atoms in axial positions with the thallium lone pair electrons in the apical vertex. In the crystal lattice of **106**, nearly linear Tl···Tl (3.9371(3) Å) chains align along the *a*-axis with the ligand planes parallel to the *bc*-plane. Tl^I ion in **107** has Tl···S_5 coordination sphere with four S atoms from D-pen/L-pen and one S atom from –NCS ligands. The octahedral arrangement of two Tl^I ions and four sulfur atoms of D-pen/L-pen form 1D double-chain structure.

TlCp (**108**) [109], Tl(CPMEF) (**109**) [110], Tl(PFSCp) (**110**) [111], Tl(QtmCp) (**111**) [112], [Tl_3Cp_2][CpMo(CO)$_3$] (**112**) [109], [Tl_2($FeCp_2$)$_3$][H_2N{B(C_6F_5)$_3$}$_2$]$_2$.5CH_2Cl_2 (**113**) [95], [Tl($P_2C_3Bu^t_3$)] (**114**) [113], [Tl(η^5-$P_3C_2Bu^t_2$)] (**115**) [114] and [{Tl(μ-η^5:η^5-1,4,2-$P_2SbC_2Bu^t_2$)}$_\infty$] (**116**) [115] form interesting 1D supramolecular chains with cyclopentadiene or substituted ligands. Compound **108** forms zigzag-shaped chain polymers in the solid state with Tl···$\pi_{(centroid)}$ distance of 2.698, 2.755 Å for Tl1 and 2.743, 2.797 Å for Tl1C. **109** exists as two polymorph; in both structures Tl^I ion is coordinated to three aromatic systems and the primary interaction is an η^5 Tl–Cp coordination with Tl···$\pi_{(centroid)}$ distances of 2.604 (**109a**) and 2.507 Å (**109b**). Two other secondary interactions lead to formation of chains (**109a**) or 3D network (**109b**) as shown in Fig. 28. In **109a** the coordination sphere of Tl^I ion is completed by intramolecular η^3,η^5 π–arene contacts to the $CPMEF^-$ system, but no bridging Cp ligands are found in **109b** and Tl^I coordination sphere is completed by η^2,η^3 π–arene contacts to the $CPMEF^-$ system.

Compound **110** is a 1D supramolecular compound with the bent chain of rings linked through the Tl^+ ions with Tl···C distances of 3.027(6)–3.149(5) Å. The coordination number at the thallium

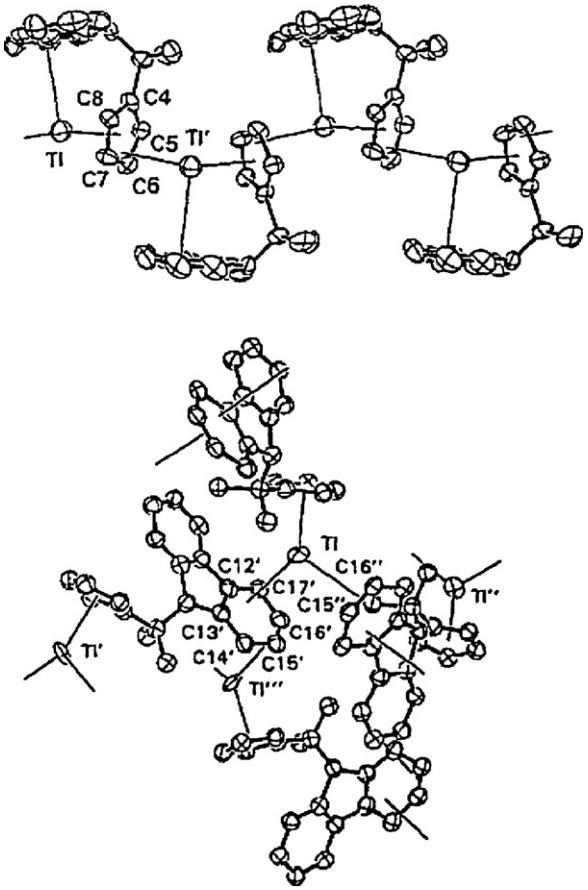

Fig. 28. A section of a polymeric chain in Tl(CPMEF) (**109a**) [110] (top) and 3D supramolecular network in **109b** (bottom).
Reproduced with permission of Wiley-VCH Verlag GmbH & Co. KGaA.

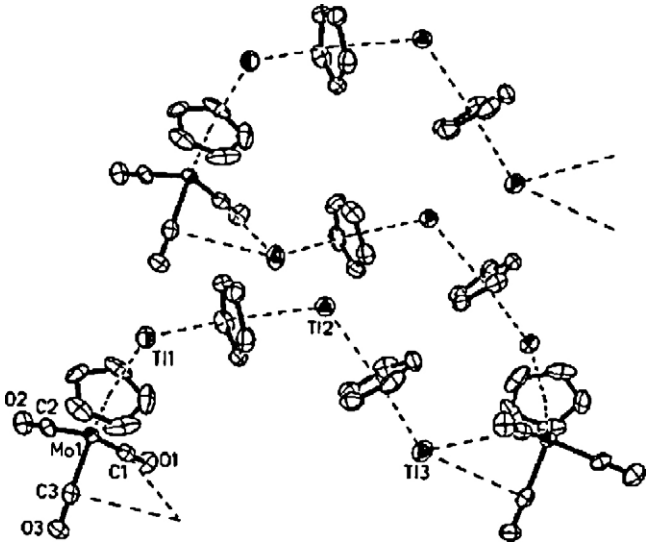

Fig. 30. Formation of u-shaped units which are arranged through additional Tl–CO contacts to helices along [010] in $[Tl_3Cp_2][CpMo(CO)_3]$ (**112**) [109].
Reproduced with permission of Wiley-VCH Verlag GmbH & Co. KGaA.

center is increased by the coordinated THF molecule and lead to O**Tl**···C_{10} coordination environment (Fig. 29).

The crystal structure analysis of **111** shows the tendency to form an infinite zigzag polymeric chain in the solid state. The thallium atom is coordinated by the substituted Cp ring and the nitrogen atom. The distance between the metal and the center of the Cp ring is 2.63 Å. A longer contact of 2.90 Å is observed to a neighboring Cp ligand. Although this distance is quite long, **111** can be described as a zigzag chain polymer. The NMR investigation indicates a monomeric structure exists in solution. Compound **112** forms u-shaped units which are arranged through additional Tl–CO contacts to helices along [0 1 0]. There are three types of Tl^I ion in **112**, Tl1 and Tl2 interact with two Cp in an η^5 fashion, while Tl3 interacts with two carbon atoms of CO group and one Cp in an η^5 fashion (Fig. 30).

The structure of **113** shows the presence of two different complex cations, $[Tl(FeCp_2)]^+$ and $[Tl(FeCp_2)_2]^+$, in a 1:1 ratio, with sandwich and half sandwich structures, respectively. The anion acts as a bridging ligand between the two different types of cations via Tl···F contacts. In the $[Tl(FeCp_2)_2]^+$ fragment, the environment around Tl(2) consists of two η^5-coordinated aromatic rings with Tl···$\pi_{(centroid)}$ distance of 2.9309 Å and two relatively close fluorine atoms. In the $[Tl(FeCp_2)]^+$ fragment, the Tl···$\pi_{(centroid)}$ interaction has the distance of 2.923 Å to the centroid of the η^5-C_5H_5 ring. The coordination environment around Tl(1) is completed by two fluorine and two chlorine atoms. Compound **114** shows infinite one-dimensional polymer strands in solid state with the mean thallium-ring centroid distance of 2.84 Å resulting in **Tl**C_6P_4 coordination sphere but in **115**, the triphospholyl ring is η^5 bound to the metal and the individual monomeric units are linked into almost linear chains by weak interactions between the metal center and alternate rings. The thallium-centroid distance to the bonded ring is 2.85 Å whilst the distance of the thallium to the centroid of the adjacent half sandwich unit is markedly longer at 3.22 Å. Compound **116** forms a double-stranded zigzag polymeric chain structure with intermolecular thallium–phosphorus interactions and Tl···$\pi_{(centroid)}$ distance of 2.835 and 2.890 Å forming **Tl**$C_4P_5Sb_2$ coordination sphere (Fig. 31).

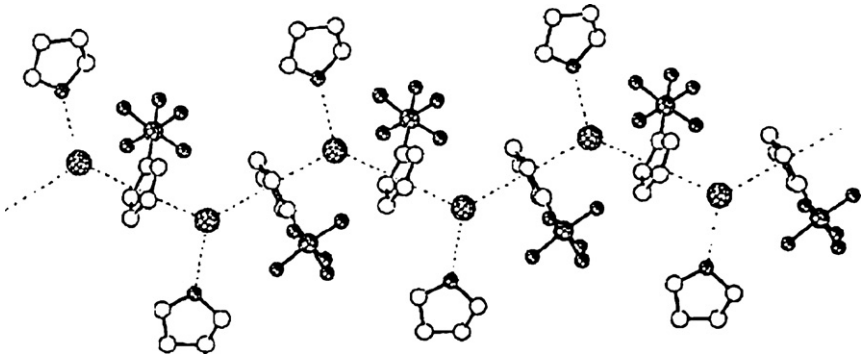

Fig. 29. A section of a polymeric chain in Tl(PFSCp) (**110**) [111], hydrogen atoms was omitted for clarity.
Reproduced with permission of Wiley-VCH Verlag GmbH & Co. KGaA.

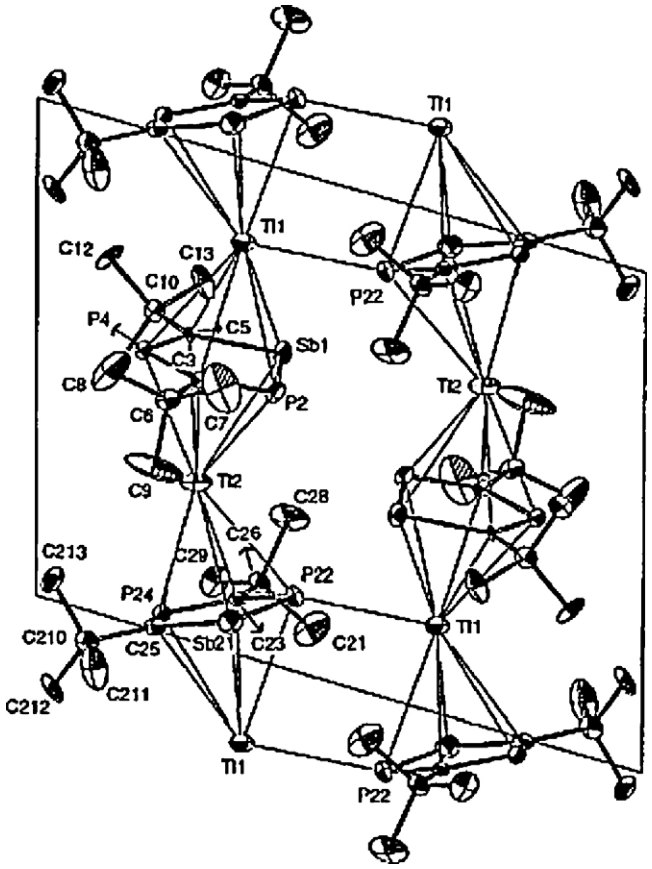

Fig. 31. Unit cell diagram of $[\{Tl(\mu\text{-}\eta^5\text{:}\eta^5\text{-}1,4,2\text{-}P_2SbC_2Bu^t_2)\}_\infty]$ (**116**) [115]. Reproduced with permission of American Chemical Society.

The thallium-centroid-thallium connections are approximately linear.

$[Tl^+][(\eta^{2-3}\text{-DMP})Ti(DMP)_4^-]$ (**117**) [116] and $[\{[(3,5\text{-}Me_2Ph)_2B(CH_2P^tBu_2)_2]Cu\}_2(\mu\text{-Br})]Tl$ (**118**) [117] are mixed metal 1D supramolecular compounds aggregated from Tl···π interactions. The Ti metal center is in a TBP geometry in **117**, and the "naked" Tl cation has π-interactions with four DMP π-arene electrons with the average distance of 3.45 Å (Fig. 32). One of the shortest distance which was reported up to date is between the Tl^I and one of the nearest neighbor's DMP ligands with Tl···$\pi_{(centroid)}$ distance of 2.592 Å.

The structure of **118** shows two copper centers connected by a linear bromide bridge, thus providing a monoanionic dinuclear copper species with one thallium counter-cation. In the molecular structure, the thallium atom resides in the hole formed by the four aryl rings of the borate anion with Tl···$\pi_{(centroid)}$ distances of 2.867, 2.901, 3.568 and 3.702 Å, lead to 1D supramolecular compound (Fig. 33).

3.2. Two-dimensional supramolecular compounds

Compound $[Tl(HB)]_n$ (**119**) [118] with carboxylate donor groups which is stable up to 185 °C has four-coordinate Tl atoms. Tl^I ions in **119** may also be involved in an $2 \times \eta^6$ interactions with the phenyl groups of neighboring molecules (Fig. 34). Hence, the Tl(I) coordination sphere could be considered as O_4**Tl**···C_{12}. The Tl···$\pi_{(centroid)}$ distances of the two phenyl groups with Tl^I ion are 3.291 and 3.297 Å. Tl···π interactions and hydrogen bonding network exist in **119**, finally resulting in a 2D supramolecular network.

Compound $[Tl_4(\mu_3\text{-dcp})_4]$ (**120**) [119], which is stable until 183 °C, shows that the complex has a tetranuclear cubic cage as a result of bridging dcp^- ligands. There are interactions between the Tl1 and two other thallium atoms in the cage with distances of 3.845(2) Å resulting in O_3**Tl**...Tl_2 coordination sphere. Compound **120** is luminescent in the solution state with emission maxima at 397 nm which could be tentatively assigned to MMCT and the existence of thallium–thallium interactions in the solution state, indicates that the structure of this complex is retained in solution. These tetranuclear cubic cages act as nodes and are connected through Cl···Cl interactions to four other nodes resulting in a two-dimensional network as shown in Fig. 35.

Tl_2Pc (**121**) [120], $[Tl^I(RC_6H_4NNNC_6H_4R)]_2$ (R = p-NO_2) (**122**) [121] and $TlTp^{Ph,4CN}$ (**123**) [122] all form 2D supramolecular networks with N-donor ligands. In compound **121** there are two metal ions per phthalocyanine macromolecule. The two thallium cations are linked to the same four isoindole nitrogen atoms and form an octahedron with thallophilic interactions. The weak interaction between T1 and the N atom of the neighboring molecule (3.516 Å) lead to a 2D supramolecular network. In compound **122** the centrosymmetric tectons attain unidimensional chains along the *c*-axis through Tl···O interactions. The 2D supramolecular network assembling of the dimeric tectons is achieved through weak secondary π interactions of the type Tl–η^2–arene between the unidimensional chains with distances of 3.926(13) and 4.115(13) Å. A thallophilic interaction (3.846 Å) and short distance of Tl^I ion with two N atoms also observed in **122**, resulting in N_3**Tl**···$TlN_2O_2C_2$ coordination sphere. In compound **123** the Tl ion is coordinated by the three available pyrazole N atoms of the Tp ligand. In addition,

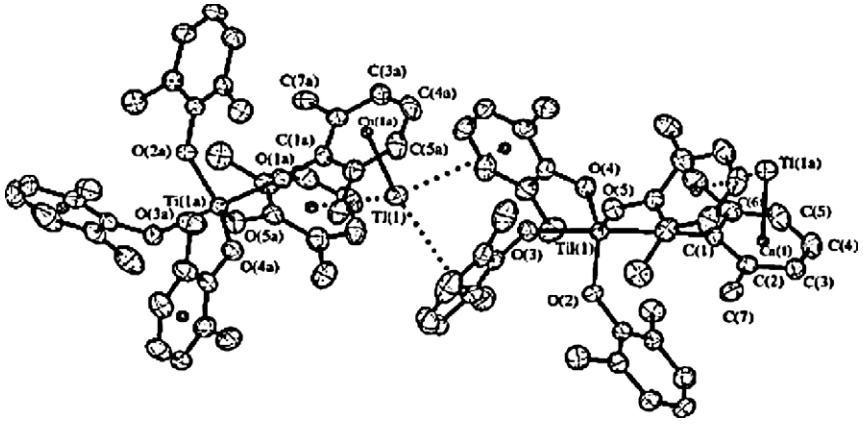

Fig. 32. Thermal ellipsoid plot of $[Tl^+][(\eta^{2-3}\text{-DMP})Ti(DMP)_4^-]$ (**117**) [116], showing interaction with nearest neighbor ellipsoids are drawn at 30% theoretical. Reproduced with permission of American Chemical Society.

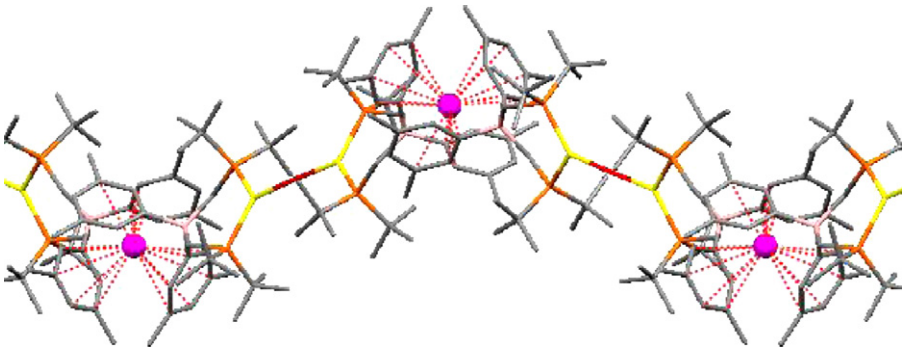

Fig. 33. A fragment of 1D supramolecular compound in [{[(3,5-$Me_2Ph)_2B(CH_2P^tBu_2)_2$]Cu}$_2$(μ-Br)]Tl (**118**) [117], hydrogen atoms and solvent molecules are omitted for clarity (C: gray, Tl: violet, B: pink, Cu: yellow, P: orange, Br: red). (For interpretation of the references to color in this figure legend, the reader is referred to the web version of the article.)
Reproduced with permission of Elsevier.

there are short contacts (Tl···N 3.211 Å) between the Tl atom and N atoms from the CN substituents of three adjacent Tp ligands. There is also a short contact between the Tl atom and the B–H group of the Tp ligand directly beneath it (Tl···B 3.071 Å), finally led to 2D supramolecular compound (Fig. 36) with N_3**Tl**···N_3H coordination environment around Tl^I ion.

Tl[Cr^{III}(D-pen)$_2$] (**124**) [108], has square planar geometry around Tl^I ion with four S atoms lead to 2D supramolecular compound. The thallium complex {[Bm^{Me}]Tl}$_x$ (**125**) [123] is oligonuclear with the metal centers being bridged by sulfur atoms of the mercaptoimidazolyl groups and four-membered [Tl_2S_2] cores, but one of the sulfur atoms on each of the [Bm^{Me}] ligands in the dinuclear thallium fragment also interacts with another thallium center, thereby resulting in a polynuclear structure. In **125** short contacts (2.69 Å) of Tl^I ion with one hydrogen atom of [Bm^{Me}] ligand are observed, thus we could consider a S_2**Tl**. . .SH coordination sphere around Tl^I ion.

[(η^5:η^5-$C_5H_4PPh_2$)Tl]$_\infty$ (**126**) [124], Tl($C_5H_3Ph_2$)(THF) (**127**) [125] and [Tl(C_4H_4P)] (**128**) [126] are 2D supramolecular compounds with cyclopentadiene derivative ligands. Two-dimensional network of **126** formed from polymeric zigzag chains of alternating thallium ions and cyclopentadienyl rings by the weak interactions between phosphorus and thallium atoms with C_5**Tl**···C_5P environment (Fig. 37) and Tl···$\pi_{(centroid)}$ distances of 2.80(1) and 2.88(1) Å. ^{31}P NMR spectrum of **126** in THF at room temperature, indicating that the Tl···P interaction is retained in solution.

Compound **127** forms 2D supramolecular network with $2 \times \eta^5$ coordination of the Tl^I ion with Cp groups, results in O**Tl**···C_{10} environment with Tl···$\pi_{(centroid)}$ distance of 2.83 and 2.87 Å. The polymeric solid-state structure of **128** consists of parallel zigzag strands in which the thallium atoms are η^5-bonded to both sides of the phospholyl ring with Tl···$\pi_{(centroid)}$ distance of 2.810 and 2.847 Å. There are two noticeable interstrand close contacts in **128** lead to 2D supramolecular network. One involves two thallium atoms (*d*Tl-Tl) 3.7953(3) Å) and the other is observed between a thallium atom and a phosphorus atom (*d*Tl–P) 3.673(2) Å), resulting in C_8P_2**Tl**···TlP coordination sphere. These Tl···Tl and Tl···P interstrand contacts could contribute to the low solubility of **128**.

3.3. Three-dimensional supramolecular compounds

Our search shows that [Tl(pydcH)]$_n$ (**129**) [127], is a 3D supramolecular compound with Tl···C interactions in a $2 \times \eta^2$ fashion with distances of 3.497 and 3.547 Å. Additional Tl···O interactions are also present in **129** leading to a O_2N**Tl**···C_4O_4 environment. In [$Tl_4(\mu^3$-OH)$_2$][H_2N{B(C_6F_5)$_3$}$_2$]$_2$·4CH_2Cl_2 (**130**) [95], [$Tl_4(\mu^3$-OH)$_2$]$^{2+}$ cation has a central $Tl_2(OH)_2$ core with two oxy-

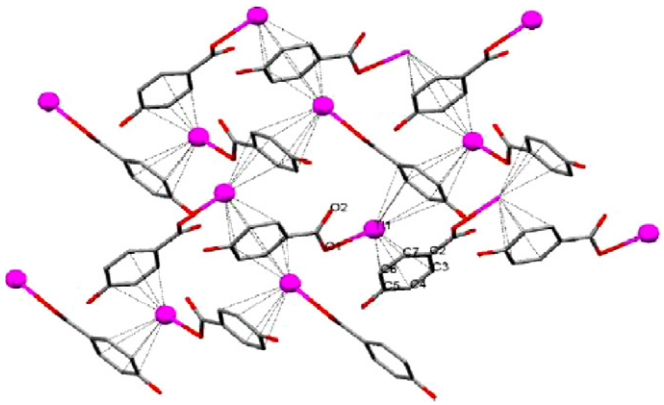

Fig. 34. A fragment of the two-dimensional layer in compound [Tl(HB)]$_n$ (**119**) [118], showing the π···Tl···π and Tl···π···Tl interactions. H atoms are omitted for clarity.
Reproduced with permission of Elsevier.

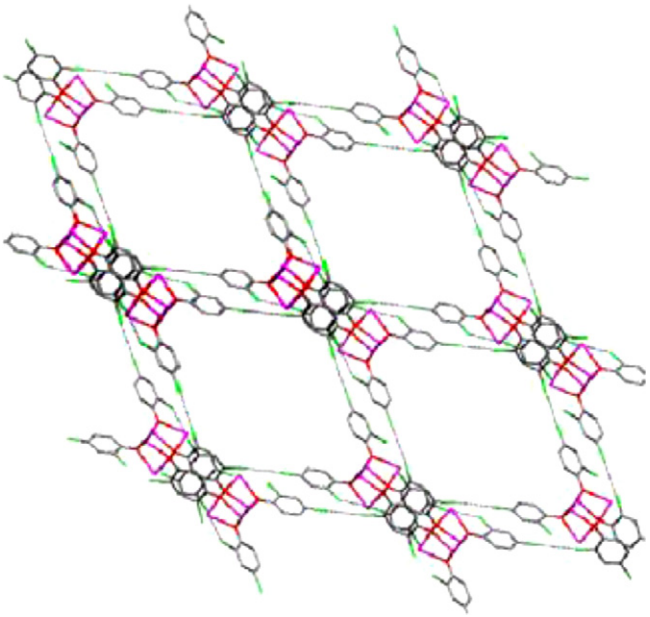

Fig. 35. A fragment of the two-dimensional layer in [$Tl_4(\mu_3$-dcp)$_4$] (**120**) [119], showing the Cl···Cl interactions. H atoms are omitted for clarity (Tl = purple, O = red, C = gray, Cl = green). (For interpretation of the references to color in this figure legend, the reader is referred to the web version of the article.)
Reproduced with permission of Elsevier.

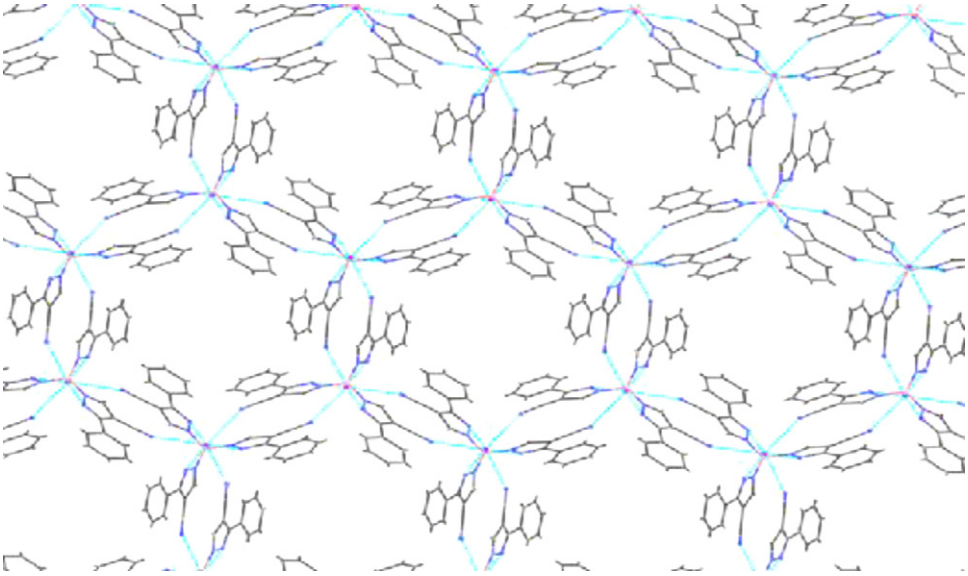

Fig. 36. A fragment of 2D network in $TlTp^{Ph,4CN}$ (**123**) [122]. Reproduced with permission of American Chemical Society.

gen atoms coordinated to the two bridging thallium atoms and to two terminal Tl atoms. The counteranions bridge between distinct cations via C–F···Tl and C–F···H–O contacts and a Tl···C (3.522 Å) interaction in Tl(2) and Tl(2A). Each of the terminal Tl atoms and two bridging Tl atoms are four-coordinate with $OF_2Cl\mathbf{Tl}\cdots C$ and $\mathbf{Tl}O_2F_2$ environment, respectively. Four intramolecular N–H···F hydrogen bonds are found in $[H_2N\{B(C_6F_5)_3\}_2]_2^-$, finally leading to a 3D supramolecular network. $Tl[C_5H_4C(CN)=C(CN)_2]$ (**131**) [128] shows the formation of a 3D supramolecular compound in which each thallium is bonded to four nitrogen atoms and a single cyclopentadienide ring with $Tl\cdots\pi_{(centroid)}$ distance of 3.040 and 3.069 Å. This situation is entirely consistent with the behaviour of this compound in solution in which the fulvenoid isomer is dominant. Compound **109** also has 3D supramolecular polymorph which was illustrated in Fig. 28 (bottom). In the case of $T1L^5$ (**132**) [129], each thallium ion in the unit cell was surrounded by five gallacarborane anions, resulting in a 3D supramolecular compound from Tl···H–B interactions with distances near 3.0 Å. The unit cell of $T1L^6$-$2/3C_7H_8$ (**133**) [129] consists of three crystallographically unique aluminacarborane anions, as well as three $T1^+$ cations and two toluene solvate molecules. Each toluene molecule in **133** lies close to a thallium ion, while a third thallium ion lies in a special position closer to one of the L^6 anions. The toluene-coordinated thallium atoms in **133** also exhibit six similar non-bonded close approaches to carborane cage hydrogen atoms averaging 2.84 Å. Finally three Tl^I ions with $\mathbf{Tl1}\cdots H_8$, $\mathbf{Tl2}\cdots H_6C_6$ and $\mathbf{Tl3}\cdots H_6C_6$ environments lead to 3D supramolecular compound.

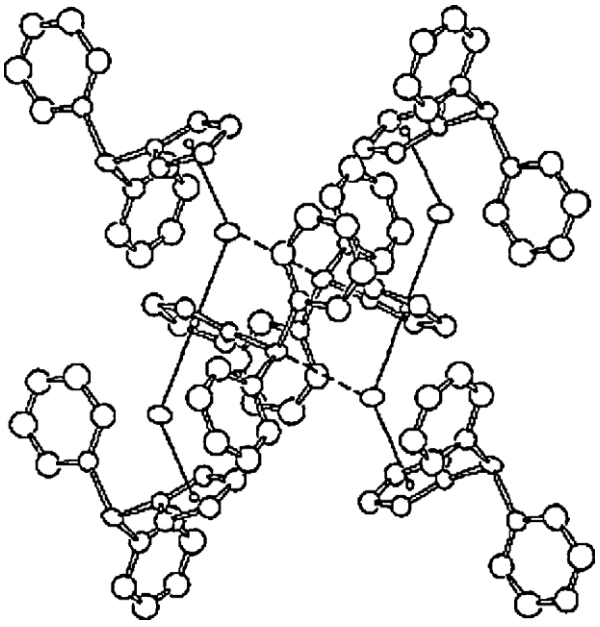

Fig. 37. Packing diagram for $[(\eta^5{:}\eta^5\text{-}C_5H_4PPh_2)Tl]_\infty$ (**126**) [124]. Reproduced with permission of Elsevier.

4. Thallium(I) polymeric compounds from linear Tl–M (M = other metal ions) arrays

Metal ions with the closed shell and pseudo-closed shell d^8, d^{10}, and s^2 electronic structures, such as Pt(II), Au(I), and Tl(I), can interact with one another to form weak metal–metal bonds [21,130,131] thus in this section we consider polymeric compounds obtained from Tl–M (M = Pt, Au or Ni) bonds.

4.1. Supramolecular compounds with Tl–Pt polymeric chains

In this section we consider supramoleular polymeric compounds obtained from linear Pt–Tl–Pt–Tl chains. The bonding interactions between the metal centers in the s^2–d^8 ($Tl^I\cdots Pt^{II}$) complexes result from a combination of metallophillic and coulombic factors. The metallophillic interaction in these $Tl^I\cdots Pt^{II}$ complexes results from σ-bonding that involves the filled 6s and empty 6pz orbitals on thallium and the filled dz^2 and empty pz orbitals on platinum [132,133]. With complexes that involve $Tl^I\cdots Pt^0$ interactions, the Tl–Pt distances fall in the range 2.77–2.89 Å and complexes with $Tl^I\cdots Pt^0$ interactions; the Tl–Pt distances fall in the 2.79–3.44 Å range. The range of distances in complexes with the s^2–d^8 ($Tl^I\cdots Pt^{II}$) and s^2–d^{10} ($Tl^I\cdots Pt^0$) electronic structures are similar. In part, this might be expected, since platinum uses filled dz^2 and empty pz orbitals to interact with the filled s^2 and empty pz orbitals on thallium in both cases [134,135].

$[PtTl_2(C{\equiv}C\text{-}(4\text{-}CF_3C_6H_4)_4(acetone)dioxane]_\infty$ (**134**) [136], $\{Tl[Tl\{cis\text{-}Pt(C_6F_5)_2(CN)_2\}]\cdot(H_2O)\}_n$ (**135**) [137], $Cis\text{-}[(NH_3)_2Pt(1\text{-}$

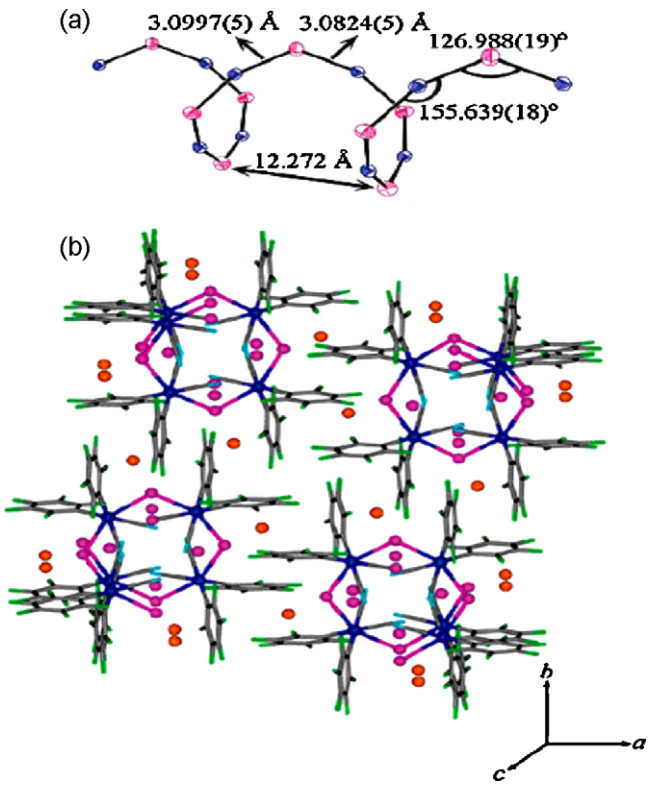

Fig. 38. (a) Schematic view of the core Pt-Tl(1) in the $\{Tl[Tl\{cis\text{-}Pt(C_6F_5)_2(CN)_2\}]\cdot(H_2O)\}_n$ (**135**) [137] helical chain. (b) View of four helical chains packing diagram projected down the crystallographic *c*-axis. Reproduced with permission of American Chemical Society.

$MeT)_2Tl(1\text{-}MeT)_2Pt(NH_3)_2]NO_3\cdot 7H_2O$ (**136**) [138], $Tl^I[(C_4H_9N_4)Pt^{II}(dmg\text{-}H)].5H_2O$ (**137**) [135], $Tl^I[(C_4H_9N_4)Pt^{II}(mnt)]$ (**138**) [135], {trans,trans,trans-$[PtTl_2(C_6F_5)_2(C{\equiv}C^tBu)_2](acetone)_2$} (**139**) [139], $[Pt(NH_3)_2(NHCO^tBu)_2Tl](NO_3)$ (**140**) [93], $[Pt(NH_3)_2(NHCO^tBu)_2Tl](ClO_4)$ (**141**) [93], $[\{Pt(NH_3)_2(NHCO^tBu)\}_2Tl_2](PF_6)_2\cdot(CH_3)_2CO\cdot H_2O$ (**142**) [93], $[\{Pt(NH_3)_2(NHCO^tBu)\}_2Tl_2](NO_3)_2\cdot EtOH\cdot H_2O$ (**143**) [93], $[\{Pt(NH_3)_2(NHCO^tBu)\}_2Tl_2](PF_6)_2.2(CH_3)_2CO$ (**144**) [93], $[\{Pt(DACH)(\mu\text{-}NHCO^tBu)_2\}_2Tl_2]\text{-}X_2$ (X = ClO^{4-}, **145**; PF^{6-}, **146**) [93] and $[\{Pt(DACH)(NHCOCH_3)_2\}_2Tl_2]X_2$ (X = NO^{3-}, **147**; ClO^{4-}, **148**; PF^{6-}, **149**) [93] form 1D supramolecular compounds aggregate from Tl–Pt bonds. Compound **134** forms an extended columnar structure from Tl–Pt bonds with secondary Tl···(η^2-acetylenic) interactions (distances from 2.980 to 3.267 Å). The blue phosphorescence of **134** in solution is very different to that in the solid state (orange). The solvent molecules are located in channels and have secondary interactions with Tl^I ion, finally leading to a Pt_2**Tl1**···$C_4O_{(dioxane)}$ and Pt_2**Tl2**···$C_2O_{(acetone)}$ coordination sphere around the Tl^I ions. Compound **135** forms an extended 1D helicoidal chain composed of both P (right-handed) and M (left-handed) helices (Fig. 38), affording an internal racemate. Two types of Tl^I ions exist in **135** with Pt_2**Tl1**…F_5O and **Tl2**…F_3N_4 coordination sphere. Low energy absorption observed in **135** compared with $[Tl_2\{Pt(C_6F_5)_2(CN)_2\}\cdot(CH_3COCH_3)_2]_n$ (**150**) [137], arises because of the presence of shorter Pt–Tl separations in **135**. In addition the lower emission energy for the helical chain in **135** compared with **150** could be attributed to the expected lower band gap energy in the extended chain. In contrast to the initial precursors, compound **135** is phosphorescent in the solid state, but loses its emissive properties in solution probably because of partial rupture of the Pt-Tl bonds.

Compound **136** forms 1D polymer with O_4Pt_2**Tl**…O_2 coordination sphere. The protons of the water molecules would then be in a position to make H bonding contacts with the lone pair at the Tl^I center. Compound **137** forms as dimers with close $Tl^I\cdots Pt^{II}$ separations of 3.0843(5) Å. Additionally, the dimers of **137** are linked via hydrogen bonding of the dimethylglyoximate oxygen atoms to chains of water molecules. These interstitial water molecules form ribbons of $(H_2O)_4$ tetramers with a T4(0)A(0) topology, lead to 2D supramolecular network, while compound **138** has much longer $Tl^I\cdots Pt^{II}$ separations of 3.4400(2) Å and forms loosely associated helical polymers. Compound **137** shows a band at about 415 nm in the solid-state UV–vis spectrum, this band occurs at lower energy in DMF and DMSO displaying a negative solvatochromic effect in these more-polar solvents. This band tentatively assigned to Pt–π^*(carbene) metal-to-ligand charge transfer (MLCT). The 1D polymeric complex of **139** can be regarded as trinuclear octahedral fragments linked through weak four Tl···C interactions with distances of 2.905, 3.114 Å from alkynyl group and 3.495, 3.650 Å from pentafluorophenyl group. Secondary Tl···F interactions of *o*-F atoms on each ring and weak Tl–O bond with acetone molecule were also observed, lead to PtO**Tl**···C_4F_2 coordination environment for Tl^I ion. The solid sample of **139** shows emission at 640 nm upon excitation at 441 nm. Despite crystallizing in different space groups, compounds **140** and **141** displays an identical supramolecular motif consisting of infinite zigzag chains. The geometry around the Tl atom may be described as a distorted tetrahedron. In compound **142**, the Pt–Tl chains run along 3_1 screw axes to give a helical motif. The helical pitch Pt_6Tl_6 is ~34.38 Å. Compound **143** consists of linear chains the same as those of **142**, and the chains stack to generate a trigonal architecture. Compound **144** has a basically similar structure to that of **143**, but all thallium centers have the same single absolute configuration, Δ or Λ, a P or M helical arrangement of strands would result, respectively lead to the achiral compound with space group of $P2_1/n$. Reaction of $[Pt(DACH)(NHCO^tBu)_2]$ with $TlNO_3$ in the presence of $NaClO_4$ or $NaPF_6$, gave supramolecular compounds of **145** and **146** and the reactions of $[Pt(DACH)(NHCOCH_3)_2]$ with Tl^+ always yielded the supramolecular compounds of **147**–**149**. The structures of the cations of **145**–**149** are essentially the same. The polymers adopt a helical structure in the solid state. The geometry about the thallium ion can be viewed as a distorted trigonal bipyramid. The amidate oxygen atoms and the nonbonding lone pair are located in the equatorial plane, and two platinum atoms are at the apical positions. In compounds **140**–**149**, Tl^I ions have **Tl**Pt_2O_2 coordination sphere with stereoactive lone pair on Tl^I ions. The remarkable overlap between the filled $5d_z^2$ orbitals of Pt and the empty $6p_z$ orbitals of Tl is responsible for the emissive behavior observed in **135** and **140**–**149**.

Compound $[Tl_2\{Pt(C_6F_5)_2(CN)_2\}\cdot(CH_3COCH_3)_2]_n$ (**150**) [137] forms a two-dimensional framework and the CN ligand shows an unusual μ_3-κC:κN:κN bridging mode, C-bound to the platinum center and N-contacting to two thallium atoms. Weak interactions of Tl^I ion with *o*-F of the C_6F_5 rings and O atom of acetone molecule were also observed, leading to a Pt**Tl**···$N_2F_2O_2$ coordination environment. Compound **150** shows similar emission properties observed for **135**. $Tl^I[(C_4H_9N_4)Pt^{II}(CN)_2]$ (**151**) [131] exists in two polymorphs; red and yellow as shown in Fig. 39. The red polymorph involves an extended ···Pt···Tl···Pt···Tl··· chain with **Tl**Pt_2N_2 coordination environment. These layers are, in turn, joined vertically through the Pt···Tl interactions. The yellow form lacks the extended ···Pt···Tl···Pt···Tl··· chain seen in the red polymorph. Rather, dimers connected by pairs of shorter Pt···Tl interactions are present. The thallium ion in the yellow polymorph has three-coordinate pyramidal geometry with **Tl**PtN_2 coordination environment.

In $[\{Pt(DACH)(NHCO^tBu)_2\}_2\{Fe(CpCO_2Tl)_2\}]$ (**152**) [93], the neighboring helical chains are linked by 1,1′-ferrocenyldicarboxylate anions to yield the two-dimensional supramolecular

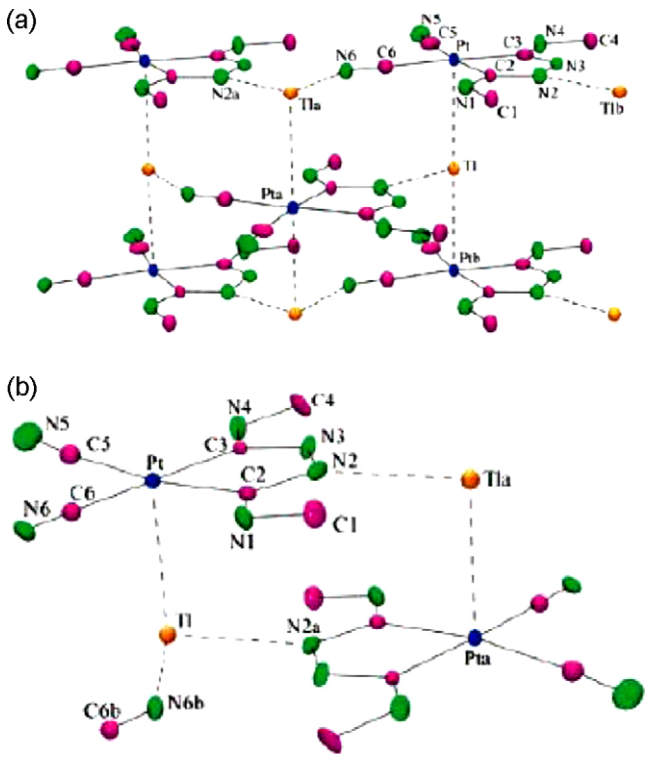

Fig. 39. (a) A view of the red polymorph and (b) dimeric unit in the yellow polymorph of $Tl^{I}[(C_4H_9N_4)Pt^{II}(CN)_2]$ (**151**) [131] with 50% thermal contours for all non-hydrogen atoms (atom colors: carbon, purple; nitrogen, green; platinum, blue; thallium, orange). (For interpretation of the references to color in this figure legend, the reader is referred to the web version of the article.)
Reproduced with permission of American Chemical Society.

grid like structure with **Tl**O_2Pt_2 coordination environment and a chiral space group of $P2_1$ (Fig. 40). The grids stack and form "stacked layers". The stacking exhibited by the grids forms microchannels which run approximately perpendicular to the layers and water molecules filled between layers.

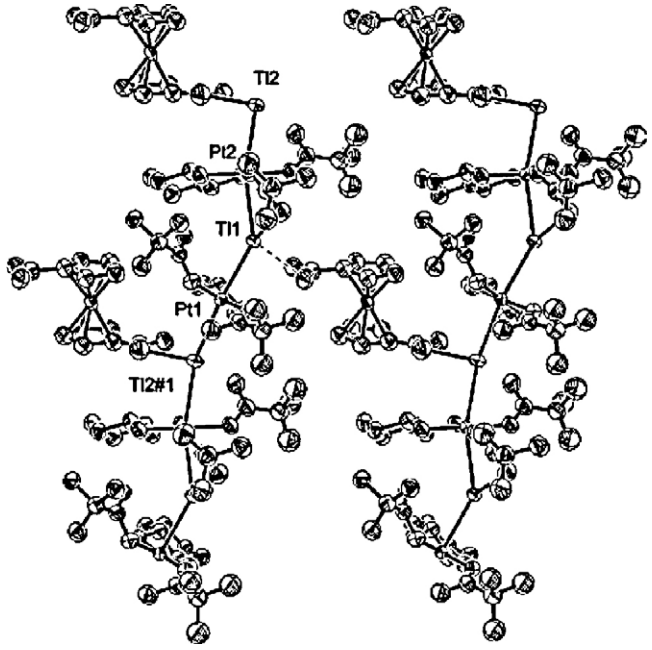

Fig. 40. Perspective drawing (30% thermal ellipsoids) of the asymmetric unit in complex [{Pt(DACH)(NHCO^{t}Bu)$_2$}$_2${Fe(CpCO$_2$Tl)$_2$}] (**152**) [93].
Reproduced with permission of American Chemical Society.

The compound {Pt(pda)(NHCOtBu)$_2$}$_4$Tl$_4$][Pt(CN)$_4$]$_2$.2H$_2$O (**153**) [140], exhibits a novel 3D network structure consisting of [Pt(CN)$_4$]$_2$) connected 1D infinite Pt–Tl–Pt–Tl chains via strong Pt–Tl bonds. Within **153**, Tl(1) and Tl(3) ions are coordinated by two [Pt(pda)(NHCOtBu)$_2$] units and one [Pt(CN)$_4$]$_2^-$ anion in a severely distorted trigonal pyramidal geometry with a **Tl**Pt_3O_2 coordination environment.

4.2. Supramolecular compounds with Tl–Au polymeric chains

In the last few years, Fernández et al. studied the synthesis of new strongly luminescent gold–thallium systems through acid–base reactions between $[AuR_2]^-$ (R = C_6F_5, C_6Cl_5) complexes and Tl^+ salts [141]. The photoluminescent properties of gold–thallium systems are very sensitive to the environment of thallium [142]. Short metal–metal contacts in the solid state are of great interest because of their influence on the molecular structure and physical properties of the materials in which they are present, such as luminescence. Moreover, the spectroscopic properties of such species can be useful for the development of, for example, volatile organic vapor (VOCs) sensors or light emitting devices (LEDs) [143]. The interactions between Au(I) and Tl(I) centers, in extended metal complexes is estimated at about 276 kJ mol^{-1}, of which about 80% consists of an ionic interaction and 20% van der Waals [144].

Compounds $[AuTl_3(acac)_2(C_6F_5)_2]$ (**154**) [44], {NBu_4[Tl_2{Au(C_6Cl_5)$_2$}{μ-Au(C_6Cl_5)$_2$}$_2$]}$_n$ (**155**) [145], {NBu_4[Tl{Au(3,5-$C_6Cl_2F_3$)$_2$}$_2$]}$_n$ (**156**) [145], {NBu_4[Tl{Au(C_6Cl_5)$_2$}{Au(3,5-$C_6Cl_2F_3$)$_2$}]}$_n$ (**157**) [145], [AuTl(C_6Cl_5)$_2$(L^{15})] (**158**) [146], [AuTl(C_6X_5)$_2$(L^{16})] (X = Cl, **159**; F, **160**) [146], {Tl[Au(C_6Cl_5)$_2$]}$_n$ (**161**) [147], {NBu_4[Tl_2(AuR_2)$_3$]}$_n$ with R = 2-C_6BrF_4 (**162**), 2-C_6F_4I (**163**) [148], {NBu_4[Tl(Au(2-C_6BrF_4)$_2$)$_2$]}$_n$ (**164**) [148], [Tl(OPPh$_3$)$_2$][Au(C_6F_5)$_2$] (**165**) [149], [Au(C_6Cl_5)$_2$]$_2$[Tl(OPPh$_3$)][Tl(OPPh$_3$)(L)] (L = THF (**166**), acetone (**167**)) [150], {Tl(THF)$_2$[Au(C_6Cl_5)$_2$]}$_n$ (**168**) [151], {Tl(acacH)$_2$[Au(C_6Cl_5)$_2$]}$_n$ (**169**) [151], {Tl(THF)$_{0.5}$[Au(C_6Cl_5)$_2$]}$_n$, (**170**) [151], [Tl_2{Au(C_6F_5)$_2$}$_2${μ-DMSO}$_3$]$_n$ (**171**) [144] and [Tl_2{Au(C_6Cl_5)$_2$}$_2${μ-DMSO}$_2$]$_n$ (**172**) [144] form 1D supramolecular compounds from the formation of Tl–Au bonds. Compound **154** forms a double-chain polymer and displays $Tl_2(acac)_2$ units acting as bridges between $[AuTl(C_6F_5)_2]$ units with three types of Tl^I ions with O_2**Tl1**···Au and **Tl2**,**3**···O_4 coordination spheres. In **154** Tl···Tl contacts also appear which are considered to be in part responsible for the luminescent behavior. Finally some short Tl···F contacts stabilize the structure of **154**. The comparison of these properties in solution to that of the starting complex [Tl(acac)] allows us to propose the presence of Tl···Tl interactions also in solution. Complex **154** shows a second band at lower energy with independent excitation profiles. These energies are likely to be attributable to electronic excited states coming from the d^{10}–s^2 interactions between Au^I and Tl^I centers. These emissions do not appear in solution at room temperature, where the Au···Tl interactions are probably lost. Compounds **155**–**157** form 1D polymers with a half (**155**) or one (**156**, **157**) additional gold center per thallium atoms. These compounds display a strong visible luminescence at room temperature and at 77 K in the solid state, which originates from an admixture of MMCT (Au to Tl charge transfer) and LMCT (ligand (perhalophenyl) to metal charge transfer). These compounds showing bridging loosely bound butterfly Au_2Tl_2 clusters which are joined together by an anionic $[Au(C_6Cl_5)_2]^-$ fragment (**155**, Fig. 41a) or terminal (**156** and **157**, Fig. 41b) $[AuR_2]^-$ fragments bonded to the thallium centers of the principal Au/Tl chain with an almost planar **Tl**Au_3 environment for the thallium atoms. Secondary Tl···X interactions with X = Cl (**155**) and X = F,Cl (**156**,**157**) also exist in these compounds.

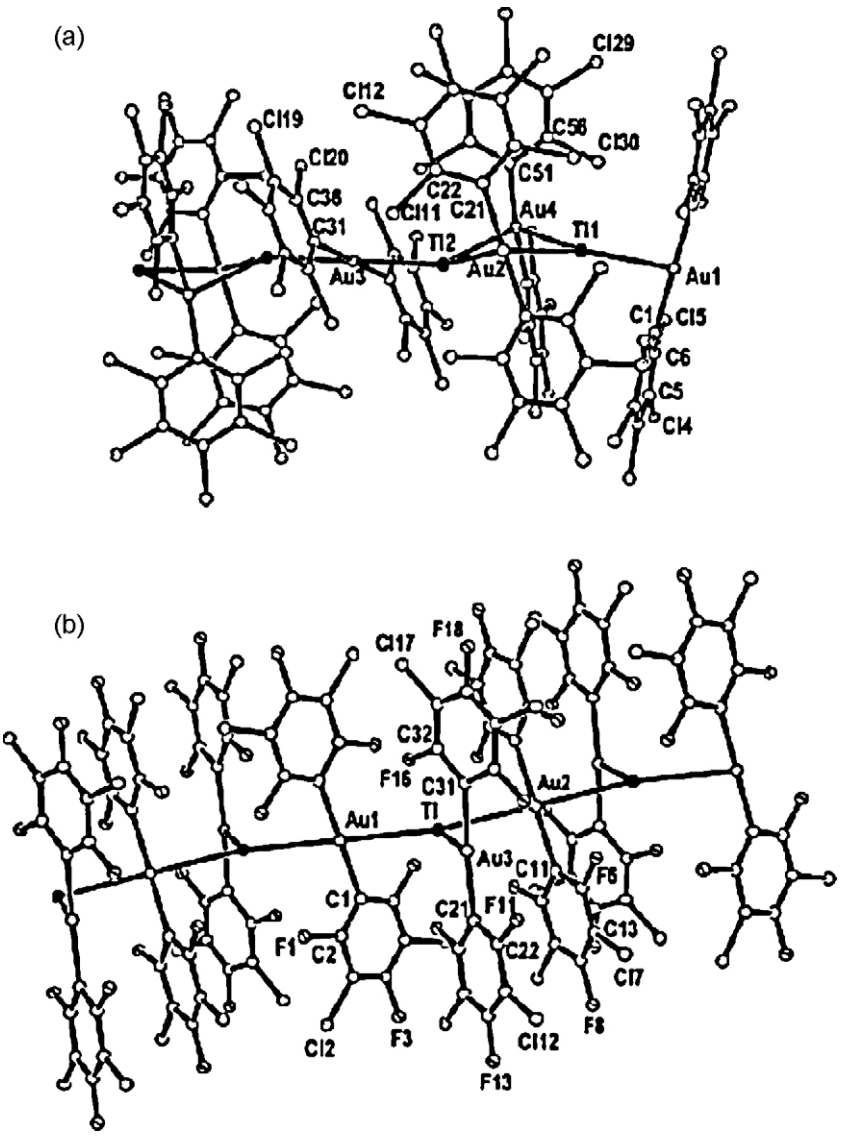

Fig. 41. (a) Different structures of compounds $\{NBu_4[Tl_2\{Au(C_6Cl_5)_2\}\{\mu\text{-}Au(C_6Cl_5)_2\}_2]\}_n$ (**155**) [145] and $\{NBu_4[Tl\{Au(3,5\text{-}C_6Cl_2F_3)_2\}_2]\}_n$ (**156**) [145] anions with the labeling scheme of the atom positions. H atoms are omitted for clarity.
Reproduced with permission of American Chemical Society.

All three compounds of **158**–**160**, show the formation of 1D polymeric chain in solid state. Each thallium binds two nitrogen atoms of a chelating amineimine (**158**) or diimine ligand (**159**, **160**) with **Tl**N_2Au_2 coordination sphere, but the environment for Tl is distorted trigonal bipyramidal with a vacant equatorial coordination site apparently associated with the stereochemically active lone pair. In addition in **158**, a series of N–H···Cl hydrogen bonds are present between atoms of the same polymeric chain. All compounds exhibit a bright luminescence in the solid state, but not in deoxygenated tetrahydrofuran solutions. Compound **161** consists of 1D linear polymer chains with unsupported Au-Tl interactions between the $[Au(C_6Cl_5)_2]$ anions and Tl(I) cations, although with channels which run parallel to the *z* axis structure with Au_2**Tl**...Cl_8 environment around Tl^I ion. Through decreasing the temperature from r.t. to 77 K, the emission is shifted to lower energy. Compound **161** also displays a vapochromic behavior with reversible changes of color when the solid is exposed to a variety of organic vapors. Compounds **162** and **163** consist of anionic chains formed by the association of loosely bound Au_2Tl_2 clusters interconnected by $[AuR_2]^-$ anions via unsupported Au···Tl interactions. Compound **164** shows infinite polymetallic Au/Tl chains with an additional $[AuR_2]^-$ fragment bonded to each Tl^I via unsupported Au···Tl contacts. All three compounds have Au_3**Tl**···X {X = Br(**162** and **164**) and I (**163**)} coordination sphere. The heterometallic bromotetrafluorophenyl complexes **162** and **164** display luminescence in the solid state, which is assigned to excited states that appear as result of the interactions between the metal centers. At 77 K different emissions appear in glassy solutions, which are assigned to the presence of oligomers of different length. In the case of the iodotetrafluorophenyl derivatives, in spite of presenting similar structures, complex **163** is weakly luminescent. This result is probably a consequence of the heavy-atom effect (HAE) due to the presence of iodine instead of bromine. Therefore, the emitting states responsible for the luminescence in the solid state for these complexes are likely to arise from a mixture of MMCT and LMCT. Compound **165** forms a one-dimensional polymer parallel to the crystallographic *z*-axis, including the metal–metal interactions. The geometry at thallium is distorted trigonal bipyramidal with a vacant equatorial coordination site and Au_2O_2**Tl**···F coordination environment, presumably associated with the stereochemically active lone pair. Four

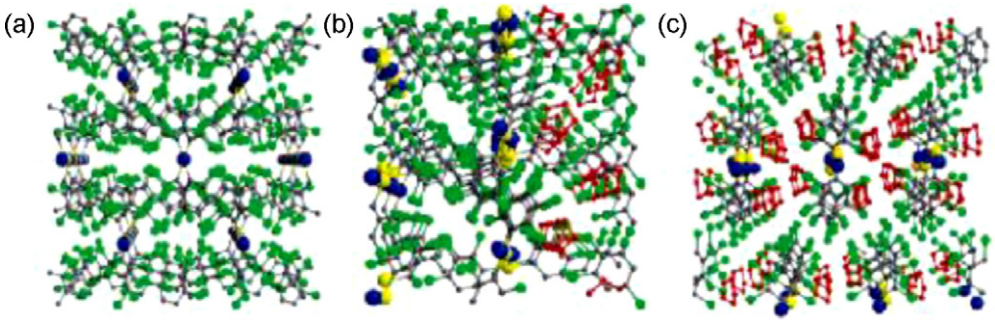

Fig. 42. View of the crystal structure of complexes: (a) $\{Tl[Au(C_6Cl_5)_2]\}_n$ (**161**) [147]; (b) **161** exposed to THF vapor: **170** and (c) $\{Tl(THF)_2[Au(C_6Cl_5)_2]\}_n$ (**168**) [151]. THF molecules are in red. (For interpretation of the references to color in this figure legend, the reader is referred to the web version of the article.)
Reproduced with permission of American Chemical Society.

weak Tl···F contacts may also contribute to the stability of the system. Compound **165** is fluorescent both at room temperature and at 77 K in the solid state. Thus, a feature of this excited state is that the transfer of an electron from a HOMO antibonding orbital (s* orbital mainly of Tl^I) to a LUMO bonding orbital (s orbital of both Au^I and Tl^I) resulting in a net increase of intermetallic bonding in the excited state. Compounds **166** and **167** display extended unsupported chains with short intermolecular interactions between alternating Au^I and Tl^I centers. Moreover, the Tl^I centers show two different types of geometrical environments, such as pseudotetrahedral with **Tl2**Au_2O environment and distorted trigonal-bipyramidal with **Tl1**Au_2O_2 environment, due to the presence of solvent molecules which act as ligands in the solid-state structure. Some Tl···Cl interactions between adjacent chains lead to more stability of these compounds. Two complexes are luminescent in the solid state at room temperature and at 77 K. Complexes **166** and **167** show site-selective excitation, probably due to the different environments around the Tl^I centers, which was confirmed by DFT and (TD)-DFT calculations. In **168** and **169** the thallium atoms show pseudo trigonal bipyramidal coordination with **Tl**Au_2O_2 environment and a vacant equatorial coordination site. Each acetylacetone molecule in the crystal structure of **169** coordinates in its enol form, stabilized by intramolecular O–H···O hydrogen bonding. Compound **170** obtained from treatment of solid **161** with THF as a VOC. Structure of **170** is intermediate between the structure of **161** in which there is no ligand coordinated to thallium, and complex **168**, which has two THF molecules per thallium (Fig. 42). In **161** there are vacant channels parallel to the crystallographic *z*-axis with hole diameters as large as 10.471 Å to accommodate the VOCs. In **161**, the observed shift of the emission to higher energies with increase in temperature is consistent with an increase in the metal–metal separation as a result of thermal expansion. This interaction is also influenced by the presence of the organic molecules in the lattice channels.

Compounds **171** and **172** can be viewed as extended linear chains built with Tl–Au–Tl units in which the thallium atoms are bridged by the oxygen atoms of DMSO ligands with **Tl1**AuO_3 and Au_2O_2**Tl2**···O coordination sphere in **171** and Au_2O_2**Tl1**,**2**···Tl coordination sphere in **172** (Fig. 43). Additional $[Au(C_6X_5)_2]^-$ fragments interact with one or two thallium centers, respectively, giving rise to two different types of metal–metal interaction in each molecule. Both show a strong fluorescence in the solid state and compound **172** also in solution. The thallium–thallium interaction in this complex is considered to be the responsible for its luminescence, which remains in solution. Finally, each metallic center displays several metal–halogen secondary interactions.

$[Tl(bipy)][Tl(bipy)_{0.5}(THF)][Au(C_6Cl_5)_2]_2$ (**173**) [152], consist of 2D planar polymers formed by repetition of Tl–Au–Tl–Au moieties linked through bidentate bridging bipy ligands. In **173** there are two nonequivalent thallium centers, Tl(1) with **Tl**N_2Au_2 environment displays a trigonal bipyramidal geometry with a vacant equatorial coordination site and Tl(2) with **Tl**$NOAu_2$ environment. No Tl···Cl contacts are observed in this case. Compound **173** is strongly luminescent at room temperature and at 77 K in the solid state, losing this characteristic in solution even at high concentrations. In $[AuTl(C_6Cl_5)_2(bipy)_{0.5}]_n$ (**174**) [142], the thallium center has trigonal planar geometry with **Tl**Au_2N environment, the bipy ligands bridge thallium centers of adjacent polymetallic chains giving rise to a two-dimensional polymer as shown in Fig. 44. Some short Tl···Cl contacts were also observed in **174**. The fluorescence in this complex is temperature dependent and shifted to lower energies with decreasing temperature. No emission was

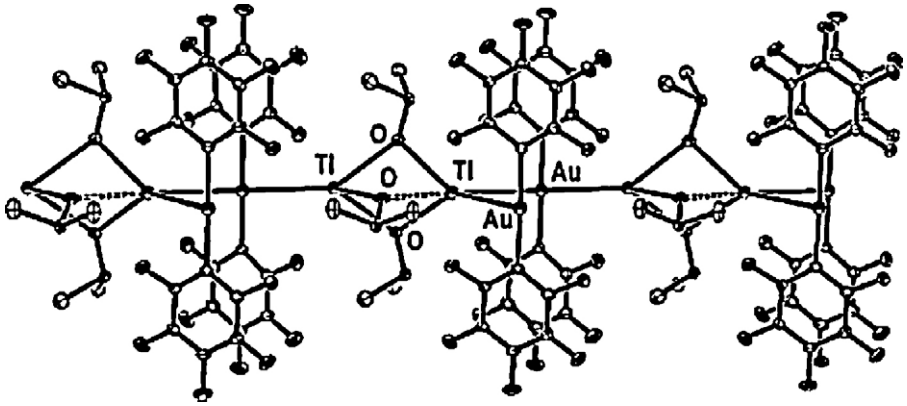

Fig. 43. Molecular structure of $[Tl_2\{Au(C_6F_5)_2\}_2\{\mu\text{-DMSO}\}_3]_n$ (**171**) [144]. H atoms are omitted for clarity.
Reproduced with permission of Elsevier.

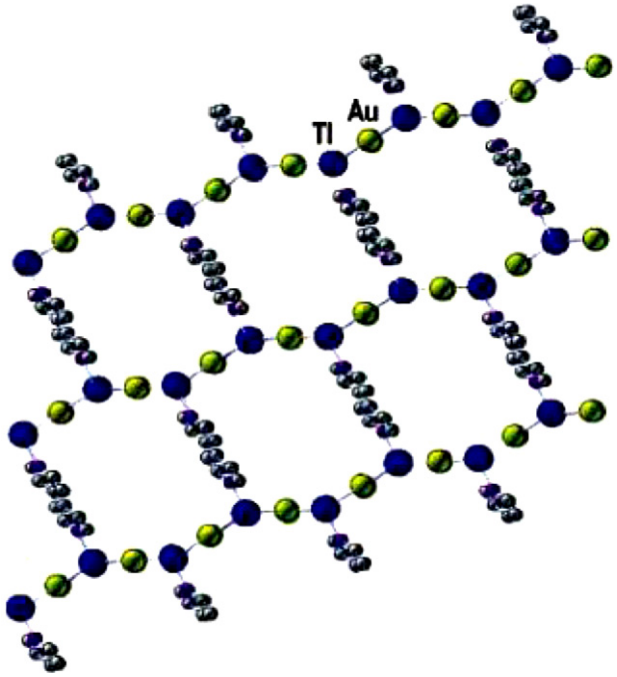

Fig. 44. Polymeric layer structure of $[AuTl(C_6Cl_5)_2(bipy)_{0.5}]_n$ (**174**) [142]. Hydrogen atoms and C_6Cl_5 groups have been omitted for clarity reasons.
Reproduced with permission of The Royal Society of Chemistry.

observed in solution, due to the dissociation caused by the solvent.

$[AuTl_2(acac)(C_6Cl_5)_2]$ (**175**) [44], displays $Tl_2(acac)_2$ units acting as bridges between linear chains of $[AuTl(C_6Cl_5)_2]_n$, giving rise to a two-dimensional structure (Fig. 45). In **175**, in addition to the Au···Tl interactions, Tl···Tl contacts also appear which are considered to be in part responsible for the luminescent behavior. The luminescence behavior and coordination spheres observed in **175** are similar to those observed in **154**.

Compound $[Tl(bipy)]_2[Au(C_6F_5)_2]_2$ (**176**) [152] consists of 3D polymers formed by repetition of Au–Tl–Au–Tl moieties linked through bidentate bridging bipy ligands. Secondary Tl···F contacts with C_6F_5 ring were also observed in **176**, lead to AuN_2**Tl**···F_2 coordination sphere around Tl^I ion. Compound **176** shows similar emission properties as observed in **173**. Compounds $[AuTl(C_6Cl_5)_2(bipy)]_n$ (**177**) [142], $\{[Tl(bipy)][Tl(bipy)_{0.5}(THF)][Au(C_6Cl_5)_2]_2\}_n$ (**178**) [142], $[Tl(bipy)][Tl(bipy)_{0.5}(THF)][Au(C_6Cl_5)_2]_2{\cdot}THF\}_n$ (**179**) [142] and $\{[AuTl(C_6Cl_5)_2(bipy)]{\cdot}0.5toluene\}_n$ (**180**) [142] are coordinated at least by one bipy ligand which bridges adjacent polymeric chains giving rise to three-dimensional networks. The thallium atoms have trigonal-bipyramidal geometry with **Tl**Au_2N_2 or **Tl**Au_2NO coordination sphere and a vacant equatorial coordination site apparently associated with the stereochemically active lone pair. The structures of **178** and **179** are similar, but the supramolecular structure resulting from the interconnection of polymetallic chains through bridging N-donor ligands and the presence of a crystallization THF molecule disordered into two positions in complex **179** is not present in **178**. Finally, additional Au···Cl and Tl···Cl contacts stabilize the systems. The luminescence properties in these compounds are similar to those observed in **174**.

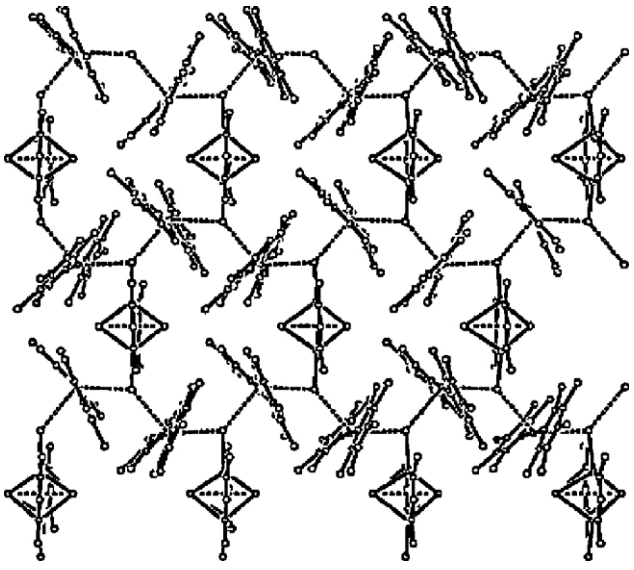

Fig. 45. Molecular structure of $[AuTl_2(acac)(C_6Cl_5)_2]$ (**175**) [44]. H atoms are omitted for clarity.
Reproduced with permission of American Chemical Society.

4.3. Supramolecular compounds with Tl–Ni polymeric chains

$Tl[Ni^{II}(D\text{-pen})_2H]{\cdot}H_2O$ (**181**) [108], is the only polymer which obtained from formation of Tl–Ni bond and shows 1D double-chain polymer with secondary Tl···S interaction and Ni_2**Tl**···S coordination sphere around Tl^I ion.

5. Additional remarks

Several different synthetic approaches have been offered for the preparation of single crystals of thallium(I) supramolecular compounds. Some of them, in order of the most use, are (1) slow evaporation of the solvent at ambient or reduced temperatures (compounds **1**–**8**, **12**, **17**, **24**, **28**, **30**, **31**, **34**, **36**, **39**, **43**, **44**, **47**–**54**, **58**–**61**, **64**, **66**, **67**, **69**–**73**, **77**–**80**, **82**, **84**, **86**, **89**, **92**, **99**, **100**, **109b**, **117**, **119**, **120**, **122**, **123**, **125**, **129**, **134**–**138**, **140**–**149**, **151**–**153**, **174** and **180**), (2) slow diffusion (compounds **26**, **45**, **57**, **62**, **63**, **132**, **139**, **150**, **154**–**157**, **162**–**169**, **173** and **176**–**179**), (3) recrystallization at low temperatures (compounds **131** at 10 °C, **101** at 4 °C, **106** at −10 °C, **41** at −25 °C, **90**, **113** and **130** at −28 °C, **96** and **103** at −35 °C, **110** at −78 °C), (4) slow cooling of hot saturated solution (compounds **13**, **14**, **32**, **55** and **126**), (5) vapor diffusion (compounds **27**, **38**, **93** and **118**), (6) sublimation at reduced pressure (compounds **114**, **115** and **128**), (7) layering technique (compounds **37** and **56**), (8) electrocrystallization (compound **81**), and (9) branch tube (compound **76**) and (10) combination of some methods with each other (compounds **29** and **97** from layering technique with slow diffusion and evaporation of the solvent).

With the exception of compounds **30**, **36**, **53**, **59**, **79**, **81**–**83**, **155**–**157**, **162**–**164** and **174** which have an inactive electron lone pair, all thallium compounds which were considered here have a stereochemically active lone pair. There are several compounds where the stereochemical activity of the lone pair is not distinguished (Compounds **113**, **115**, **117**, **118**, **129**, **132**, **133**, **135**, **150** and **153**).

The results of studies the stoichiometry and formation of compounds **59**, **119** and **120** by spectrophotometric and conductometric methods in solution state were in support of their solid-state stoichiometry.

6. Conclusions

Considering the structures discussed in this paper, Tl^I favors to forms neutral species with anionic ligands. One-dimensional polymers constitute a great portion of thallium(I) supramolecular

compounds and two and three-dimensional polymers are less common. This may be related to existence of a vacant site on thallium(I) environment and hemidirected coordination sphere of Tl^{I} ion due to the stereochemical activity of its lone pair (however the stereochemical activity of the lone pair was also observed in 2D and 3D supramolecular compounds) and effects which relate to structure, size and rigidity of ligands. In addition thallium(I) usually favors the formation of Tl···Tl, Tl···C, Tl···H secondary interactions especially through the stereochemically active lone pair indicating that thallium(I) ions act as both a Lewis acid and a Lewis base. With phenolate derivatives ligands, Tl^{I} usually forms two structures; disordered cubic units which are retained also in solution with thallophilic interactions and stair-like polymers. Furthermore Tl^{I} favors the formation of organometallic zigzag chains with cyclopentadiene derivatives. Tl^{I} also forms polymeric compounds from Tl–M (M = Pt, Au or Ni) bonds, these materials show unique emission properties arising from metal–metal interactions.

Acknowledgement

This work was supported by Tarbiat Modares University.

References

[1] H. Sadeghzadeh, A. Morsali, Inorg. Chem. 48 (2009) 10871.
[2] H. Sadeghzadeh, A. Morsali, Cryst. Eng. Commun. 12 (2010) 370.
[3] A. Aslani, A. Morsali, M. Zeller, J. Chem. Soc., Dalton. Trans. (2008) 5173.
[4] A. Aslani, A. Morsali, J. Chem. Soc., Chem. Commun. (2008) 3402.
[5] N. Soltanzadeh, A. Morsali, Polyhedron 28 (2009) 703.
[6] N. Soltanzadeh, A. Morsali, Polyhedron 28 (2009) 1343.
[7] A.V. Mudring, F. Rieger, Inorg. Chem. 44 (2005) 6240.
[8] A. Askarinejad, A.A. Torabi, A. Morsali, Z. Naturforsch. 61b (2006) 565.
[9] F. Wiesbrock, H. Schmidbaur, J. Inorg. Biochem. 98 (2004) 473.
[10] S. Hünig, H. Meixner, T. Metzenthin, U. Langohr, J.U. Schütz, H.-C. Wolf, E. Tillmanns, Adv. Mater. 2 (1990) 361.
[11] F. Wiesbrock, H. Schmidbaur, J. Am. Chem. Soc. 125 (2003) 3622.
[12] S.-H. Huang, R.-J. Wang, T.C.W. Mak, J. Chem. Soc., Dalton Trans. (1991) 1379.
[13] J. Emsley, The Elements, Clarendon Press, Oxford, UK, 1995, p. 192.
[14] A. Bondi, J. Phys. Chem. 68 (1964) 441.
[15] H. Schmidbaur, Angew. Chem. Int. Ed. 24 (1985) 893.
[16] M. Bochmann, Coord. Chem. Rev. 253 (2009) 2000.
[17] H. Schmidbaur, W. Bublak, J. Riede, G. Müller, Angew. Chem. Int. Ed. 24 (1985) 414.
[18] S.D. Waezsada, T. Belgardt, M. Noltemeyer, H.W. Roesky, Angew. Chem. Int. Ed. 33 (1994) 1351.
[19] R.J. Wright, A.D. Phillips, S. Hino, P.P. Power, J. Am. Chem. Soc. 127 (2005) 4794.
[20] P. Ghosh, A.L. Rheingold, G. Parkin, Inorg. Chem. 38 (1999) 5464.
[21] P. Pyykkö, Chem. Rev. 97 (1997) 597.
[22] R.D. Hancock, J.H. Reibenspies, H. Maumela, Inorg. Chem. 43 (2004) 2981.
[23] T. Fillebeen, T. Hascall, G. Parkin, Inorg. Chem. 36 (1997) 3787.
[24] C. Dowling, P. Ghosh, G. Parkin, Polyhedron 16 (1997) 3469.
[25] M. Brookhart, M.L.H. Green, L.-L. Wong, Prog. Inorg. Chem. 36 (1988) 1.
[26] H. Li, M. Eddaoudi, M. O'Keeffe, O.M. Yaghi, Nature 402 (1999) 276.
[27] T. Loiseau, C. Serre, C. Huguenard, G. Fink, F. Taulelle, M. Henry, T. Bataille, G. Férey, Chem. Eur. J. 10 (2004) 1373.
[28] S.S.-Y. Chiu, S.M.-F. Lo, J.P.H. Charmant, A.G. Orpen, I.D. Williams, Science 283 (1999) 1148.
[29] A.K. Cheetham, C.N.R. Rao, Science 318 (2007) 58.
[30] A. Morsali, M.Y. Masoomi, Coord. Chem. Rev. 253 (2009) 1882.
[31] K. Akhbari, A. Morsali, Cryst. Growth Des. 7 (2007) 2024.
[32] O.T. Ilkun, S.J. Archibald, C.L. Barnes, N. Gerasimchuk, R. Biagioni, S. Silchenko, O.A. Gerasimchuk, V.N. Nemykin, J. Chem. Soc., Dalton Trans. (2008) 5715.
[33] N.K. Szymczak, F. Han, D.R. Tyler, J. Chem. Soc., Dalton Trans. (2004) 3941.
[34] K. Akhbari, A. Morsali, J. Organomet. Chem. 692 (2007) 5141.
[35] O. Kristiansson, Eur. J. Inorg. Chem. (2002) 2355.
[36] A. Askarinejad, A. Morsali, Helv. Chim. Acta 89 (2006) 265.
[37] K. Akhbari, A. Morsali, Inorg. Chim. Acta 362 (2009) 1692.
[38] J.M. Harrowfield, R.P. Sharma, B.W. Skelton, A.H. White, Aust. J. Chem. 51 (1998) 735.
[39] A.R. Mahjoub, A. Morsali, H. Bagherzadeh, Polyhedron 21 (2002) 2555.
[40] M.V. Childress, D. Millar, T.M. Alam, K.A. Kreisel, G.P.A. Yap, L.N. Zakharov, J.A. Golen, A.L. Rheingold, L.H. Doerrer, Inorg. Chem. 45 (2006) 3864.
[41] D. Robertson, Ch. Barnes, N. Gerasimchuk, J. Coord. Chem. 57 (2004) 1205.
[42] D. Robertson, J.F. Cannon, N. Gerasimchuk, Inorg. Chem. 44 (2005) 8326.
[43] C.A. Zechmann, T.J. Boyle, D.M. Pedrotty, T.M. Alam, D.P. Lang, B.L. Scott, Inorg. Chem. 40 (2001) 2177.
[44] E.J. Fernández, A. Laguna, J.M. López-de-Luzuriaga, M. Monge, M. Montiel, M.E. Olmos, J. Pérez, Organometallics 23 (2004) 774.
[45] A. Askarinejad, A. Morsali, L.-G. Zhu, Solid State Sci. 8 (2006) 537.
[46] R. Atencio, J. Barberá, C. Cativiela, F.J. Lahoz, J.L. Serrano, M.M. Zurbanot, J. Am. Chem. Soc. 116 (1994) 11558.
[47] G.B. Deacon, E.E. Delbridge, C.M. Forsyth, B.W. Skelton, A.H. White, J. Chem. Soc., Dalton Trans. (2000) 745.
[48] K. Singh, J.R. Long, P. Stavropoulos, J. Am. Chem. Soc. 119 (1997) 2942.
[49] J.F. Ojo, P.A. Slavin, J. Reglinski, M. Garner, M.D. Spicer, A.R. Kennedy, S.J. Teat, Inorg. Chim. Acta 313 (2001) 15.
[50] P.J. Schebler, C.G. Riordan, I.A. Guzei, A.L. Rheingold, Inorg. Chem. 37 (1998) 4754.
[51] S. Welsch, L.J. Gregoriades, M. Sierka, M. Zabel, A.V. Virovets, M. Scheer, Angew. Chem. Int. Ed. 46 (2007) 9323.
[52] J.C. Thomas, J.C. Peters, Inorg. Chem. 42 (2003) 5055.
[53] V.A. Trush, K.E. Gubina, V.M. Amirkhanov, J. Swiatek-Kozlowska, K.V. Domasevitch, Polyhedron 24 (2005) 1007.
[54] C. Janiak, S. Temizdemir, C. Röhr, Z. Anorg. Allg. Chem. 626 (2000) 1265.
[55] E. Craven, E. Mutlu, D. Lundberg, S. Temizdemir, S. Dechert, H. Brombacher, C. Janiak, Polyhedron 21 (2002) 553.
[56] O. Renn, H. Preut, B. Lippert, Inorg. Chim. Acta 188 (1991) 133.
[57] B. Krebs, A. Brömmelhaus, Z. Anorg. Allg. Chem. 595 (1991) 167.
[58] K. Akhbari, A. Morsali, A.D. Hunter, M. Zeller, Inorg. Chem. Commun. 10 (2007) 178.
[59] V.V. Ponomarova, K.V. Domasevitch, Cryst. Eng. 5 (2002) 137.
[60] H. Adams, S.R. Batten, G.M. Davies, M.B. Duriska, J.C. Jeffery, P. Jensen, J. Lu, G.R. Motson, S.J. Coles, M.B. Hursthoused, M.D. Ward, J. Chem. Soc., Dalton Trans. (2005) 1910.
[61] G.M. Davies, J.C. Jeffery, M.D. Ward, New J. Chem. 27 (2003) 1550.
[62] C. Janiak, L. Braun, F. Girgsdies, J. Chem. Soc., Dalton Trans. (1999) 3133.
[63] S. Guo, J.W. Bats, M. Bolte, M. Wagner, J. Chem. Soc., Dalton Trans. (2001) 3572.
[64] F. Jäkle, K. Polborn, M. Wagner, Chem. Ber. 129 (1996) 603.
[65] E. Psillakis, J.C. Jeffery, J.A. McCleverty, M.D. Ward, J. Chem. Soc., Dalton Trans. (1997) 1645.
[66] A.J. Blake, D. Fenske, W-Sh. Li, V. Lippolis, M. Schröder, J. Chem. Soc., Dalton Trans. (1998) 3961.
[67] W. Rensch, M. Schuster, Z. Anorg. Allg. Chem. 619 (1993) 1689.
[68] A. Askarinejad, A. Morsali, J. Organomet. Chem. 691 (2006) 3563.
[69] M. Akkurt, S.Ö. Yıldırım, F.-Z. Khardli, M. Mimouni, V. McKee, T.B. Hadda, Arkivoc xv (2008) 121.
[70] M.R. Fadaei, A. Morsali, A.R. Mahjoub, Z. Naturforsch. 60b (2005) 741.
[71] K. Akhbari, A. Morsali, J. Mol. Struct. 878 (2008) 65.
[72] R.P. Sharmaa, R. Bala, R. Sharma, J. Raczyńska, U. Rychlewska, J. Mol. Struct. 738 (2005) 247.
[73] A.V. Ivanov, O.A. Bredyuk, A.V. Gerasimenko, I.A. Lutsenko, O.N. Antzutkin, W. Forsling, Russ. J. Inorg. Chem. 32 (2006) 339.
[74] K. Akhbari, K. Alizadeh, A. Morsali, M. Zeller, Inorg. Chem. Acta 362 (2009) 2589.
[75] A. Askarinejad, M.R. Fadaei, A. Morsali, A.R. Mahjoub, J. Coord. Chem. 60 (2007) 753.
[76] A. Askarinejad, A. Morsali, J. Coord. Chem. 59 (2006) 997.
[77] B.H. Hamilton, C.J. Ziegler, Inorg. Chem. 43 (2004) 4272.
[78] J.A.R. Navarro, E. Barea, J.M. Salas, N. Masciocchi, S. Galli, A. Sironi, Inorg. Chem. 46 (2007) 2988.
[79] V. Latorre, P.G. Jones, O. Moers, A. Blaschette, Z. Anorg. Allg. Chem. 629 (2003) 1515.
[80] R. Ahlers, U. Ruschewitz, Solid State Sci. 11 (2009) 1058.
[81] A. Askarinejad, A. Morsali, J. Coord. Chem. 60 (2007) 1903.
[82] P. Nagy, A. Fischer, J. Glaser, A. Ilyukhin, M. Maliarik, I. Tóth, Inorg. Chem. 44 (2005) 2347.
[83] A. Askarinejad, A. Morsali, Inorg. Chim. Acta 359 (2006) 3379.
[84] M. Rafizadeh, F. Manteghi, Acta Crystallogr. E 65 (2009) m17.
[85] H. Aghabozorg, F. Ramezanipour, B. Nakhjavan, J. Soleimannejad, J. Attar Gharamaleki, M.A. Sharif, Cryst. Res. Technol. 42 (2007) 1137.
[86] A. Adam, Y.Q. Zheng, Z. Anorg. Allg. Chem. 620 (1994) 1707.
[87] A. Askarinejad, A. Morsali, Inorg. Chem. Commun. 9 (2006) 143.
[88] M. Botoshansky, F.H. Herbstein, M. Kapon, Acta Crystallogr. B50 (1994) 589.
[89] K.P. Rao, K. Vidyasagar, Eur. J. Inorg. Chem. (2006) 813.
[90] W.T.A. Harrison, L.L. Dussack, A.J. Jacobson, J. Solid State Chem. 138 (1998) 365.
[91] G. Glover, N. Gerasimchuk, R. Biagioni, K.V. Domasevitch, Inorg. Chem. 48 (2009) 2371.
[92] K.W. Hellmann, L.H. Gade, R. Fleischer, D. Stalke, J. Chem. Soc., Chem. Commun. (1997) 527.
[93] W. Chen, F. Liu, D. Xu, K. Matsumoto, S. Kishi, M. Kato, Inorg. Chem. 45 (2006) 5552.
[94] K. Aoki, Il-H. Suh, H. Nagashima, J. Uzawa, H. Yamazakit, J. Am. Chem. Soc. 114 (1992) 5722.
[95] Y. Sarazin, D.L. Hughes, N. Kaltsoyannis, J.A. Wright, M. Bochmann, J. Am. Chem. Soc. 129 (2007) 881.
[96] R.J. Wright, M. Brynda, P.P. Power, Inorg. Chem. 44 (2005) 3368.
[97] E. Herdtweck, F. Peters, W. Scherer, M. Wagner, Polyhedron 17 (1998) 1149.
[98] J.C. Peters, S.B. Harkins, S.D. Brown, M.W. Day, Inorg. Chem. 40 (2001) 5083.
[99] K.W. Hellmann, L.H. Gade, I.J. Scowen, M. McPartlin, J. Chem. Soc., Chem. Commun. (1996) 2515.
[100] C.H. Galka, L.H. Gade, Inorg. Chem. 38 (1999) 1038.
[101] C. Janiak, S. Temizdemira, T.G. Scharmann, Z. Anorg. Allg. Chem. 624 (1998) 755.

[102] D.A. Bardwell, J.C. Jeffery, J.A. McCleverty, M.D. Ward, Inorg. Chim. Acta 267 (1998) 323.
[103] K.L.V. Mann, J.C. Jeffery, J.A. McCleverty, M.D. Ward, Polyhedron 18 (1999) 721.
[104] A.J. Amoroso, J.C. Jeffery, P.L. Jones, J.A. McCleverty, E. Psillakis, M.D. Ward, J. Chem. Soc., Chem. Commun. (1995) 1175.
[105] F. Zhang, M. Bolte, H.-W. Lerner, M. Wagner, Organometallics 23 (2004) 5075.
[106] D.R. Manke, D.G. Nocera, Polyhedron 25 (2006) 493.
[107] B.E. Bosch, M. Eisenhawer, B. Kersting, K. Kirschbaum, B. Krebs, D.M. Giolando, Inorg. Chem. 35 (1996) 6599.
[108] A. Müller, K.U. Johannes, M. Straube, E. Krickemeyer, H. Bögge, Z. Anorg. Allg. Chem. 619 (1993) 1037.
[109] A. Dashti-Mommertza, B. Neumüllera, S. Melle, D. Haase, W. Uhl, Z. Anorg. Allg. Chem. 625 (1999) 1828.
[110] W. Frank, D. Kuhn, S. Müller-Becker, A. Razavi, Angew. Chem. Int. Ed. 32 (1993) 90.
[111] A. Klauck, K. Seppelt, Angew. Chem. Int. Ed. 33 (1994) 93.
[112] M. Enders, J. Fink, H. Pritzkow, Eur. J. Inorg. Chem. (2000) 1923.
[113] M. Brym, M.D. Francis, G. Jin, C. Jones, D.P. Mills, A. Stasch, Organometallics 25 (2006) 4799.
[114] M.D. Francis, P.B. Hitchcock, J.F. Nixon, H. Schnöckel, J. Steiner, J. Organomet. Chem. 646 (2002) 191.
[115] M.D. Francis, C. Jones, G.B. Deacon, E.E. Delbridge, P.C. Junk, Organometallics 17 (1998) 3826.
[116] T.J. Boyle, C.A. Zechmann, T.M. Alam, M.A. Rodriguez, C.A. Hijar, B.L. Scott, Inorg. Chem. 41 (2002) 946.
[117] J.C. Thomas, J.C. Peters, Polyhedron 23 (2004) 2901.
[118] K. Akhbari, A. Morsali, J. Organomet. Chem. 692 (2007) 5109.
[119] K. Akhbari, A. Morsali, Inorg. Chem. Commun. 10 (2007) 1189.
[120] J. Janczak, R. Kubiak, J. Alloy. Compd. 202 (1993) 69.
[121] M. Hörner, G.M. Oliveira, L. Bresolin, A.B. Oliveira, Inorg. Chim. Acta 359 (2006) 4631.
[122] N. Zhao, M.J.V. Stipdonk, C. Bauer, C. Campana, D.M. Eichhorn, Inorg. Chem. 46 (2007) 8662.
[123] C. Kimblin, B.M. Bridgewater, T. Hascall, G. Parkin, J. Chem. Soc., Dalton Trans. (2000) 891.
[124] G. Lin, W.-T. Wong, J. Organomet. Chem. 495 (1995) 203.
[125] H. Schumann, A. Lentz, R. Weimann, J. Organomet. Chem. 487 (1995) 245.
[126] F. Nief, L. Ricard, Organometallics 20 (2001) 3884.
[127] M. Rafizadeha, V. Amani, B. Neumüller, Z. Anorg. Allg. Chem. 631 (2005) 1753.
[128] M. Arthurs, J.C. Bickerton, G. Hogarth, D.A. Morton-Blake, G. Kubal, M.R. Truter, J. Organomet. Chem. 571 (1998) 43.
[129] D.M. Schubert, M.A. Bandman, W.S. Rees, J.C.B. Knobler, P. Lu, W. Nam, M.F. Hawthorne, Organometallics 9 (1990) 2046.
[130] D.M. Roundhill, H.B. Gray, C.-M. Che, Acc. Chem. Res. 22 (1989) 55.
[131] J.R. Stork, M.M. Olmstead, A.L. Balch, J. Am. Chem. Soc. 127 (2005) 6512.
[132] J.K. Nagle, A.L. Balch, M.M. Olmstead, J. Am. Chem. Soc. 110 (1988) 319.
[133] J.R. Berenguer, J. Forniés, J. Gomez, E. Lalinde, M.T. Merino, Organometallics 20 (2001) 4847.
[134] P. Pyykkö, M. Patzschke, Faraday Discuss. 124 (2003) 41.
[135] J.R. Stork, M.M. Olmstead, J.C. Fettinger, A.L. Balch, Inorg. Chem. 45 (2006) 849.
[136] J.R. Berenguer, J. Forniés, B. Gil, E. Lalinde, Chem. Eur. J. 12 (2006) 785.
[137] J. Forniés, A. García, E. Lalinde, M.T. Moreno, Inorg. Chem. 47 (2008) 3651.
[138] O. Renn, B. Lippert, I. Mutikainen, Inorg. Chim. Acta 208 (1993) 219.
[139] I. Ara, J.R. Berenguer, J. Forniés, J. Gómez, E. Lalinde, R.I. Merino, Inorg. Chem. 36 (1997) 6461.
[140] G. Wu, D. Wang, J. Clust. Sci. 18 (2007) 406.
[141] E.J. Fernández, A. Laguna, J.M. López-de-Luzuriaga, Coord. Chem. Rev. 249 (2005) 1423.
[142] E.J. Fernández, A. Laguna, J.M. López-de-Luzuriaga, M.E. Olmos, J. Pérez, J. Chem. Soc., Dalton Trans. (2004) 1801.
[143] E.J. Fernández, J.M. López-de-Luzuriaga, M.E. Olmos, J. Pérez, A. Laguna, M.C. Lagunas, Inorg. Chem. 44 (2005) 6012.
[144] E.J. Fernández, A. Laguna, J.M. López-de-Luzuriaga, M. Montiel, M.E. Olmos, J. Pérez, Inorg. Chim. Acta 358 (2005) 4293.
[145] E.J. Fernández, A. Laguna, J.M. López-de-Luzuriaga, M. Montiel, M.E. Olmos, J. Pérez, Organometallics 24 (2005) 1631.
[146] E.J. Fernández, A. Laguna, J.M. López-de-Luzuriaga, M. Montiel, M.E. Olmos, J. Pérez, Organometallics 25 (2006) 1689.
[147] E.J. Fernández, J.M. López-de-Luzuriaga, M. Monge, M.E. Olmos, J. Pérez, A. Laguna, A.A. Mohamed, J.P. Fackler Jr., J. Am. Chem. Soc. 125 (2003) 2022.
[148] E.J. Fernández, A. Laguna, T. Lasanta, J.M. López-de-Luzuriaga, M. Montiel, M.E. Olmos, Organometallics 27 (2008) 2971.
[149] O. Crespo, E.J. Fernández, P.G. Jones, A. Laguna, J.M. López-de-Luzuriaga, A. Mendía, M. Monge, E. Olmos, J. Chem. Soc., Chem. Commun. (1998) 2233.
[150] E.J. Fernández, A. Laguna, J.M. López- de-Luzuriaga, F. Mendizabal, M. Monge, M.E. Olmos, J. Pérez, Chem. Eur. J. 9 (2003) 456.
[151] E.J. Fernández, J.M. López-de-Luzuriaga, M. Monge, M. Montiel, M.E. Olmos, J. Pérez, A. Laguna, A.A. Mohamed, J.P. Fackler Jr., Inorg. Chem. 43 (2004) 3573.
[152] E.J. Fernández, P.G. Jones, A. Laguna, J.M. López-de-Luzuriaga, M. Monge, J. Pérez, M.E. Olmos, Inorg. Chem. 41 (2002) 1056.